

People's Democratic Republic of Algeria
Ministry of Higher Education and Scientific Research

University of Akli Mohand Oulhadj- Bouira
FACULTY OF SCIENCE AND SCIENCE APPLIED
DEPARTEMENT OF MECHANICAL ENGINEERING



Master thesis

**For the purpose of obtaining the Academic Master's Degree in Mechanical
Engineering**

Option: Mechanical engineering

Specialty: Energetics

Subject

**Numerical study of the influence of air velocity on the cooling of hot
cylindrical blocks**

Thesis examination committee :

Dr. Messai (Mnager)

Dr. Merzouk (President)

Dr. Aberkane (Examiner)

presented by:

Bouzid Imane

Azzoune Yasmine

2022/2023



نموذج التصريح الشرفي الخاص بالالتزام بقواعد النزاهة العلمية لإنجاز بحث.

انا الممضي اسفله،

السيد(ة).....
الحامل(ة) لبطاقة التعريف الوطنية:.....
المسجل(ة) بكلية / معهد العلوم.....
والمكلف(ة) بإنجاز اعمال بحث(مذكرة، التخرج، مذكرة ماستر، مذكرة ماجستير، اطروحة دكتوراه).

عنوانها:.....
تحت إشراف الأستاذ(ة):.....
أصرح بشرفي اني ألتزم بمراعاة المعايير العلمية والمنهجية الاخلاقيات المهنية والنزاهة الاكاديمية المطلوبة
في انجاز البحث المذكور أعلاه.

التاريخ:.....

توقيع المعني(ة)

رأي هيئة مراقبة السرقة العلمية:

النسبة:

27 %

الامضاء:



Dedications

With deep gratitude and sincere words, we dedicate this modest thesis work to our dear parents, who have sacrificed their lives for our success and have illuminated our path with their wise counsel. We hope that one day we can give back to them some of what they have done for us. May god bless them with happiness and a long life.

We also dedicate this work to our brothers our sisters, our families, our friends, all our professors who have taught us, to all those dear to us, and of course to ourselves.

Imane Yasmine

Acknowledgments

In the name of Allah, the Most Gracious, the Most Merciful.

First and foremost, we extend our gratitude to ALLAH, our Creator, who granted us the strength, courage, and determination to complete this work.

We would like to express our sincere thanks to all individuals who supported and guided us throughout this endeavor.

Foremost, we extend our heartfelt appreciation to our supervisor Mr. T.MESSAI for his valuable advice and assistance that significantly contributed to the progress of this work.

Our thanks also go to who kindly agreed to evaluate our work and participate in the jury.

Their guidance, insights, and contributions have been indispensable in shaping the quality and direction of this thesis.

Abstract

This dissertation delves into the intricate thermodynamic behavior of fluid flow interacting with cylindrical obstacles, which find wide-ranging applications across diverse industrial sectors. The focus of this investigation centers on comprehending three-dimensional , employing Ansys Fluent version 18.2.

The aim of this graduation thesis is to investigate and analyze the influence of air velocity on the cooling process of hot cylindrical blocks.

The purpose of this study is to provide insights into the complex interplay between air velocity and convective heat transfer

, shedding light on how varying air velocities impact the rate of cooling of hot cylindrical blocks. and return to lower, stable temperatures.

To achieve this goal, numerical simulations and computational fluid dynamics (CFD) techniques are employed to model the convective heat transfer between hot cylindrical blocks and the surrounding air

Résumé

Cette thèse se penche sur le comportement thermodynamique complexe de l'écoulement de fluide interagissant avec des obstacles cylindriques, qui trouve de nombreuses applications dans divers secteurs industriels. L'objectif de cette étude se concentre sur la compréhension en trois dimensions, en utilisant Ansys Fluent version 18.2.

L'objectif de cette thèse de fin d'études est d'investiguer et d'analyser l'influence de la vitesse de l'air sur le processus de refroidissement de blocs cylindriques chauds. Le but de cette étude est de fournir des informations sur l'interaction complexe entre la vitesse de l'air et le transfert de chaleur par convection, en éclairant comment les différentes vitesses de l'air impactent le taux de refroidissement des blocs cylindriques chauds et leur retour à des températures plus basses et stables.

Pour atteindre cet objectif, des simulations numériques et des techniques de dynamique des fluides numérique (CFD) sont utilisées pour modéliser le transfert de chaleur par convection entre les blocs cylindriques chauds et l'air environnant.

ملخص

تتناول هذه الدراسة السلوك الحراري المعقد لتدفق السوائل المتفاعلة مع العوائق الاسطوانية والذي يجد تطبيقات كثيرة في مختلف القطاعات الصناعية. يركز هدف هذه الدراسة على فهم ثلاثي الأبعاد باستخدام انسيس فلونت 18.2

هدف رسالة الماجستير هذه هو التحقق وتحليل تأثير سرعة الهواء على عملية تبريد الكتل الاسطوانية الساخنة وتوفير معلومات حول التفاعل المعقد بين سرعة الهواء ونقل الحرارة بالتواصل من خلال القاء الضوء على كيفية تأثير السرعات المختلفة للهواء على معدل تبريد الكتل الاسطوانية الساخنة

لتحقيق هذا الهدف يتم استخدام المحاكاة الرقمية وتقنيات الديناميات السائلة الرقمية لنمذجة نقل الحرارة بالتواصل بين الكتل الاسطوانية والهواء

Table of contents

Table of contents.....	ii
List of tables	vi
List of figures	vii
Nomenclature.....	x
GENEREAL INTRODUCTION.....	xiii

Table of Contents

CHAPTER I.....	XV
I 1 Introduction.....	1
I 2 Over view on heat transfer.....	1
I 3 Heat transfer modes	2
I 3 1 Conduction heat transfer	2
I 3 2 Radiation heat transfer	4
I 3 3 Convection heat transfer	5
I 4 Mixed convection in cooling obstacles.....	8
I 5 Internal and external flows	8
I 6 Heat exchangers.....	9
I 6 1 Cross flow heat exchanger	10
I 7 Examples of hot cylindrical blocks.....	11
I 8 Literature review.....	12
I 8 1 Obstacles 2D	13
I 8 2 Obstacles 3D	15
I 9 Conclusion	17
CHAPTER II	19
II 1 Introduction	20
II 2 Free and Forced Convection Experiment(TD1005).....	20
II 2 1 Description.....	20
II 2 2 Objectives	21

II 3 Fluid kinematics	21
II 4 Different flow regimes	22
II 4 1 laminar flow	22
II 4 2 Turbulent flow	22
II 4 3 Transitional flow	23
II 5 Turbulence	23
II 6 Turbulence models	24
II 7 RANS (Reynolds-Averaged Navier-Stokes equations)	24
II 7 1 zero-equation model (Algebraic Eddy viscosity)	25
II 7 2 One-equation models (Spalart-Allmaras)	25
II 7 3 Two-equation models	26
II 7 4 Reynolds stress models	27
II 8 Simplifying hypotheses	28
II 9 Navier Stokes equations	28
II 9 1 Continuity equation	28
II 9 2 Momentum equation	29
II 9 3 Energy equation	29
II 10 The Boussinesq approximation	29
II 11 Formulation of equations in Cartesian coordinates	31
II 11 1 Continuity equation	31
II 11 2 Equation of momentum	31
II 11 3 Energy equation	32
II 12 Dimensional analysis	32
II 12 1 Continuity equation	32
II 12 2 Momentum equation	32
II 12 3 The energy equation	33
II 13 Dimensionless numbers	33
II 13 1 Grashof number	33

II 13 2 Prandtl number	33
II 13 3 Reynolds number	33
II 13 4 Nusselt number	34
II 13 5 Richardson number	35
II 14 Model Boundary conditions	35
II 15 Conclusion.....	35
CHAPTER III.....	37
NUMERICAL METHODS	37
III 1 Introduction.....	38
III 2 Solution of differential equations.....	38
III 3 Finite volume methods.....	38
III 4 Discretization of the governing equations	39
III 4 1 Discretization process	39
III 4 2 Transport equation.....	40
III 4 3 SIMPLEC Algorithm	47
III 5 The computational fluid dynamics (CFD) :	48
III 6 ANSYS Fluent :	48
III 6 1 Pre-processing	50
III 6 2 Processing.....	53
III 7 Conclusion	58
CHAPTER IV.....	61
IV 1 Introduction.....	62
IV 2 Mesh choice	62
IV 3 Volume rendering	64
IV 4 Velocity influence.....	64
IV 4 1 For P= 50 watts	64
IV 4 2 For P =70 watts	72
IV 5 Power influence	80

IV 6 Turbulence	81
IV 6 1 Turbulent kinetic energy contours and profiles	81
IV 6 2 Eddy viscosity contours and profiles	82
IV 7 Conclusion	83
GENERAL CONCLUSION.....	86
REFERENCES.....	87

List of tables

Table I. 1 Typical values of convection heat transfer coefficient.....	7
Table II. 1 Ranking for closure relations.....	24
Table II. 2 Values of model constants k - ε	27
Table III. 1 Cases for transport equation for fluid domain.....	40
Table IV.1 Noeuds and elements for different meshes.....	62
Table IV. 2 Average Nusselt number, and Reynolds number values for V from 0.5 to 3 m/s...71	
Table IV. 3 Average Nusselt number and Reynolds number for V from 0.5 to 3 m/s.....	78

List of figures

Figure I. 1 heat Transfer modes[3].....	1
Figure I. 2 conduction heat Transfer	2
Figure I. 3 One-dimensional heat transfer by conduction[3]	4
Figure I. 4 Radiation heat Transfer[4].....	4
Figure I. 5 convection heat transfer[4]	5
Figure I. 6 Heat transfer from a hot surface to air by convection[2].....	6
Figure I.7 convection heat transfer process .(a) forced convection .(b) naturel convection.(c) boiling[3]	7
Figure I. 8 Internal flow[6].....	9
Figure I. 9 External flow[7]	9
Figure I. 10 Cross flow heat exchanger.....	10
Figure I. 11 Types of cross flow heat exchanger	11
Figure I. 12 Heat exchanger	12
Figure I. 13 Thermal Management System in Li-ion Battery using Air Cooling	12
Figure I. 14 Schematic diagram of the single obstacle problem	13
Figure I. 15 Physical model illustration	14
Figure I. 16 Schematic of the physical model study	14
Figure I.17 Geometry of the problem. The horizontal channel contains two protruding heat sources, which simulate electronic components	15
Figure I. 18 Full mode of the radiator cooling system used in a transformer	16
Figure I. 19 A schematic diagram of the air-cooling BTMS.	16
Figure I. 20 geometric configuration and boundary conditions of the problem.....	17
Figure II. 1 The Free and Forced Convection Apparatus (TD1005).	20
Figure II. 2 The pinned surface.....	21
Figure II. 3 Potential flow around a cylinder.	22
Figure II. 4 Laminar, turbulent, and transitional flow.	23
Figure II. 5 Dimensions between cylinders $ST=28\text{mm}$. $SL=21\text{mm}$	34
Figure III. 1 Control volume in three dimensions	39
Figure III. 2 The discretization process	40
Figure III. 3 Face interpolation	44

Figure III. 4	Face interpolation UD scheme, (A) $F \geq 0$, (B) $F < 0$.	44
Figure III. 5	SIMPLEC Algorithm.	48
Figure III. 6	ANSYS Fluent interface	49
Figure III. 7	Fluid flow (fluent)	49
Figure III. 8	Design Modeler interface	50
Figure III. 9	Geometry part of TD1005	51
Figure III. 10	The computational model geometry	51
Figure III. 11	Different geometrical faces and volume entities, and mesh specifics.	52
Figure III. 12	The discretized domain.	53
Figure III. 13	Meshing of Pinned surface	53
Figure III. 14	The segregated Pressure-Based Algorithm.	54
Figure III. 15	Setting up physics.	54
Figure III. 16	Models selecting	55
Figure III. 17	Air properties.	55
Figure III. 18	Boundary conditions	56
Figure III. 19	Velocity inlet parameters.	56
Figure III. 20	Outlet.	56
Figure III. 21	Wall Pin Fin properties.	57
Figure III. 22	Solution Methods.	58
Figure III. 23	Scaled Residuals.	58
Figure IV. 1	Temperature profile for different Mesh in y direction.	62
Figure IV. 2	Velocity profiles for different meshes in y direction.	63
Figure IV. 3	xy plane and yz plane.	63
Figure IV. 4	(a) temperature volume rendering, (b) velocity volume rendering, $V=0.5$ m/s, $P=70$ watts.	64
Figure IV. 5	Temperature, velocity contours and streamlines $v=0.5$ m/s.	65
Figure IV. 6	Temperature, velocity contours and streamlines $v=1$ m/s.	66
Figure IV. 7	Temperature, velocity contours and streamlines $v=1.5$ m/s.	67
Figure IV. 8	Temperature, velocity contours and streamlines $v=2$ m/s.	67
Figure IV. 9	Temperature, velocity contours and streamlines $v=2.5$ m/s.	68
Figure IV. 10	Temperature, velocity contours and streamlines $v=3$ m/s.	69
Figure IV. 11	Temperature profiles for $P=50$ watts.	69

Figure IV. 12 Temperature profile in pins for P=50 watts.....	70
Figure IV. 13 Velocity profiles for P=50 watts.....	71
Figure IV. 14 Average Nusselt number VS velocity from 0.5 to 3 m/s.....	72
Figure IV. 15 Average Nusselt number Vs Reynolds number.....	72
Figure IV. 16 Temperature, velocity contours and streamlines v=0.5m/s.....	73
Figure IV. 17 Temperature, velocity contours and streamlines v=1 m/s.....	74
Figure IV. 18 Temperature, velocity contours and streamlines v=1.5m/s.....	74
Figure IV. 19 Temperature, velocity contours and streamlines v=2m/s.....	75
Figure IV. 20 Temperature, velocity contours and streamlines v=2.5m/s.....	76
Figure IV. 21 Temperature, velocity contours and streamlines v=3m/s.....	76
Figure IV. 22 Temperature profiles for P=70 watts, velocity from 0.5 to 3 m/s.....	77
Figure IV. 23 Temperature profile through Pins.....	77
Figure IV. 24 Velocity profile for P=70watts, velocity from 0.5 to 3m/s.....	78
Figure IV. 25 Average Nusselt number Vs velocity magnitude.	79
Figure IV. 26 Average Nusselt number Vs Reynolds number.....	79
Figure IV. 27 Temperature contours for v=1.5m/s.(a) P=50 W/m ² .(b) P=70 W/m ²	80
Figure IV. 28 Influence of power on air velocity.....	80
Figure IV. 29 influence of power on temperature.....	81
Figure IV.30 Turbulent kinetic energy contours, a)1m/s, b)2m/s, c)3m/s.....	81
Figure IV.31 Turbulent kinetic energy profile.....	82
Figure IV.32 Eddy viscosity, a)1m/s, b)2m/s, c)3m/s.....	82
Figure IV.33 Eddy viscosity profiles.....	83

Nomenclature

h	Convective heat transfer coefficient.	$(W.m^{-2} .K^{-1})$
k	Thermal conductivity.	$(W.m^{-1} .K^{-1})$
K	Thermal conductivity ratio.	
C_p	Specific heat at constant Pressure.	$(J.kg^{-1} .K^{-1})$
g	Gravitational acceleration.	$(m.s^{-2})$
\vec{g}	Gravity field.	
t	Time.	(s)
T	Temperature.	(K)
ΔT	Temperature difference.	(K)
T^*	Dimensionless temperature.	
t^*	Dimensionless time.	
u, v, w	Velocity components.	$(m. s^{-1})$
u^*, v^*, w^*	Dimensionless velocity components.	
\vec{V}	Velocity vector.	
V	Volume of control volume.	
w	Weight function.	
x, y, z	Cartesian coordinates.	(m)
x^*, y^*, z^*	Dimensionless Cartesian coordinates.	
ε	dimensionless turbulent dissipation rate.	
ε^*	turbulent dissipation rate.	
θ	dimensionless temperature.	
λ	thermal conductivity.	
ν	dimensionless kinematic viscosity.	

ν^* dimensionless kinematic viscosity

Greek Symbols

ρ	Density.	(kg.m ⁻³)
μ	Dynamic viscosity.	(kg.m ⁻¹ .s ⁻¹)
β	Thermal expansion coefficient.	(K ⁻¹)
Φ	Transported quantity.	
ν	Kinematic viscosity.	(m ² .s ⁻¹)
α	Thermal diffusivity.	(m ² .s ⁻¹)

Dimensionless numbers

Gr	Grashof number.
Nu	Nusselt number.
Pr	Prandtl number.
Re	Reynolds number.
Ri	Richardson number.

Abbreviations

2D	Two-dimensional
3D	Three-dimensional
CFD	Computational Fluid Dynamics.
RANS	Reynolds Average Navier Stokes
BEM	Boundary element method.
FDM	Finite difference method.
FEM	Finite element method.
FVM	Finite volume method.
PDE	Partial differential equation.

GENERAL INTRODUCTION

GENERAL INTRODUCTION

In the realm of thermal management and engineering, understanding the intricate interplay between fluid dynamics and heat transfer is of paramount importance. The cooling of hot cylindrical blocks, a common scenario in various industrial and scientific applications, presents a complex phenomenon wherein the airflow velocity plays a pivotal role. The numerical study of how air velocity influences the cooling process has emerged as a critical area of investigation, offering insights that not only enhance the efficiency of cooling strategies but also contribute to the optimization of energy utilization and system performance.

In industrial processes such as metal casting, electronics cooling, and aerospace propulsion, effective heat dissipation is essential to prevent thermal damage and ensure the durability of components.

The cooling process involves the transfer of heat from a high-temperature solid surface to the surrounding air through convection.

This convection process is highly influenced by the velocity of the air, as the movement of the fluid alters the heat transfer coefficient and affects the convective heat transfer rate.

In this study, we delve into the numerical analysis of how air velocity impacts the cooling of hot cylindrical blocks. By employing computational fluid dynamics (CFD) simulations and leveraging advanced numerical techniques, we aim to uncover the intricate relationships between fluid flow patterns, heat transfer coefficients, and temperature distributions.

in this thesis there are four chapters:

The first chapter, "Foundations and Literature Review," embarks on a journey through the fundamental principles of fluid mechanics.

In the second chapter, "Mathematical Formulations," the focus sharpens onto the mathematical underpinnings, as it delves into the equations governing the three-dimensional, incompressible fluid flow surrounding obstacles. the intricacies of flow patterns around obstacles, and the relevant corpus of research in the field.

Transitioning to the third chapter, "Finite Volume Method and CFD (Fluent)," the spotlight is cast on the finite volume method, with a dedicated exploration into the application of Computational Fluid Dynamics (CFD), particularly through the utilization of the Fluent software.

The culmination arrives with the fourth chapter, "Results Presentation and Discussion," where the spotlight shifts to the presentation and rigorous discussion of simulation results.

The objectives of this study are to:

- Investigate the effects of air velocity on the flow field around a hot cylindrical block.
- Study the effects of air velocity on the temperature distribution around a hot cylindrical block.
- Determine the optimum air velocity for cooling a hot cylindrical block

CHAPTER I
GENERAL INFORMATION AND LITERATURE REVIEW

I 1 Introduction

Convective heat transfer explores the mechanisms by which heat is transported through the movement of fluids. The term “convection” originates from the Latin verbs *convectore*-are and *convēho*-vēhēre, denoting the action of gathering or transporting to a central location. The advancement of convective heat transfer as a modern scientific discipline is driven by our imperative to comprehend and forecast how fluid flow functions as a medium for energy and substance transport.

Convective heat transfer emerges as an interdisciplinary domain, bringing together the realms of fluid mechanics and heat transfer. Its significance extends to numerous engineering applications, encompassing the cooling of electronic devices, temperature regulation in buildings, and diverse industrial processes. Moreover, it serves as a fundamental mechanism for heat transfer in nature, facilitating the transfer of solar heat to the Earth’s atmosphere and oceans, as well as the internal heat transfer within the Earth’s mantle and core.

I 2 Over view on heat transfer

Heat transfer involves the transmission of thermal energy between systems or bodies, driven by temperature differences. This scientific discipline aims to accurately predict the energy exchange that occurs when material objects exhibit varying temperatures. Heat transfer invariably occurs from regions of higher temperature to lower temperature until thermal equilibrium is achieved. The field of heat transfer not only seeks to explain the mechanisms behind heat energy transfer but also strives to provide predictive models for quantifying the rate of exchange under specific prescribed conditions.[1]

Heat can be transferred via three primary mechanisms: conduction, convection and radiation. All of these modes express the heat exchanges from regions of evaluated temperature to another with low temperatures.[2]

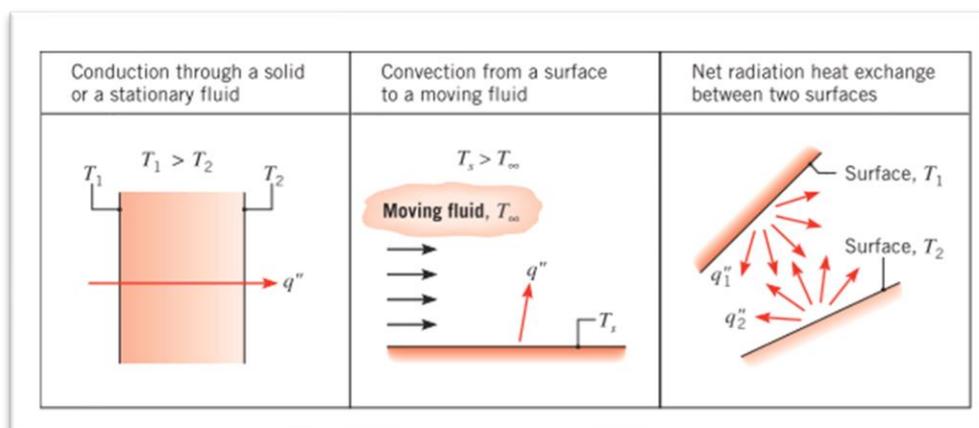


Figure I. 1 heat Transfer modes.[3]

I 3 Heat transfer modes

There are three modes of heat transfer which we will present a brief explanation about each of them in the following.

I 3 1 Conduction heat transfer

Conduction heat transfer is the process by which heat is transmitted through a material or between objects that are in direct contact. It occurs as a result of atomic or molecular collisions within the material, with higher- energy particles.

In this way, heat flows from regions with evaluated temperature to lower one. Conductors like metals, are excellent at conducting heat, while insulators, such as wood or plastic, have low conductivity and resist heat transfer, making them useful for insulation purposes.

The rate at which heat conduction occurs within a medium is influenced by several factors, including the medium's geometry, thickness, and material properties, as well as the temperature difference across the medium.[2]

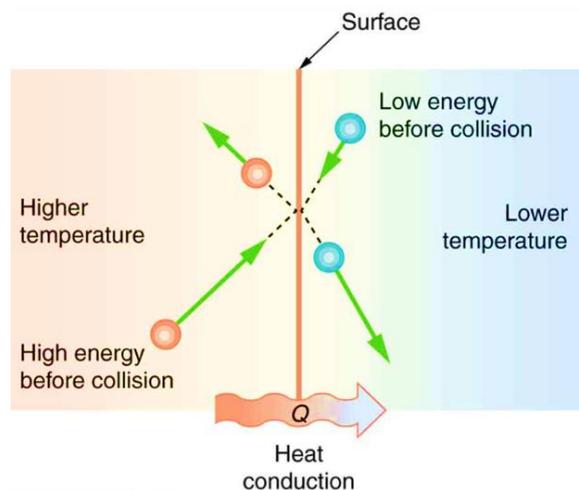


Figure I. 2 conduction heat Transfer.

I 3 1 1 Thermal conductivity

Thermal conductivity is a property of materials that determines their ability to conduct heat. It quantifies how effectively a substance can transfer heat when there is a temperature difference across it. Materials with high thermal conductivity, like metals, are efficient at conducting heat, while those with low thermal conductivity, like insulators, resist the flow heat.[2]

I 3 1 2 Thermal diffusivity

Thermal diffusivity is material property that characterizes how quickly materials responds to changes in temperature. It is defined as the ratio of a material's thermal conductivity to its heat capacity per unit volume. This property is important in various fields, including heat transfer analysis and the design of materials for specific thermal applications.[2]

The rate equation Fourier's law, for conduction can be write as follow:

$$q_x'' = -k \frac{dT}{dx} \quad \text{I. 1}$$

Such as :

q_x'' : is the heat transfer rate in the x-direction per unit area (W/m^2)

k : is the thermal conductivity ($W/m K$) and is a characteristic of the wall material .

The minus sign indicates that heat transfer occurs in the reverse direction of the temperature gradient .

under the steady-state conditions ,when the temperature gradient is linear , the temperature gradient may be expressed as :

$$\frac{dT}{dx} = \frac{T_2 - T_1}{L} \quad \text{I. 2}$$

And the heat flux :

$$q_x'' = -k \frac{T_2 - T_1}{L} \quad \text{I. 3}$$

Or :

$$q_x'' = k \frac{T_1 - T_2}{L} = k \frac{\Delta T}{L} \quad \text{I. 4}$$

This equation gives the heat flux, the rate of heat transfer per unit area. The rate of heat conduction, q_x'' (W), through a planar wall is the product of flux and area, $q_x = q_x'' \cdot A$. [3]

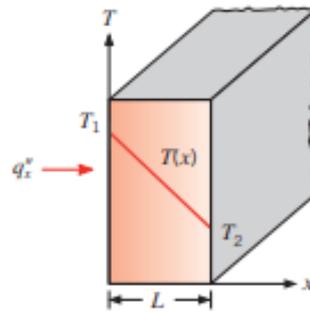


Figure I. 3 One-dimensional heat transfer by conduction.[3]

I 3 2 Radiation heat transfer

Radiation refers to the release of energy in the form of electromagnetic waves or photons when there are changes in the electronic configurations of the atoms or molecules. Unlike conduction and convection, radiation can transfer heat without the need for an intervening medium. In fact, radiation is the fastest method of heat transfer, propagating at the speed of light, and it experiences no attenuation even in a vacuum. This is how the energy from the sun reaches the Earth.

In the context of heat transfer studies, we focus on thermal radiation, which is emitted by objects due to their temperature. It differs from other forms of electromagnetic radiation, such as x-rays, gamma rays, microwaves, radio waves, and television waves, which are not directly related to temperature. All objects above absolute zero temperature emit thermal radiation.

For materials that opaque to thermal radiation, such as metals, wood, and rocks, radiation is typically considered a surface phenomenon. This is because the radiation emitted from the interior regions of such materials cannot reach the surface. Incident radiation in these bodies is usually absorbed within a few microns from the surface. [2]

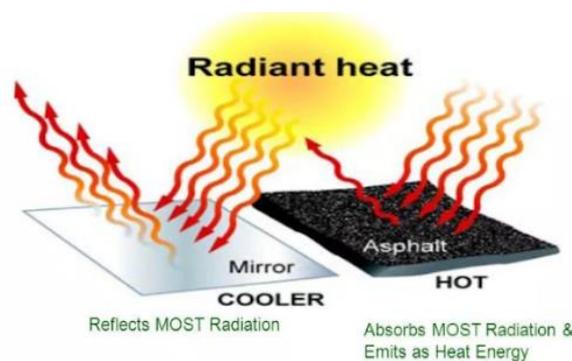


Figure I. 4 Radiation heat Transfer.[4]

I 3 3 Convection heat transfer

Convection is a mechanism through which energy is transferred between a solid surface and the surrounding fluid, whether it is a liquid or gas in motion. It arises from the combined influences of conduction and fluid movement. The intensity of convection heat transfer increases with higher fluid velocities. In situations where there is no significant fluid motion, heat transfer between the solid surface and the adjacent fluid occurs solely through conduction. However, when bulk fluid motion is present, it enhances the heat transfer between the solid surface and the fluid. Nonetheless, the determination of heat transfer rates becomes more complex due to the involvement of fluid motion.

The movement of molecules in convection often can be seen with the human eye .hence ,it is a macroscopic phenomena .

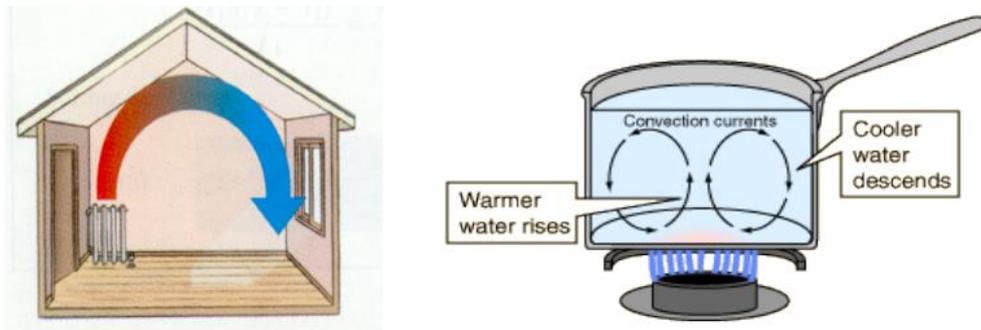


Figure I. 5 convection heat transfer.[4]

When a hot block is cooled by blowing cool air over its top surface, the heat transfer process involves two main mechanisms. Initially, heat is conducted from the block to the adjacent layer of air in direct contact with the surface. Subsequently, the heat is carried away from the surface through convection, which encompasses both conduction within the air caused by the random movement of air molecules and the bulk motion of the air that removes the heated air near the surface, replacing it with cooler air. [1]

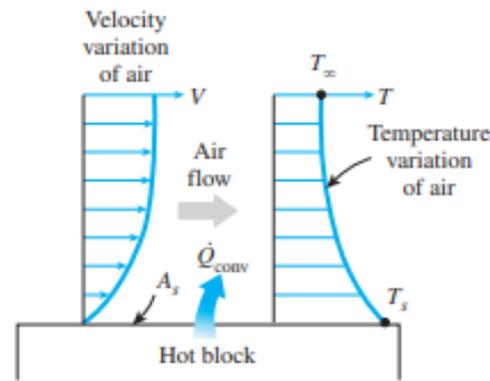


Figure I. 6 Heat transfer from a hot surface to air by convection.[2]

I 3 3 1 Naturel or free convection

If fluid motion is generated by buoyancy forces resulting from density variations caused by temperature differences within the fluid, it is referred to as free or natural convection. In this type of convection, the overall movement of the fluid is driven by body forces that depend on fluid density, which itself is influenced by temperature and or the concentration of substances present in the fluid. Free convection is a common natural phenomenon and finds numerous applications in various industries. It plays a significant role in the circulation patterns of the atmosphere and oceans, and it is increasingly utilized in passive emergency cooling systems for advanced nuclear reactors.[5]

I 3 3 2 Forced convection

Forced convection involves the deliberate circulation of a fluid, such as gas or liquid, over a surface or through a channel by external means, typically using mechanical devices like fans or pumps. This forced flow accelerate the heat transfer process in contrast to natural convection. It finds widespread use in engineering applications such as cool.[2]

I 3 3 3 Mixed convection

Mixed convection refers to the simultaneous presence of both natural convection and forced convection in a fluid. This occurs when a fluid is influenced by both buoyancy-driven flow and externally induced flow, such as when a fan is used to either assist or oppose the buoyancy flow. Mixed convection is commonly observed in various engineering applications, including heat exchangers, electronic cooling, and chemical reactors. It is a phenomenon that combines the effects of both natural and forced convection, contributing to heat transfer and fluid dynamics in these systems.

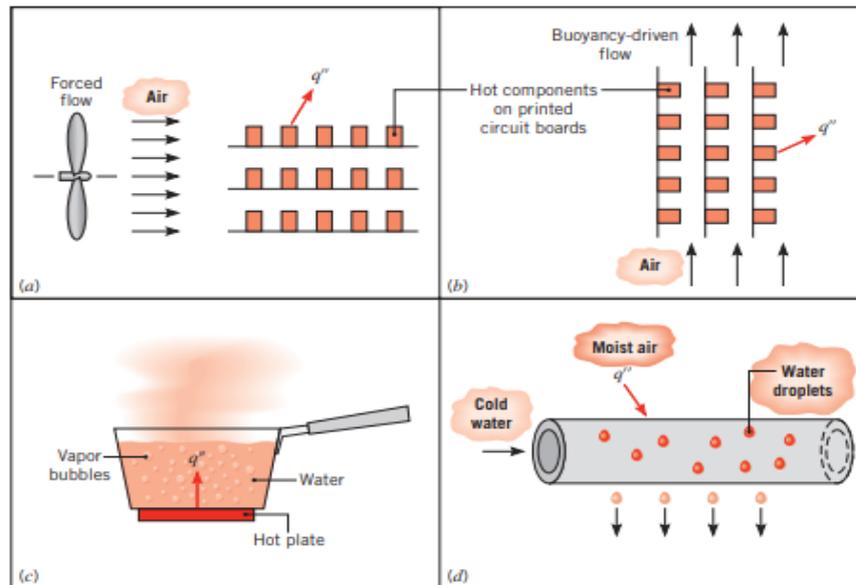


Figure I. 7 convection heat transfer process .(a) forced convection .(b) naturel convection.(c) boiling[3] .

The rate of heat transfer in convection, regardless of its nature, is directly related to the temperature difference. This fundamental principle is described by Newton's law of cooling :

$$\dot{Q}_{conv} = hA_s(T_s - T_{\infty}) \quad \mathbf{I. 5}$$

Such as :

h: convection heat transfer coefficient in $W/m^2 \cdot K$

A_s: the surface area through which convection heat transfer takes place in m^2

T_s: the surface temperature in K

T_∞:is the temperature of the fluid sufficiently far from the surface in K

The convection heat transfer coefficient, denoted as *h*, is not an inherent property of the fluid. Instead, it is a parameter determined through experimentation. Its value is influenced by various factors, including the surface geometry, fluid motion characteristic, fluid properties, and bulk fluid velocity. The table below illustrating the convection heat transfer coefficient types:

Table I. 1 Typical values of convection heat transfer coefficient.[2]

Type of convection	$h, W/m^2 \cdot K *$
Free convection of gases	2-25
Free convection of liquids	10-1000
Forced convection of gases	25-250
Forced convection of liquids	50-20,000
Boiling and condensation	2500-100,000

I 4 Mixed convection in cooling obstacles

In the cooling of hot cylindrical blocks, mixed convection can occur when a fluid (such as air or water) flows over the surface of the cylinder, and natural convection currents are also induced within the fluid due to temperature gradients near the cylinder surface.

The heat transfer coefficient for mixed convection is generally higher than that for forced convection alone, but lower than that for natural convection alone.

In cooling obstacles, mixed convection can have a significant impact on the cooling performance and efficiency. The presence of the obstacle can create regions of high and low velocity flow, which in turn can affect the heat transfer rate in different part of the domain. In addition, the buoyancy forces due to temperature differences can create convective currents that further affect the flow and heat transfer patterns.

Numerical methods such as finite volume methods or finite element method can be used to model mixed convection in cooling obstacles. These methods involve discretizing the domain into a set of cells or elements and constructing a system of equations that describe the heat transfer and fluid flow at each point in the domain.

I 5 Internal and external flows

There are two types of flows in convection :internal flows and external flows.

Internal flows occurs when the fluid is flowing inside a tube or a channel. In this case, the heat transfer occurs between the wall of the tube or channel and the fluid flowing inside it. The heat

transfer coefficient depends on the flow conditions, such as the velocity, the temperature difference between the fluid and the wall, and the viscosity of the fluid. Internal flows are commonly used in engineering applications, such as in heat exchangers, where a hot fluid is used to heat a cooler fluid.

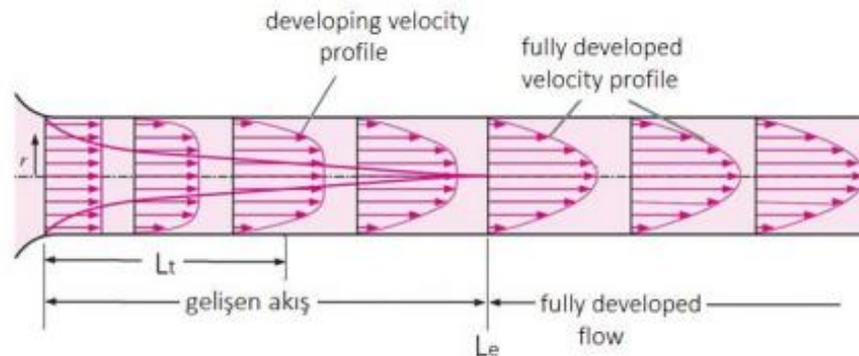


Figure I. 8 Internal flow.[6]

External flow occur when the fluid flows over a solid surface, such as in the case of a fluid flowing over a plate. In this case, the heat transfer occurs between the fluid and the solid surface. The heat transfer coefficient in external flows is influenced by velocity of the fluid, the temperature difference between the fluid and the surface, and the physical properties of the fluid, such as its viscosity and thermal conductivity. External flows are commonly used in engineering applications, such as in the cooling of electronic components or in the design of aerodynamic surfaces.

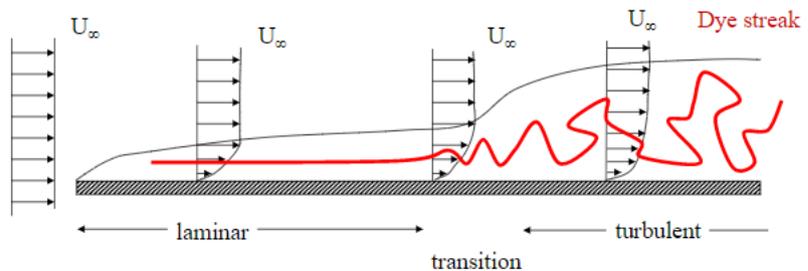
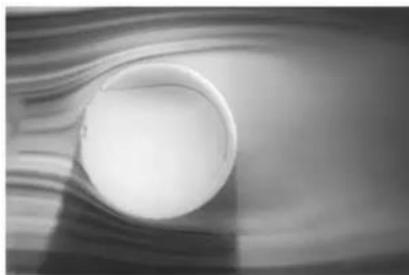


Figure I. 9 External flow.[7]

In both internal and external flows, the heat transfer coefficient can be increased by increasing the flow velocity, increasing the temperature difference between the fluid and the solid surface, and by using materials with higher thermal conductivity.[5]

I 6 Heat exchangers

A heat exchanger is a device designed to facilitate the transfer of thermal energy (enthalpy) between multiple fluids, between a solid surface and a fluid, or between solid particles and a fluid. This transfer occurs when the fluids or surfaces are at different temperatures and in thermal contact.

Heat exchangers operate without any external heat or work interactions. They find common use in applications that involve the heating or cooling of fluid streams.[8]

I 6 1 Cross flow heat exchanger

A cross flow heat exchanger is a type of heat exchanger in which the flow of two fluid occurs perpendicular (at a right angle) to each other. It is designed to transfer thermal energy between these fluids without mixing them. Typically, it consists of thin metal plates or tubes through which the fluid flow, allowing for efficient heat transfer. In a cross-flow heat exchanger, one fluid flows across the surface of the other fluid, facilitating the exchange of heat energy between the two streams. This type of heat exchanger is commonly used in applications such as air handling units(AHUs), cooling systems, and ventilation systems, where the heat needs to be transferred between two airflows while preventing moisture transfer and air flow short circuiting.

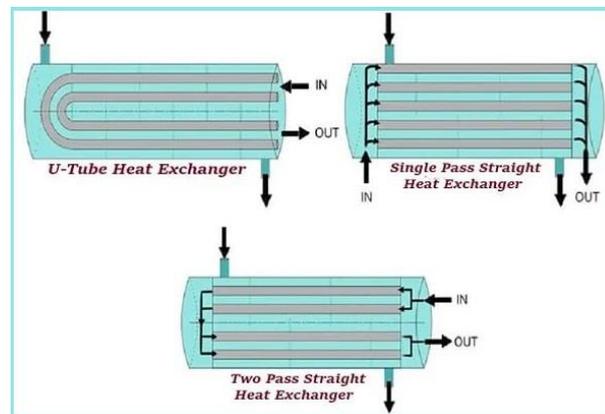


Figure I. 10 Cross flow heat exchanger.

Moisture in the air can freeze and create ice in certain types of heat exchangers. Cross-flow heat exchangers are typically more economical than other alternatives. They are commonly employed in situations where stringent hygiene standards require complete separation of airflow streams. These heat exchangers find extensive use in industries such as large-scale water bottling, hospitals, and heat recovery systems in the food industry. In contrast to rotary heat exchangers, cross-flow heat exchangers do not transfer moisture.[8]

I 6 1 1 Types of cross flow heat exchangers

Cross-flow heat exchangers find wide application in various industries. Based on the fins employed in the system, they can be categorized into mixed and unmixed cross-flow heat exchangers. Another way to refer to these types is as pinned and unpinned cross-flow heat exchangers. These designations are used to differentiate the presence or absence of fins in the heat exchanger system.

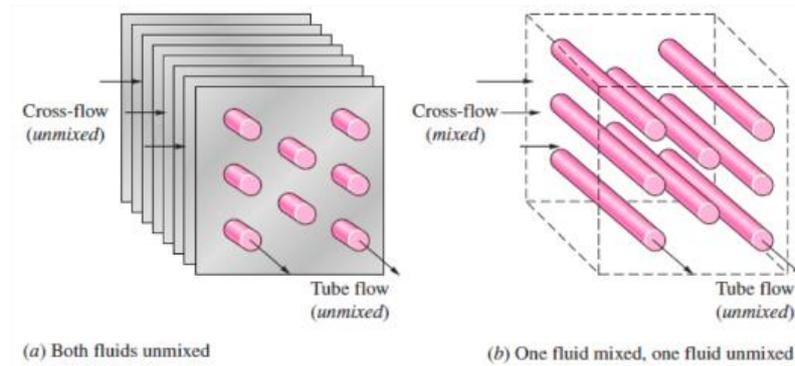


Figure I. 11 Types of cross flow heat exchanger.

➤ **Mixed cross flow heat exchanger**

In this particular type of heat exchanger, the fluid flows over the pipes in the shell side, with the flow direction perpendicular to the pipes. Unlike the other type, this heat exchanger does not incorporate any fins. Turbulent flow can occur in this configuration, which results in a higher heat transfer rate. Additionally, compared to the other type, the pressure drop is relatively lower in cross-flow heat exchangers without fins.

➤ **Unmixed cross flow heat exchanger**

In unmixed cross-flow heat exchangers, fins are added around the pipes or separate channels are used for the flow to pass over the pipes. The inclusion of fins increase the heat transfer by enlarging the effective surface area for heat transfer. However, this design choice also leads to a higher pressure drop in the system. Additionally, the weight and cost of these types of heat exchangers increase due to the addition of fins.

Uniform flow refers to a flow condition in which the velocity is constant at any given instant and at every point in the fluid, in an ideal scenario. However, in real fluid flow, the velocity varies across the section. When the size and shape of the cross-section remain constant along the length of the channel being considered, the flow is described as uniform.[9]

I 7 Examples of hot cylindrical blocks

➤ **Heat exchangers**

Heat exchangers are commonly used in mechanical engineering applications, such as HVAC systems, power plants, and refrigeration systems. These devices transfer heat between two fluids

without mixing them. Hot cylindrical blocks can be found within heat exchangers as part of the heat transfer surface, facilitating the exchange of heat between fluids.

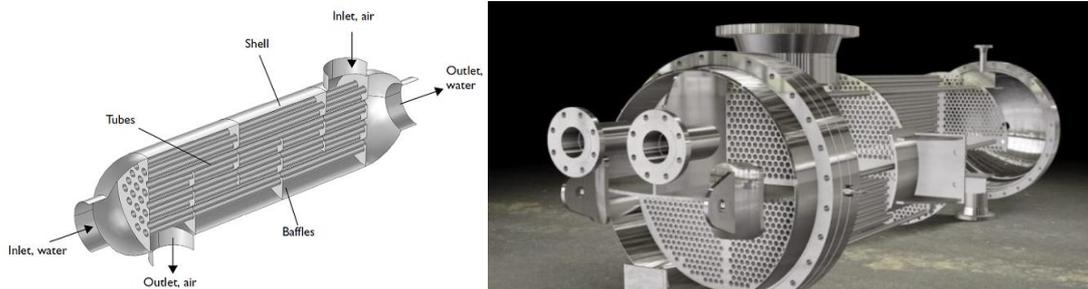


Figure I. 12 Heat exchanger.

➤ Thermal Management of Electronics

Mechanical engineers are involved in designing cooling solutions for electronic devices to prevent overheating. Cylindrical heat sinks, made of materials like aluminum or copper, are commonly used to absorb and dissipate heat generated by electronic components such as microprocessors, power transistors, or LEDs.

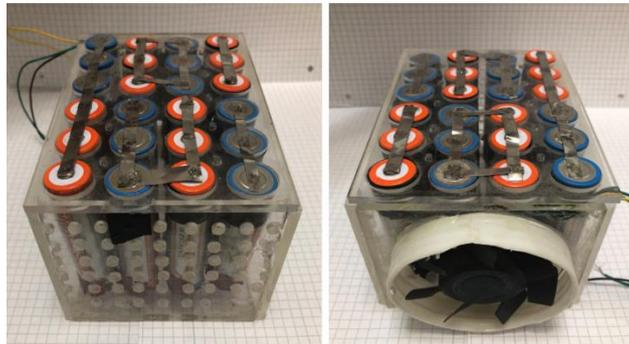


Figure I. 13 Thermal Management System in Li-ion Battery using Air Cooling.

I 8 Literature review

Cooling obstacles pose significant challenges in thermal management and energy efficiency, particularly as technology advances and the need for high-performance systems grows. These obstacles encompass issues such as limited heat dissipation, thermal resistance, system complexity, and excessive energy consumption. Addressing and understanding these obstacles are critical for developing efficient and sustainable cooling solutions.

This literature review explores the current state of research on cooling obstacles, aiming to identify their underlying causes, evaluate proposed solutions, and highlight future research directions. It

provides insights into the factors contributing to these challenges and examines innovative approaches employed by researchers.

I 8 1 Obstacles 2D

TJ. Youllg and K. Vafai.(1998) [10] performed an extensive study on forced convective cooling of a heated obstacle positioned on a channel wall. The researchers employed the Navier-Stokes equations to examine the flow pattern surrounding the obstacle and concentrated on analyzing the distribution of local Nusselt numbers and mean Nusselt numbers for each exposed surface of the obstacle. Through systematic variation of parameters including obstacle dimensions, thermal conductivity ratio, flow rate, and heating method, the study yielded important findings with both fundamental and practical implications. The investigation demonstrated the substantial impact of obstacle size, shape, and thermal conductivity on the flow behavior and heat transfer characteristic.

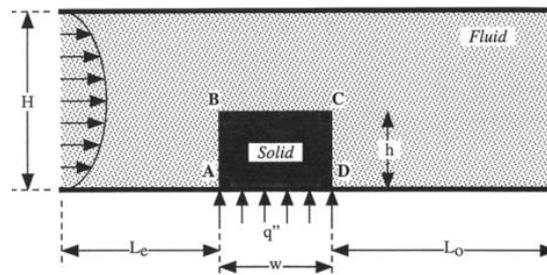


Figure I. 14 Schematic diagram of the single obstacle problem.

Shaswar Omar Osman A-O and Omar Ali (2022) [11] Numerically investigated the mixed convection phenomenon in vented square enclosure containing two horizontally aligned circular cylinders, with one heated and the other cold. The simulation utilized the Navier-Stokes and energy equations to model the heat and fluid flow behavior. The study considered various parameters such as the distance between cylinders ($0.3 \leq S \leq 0.45$), size of the vent opening ($0.125 \leq O \leq 1$), Reynolds number ($50 \leq Re \leq 400$), and Richardson number ($0.1 \leq Ri \leq 10$), while maintaining a constant Prandtl number ($Pr = 0.7$). The results presented average and local Nusselt number (Nu), streamlines, and isotherms for key factors. According to the numerical data, the average Nusselt number from the heated cylinders increased with higher values of Ri , Re , and vent opening. Additionally, increasing the spacing size ($S=0.375$) improved the average Nusselt number.

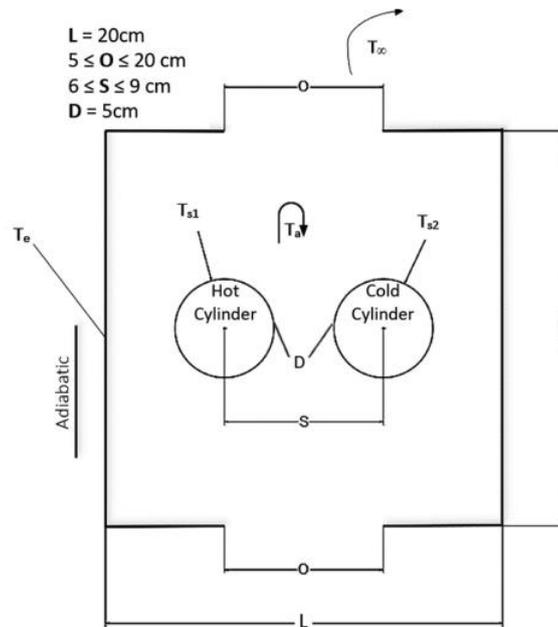


Figure I. 15 Physical model illustration.

Ait Hssain and Al.(2020) [12] conducted a numerical study on the cooling of heat sources with constant temperature in a horizontal channel using mixed convection of nanofluids. The findings indicated that the thermal exchange rate increased as the volume fraction of nanoparticles and Reynolds number were raised. However, the separation distance between heated sources was observed to have a negative impact on heat exchange. Moreover, the study demonstrated a significant 20% enhancement in heat exchange when the volume fraction of Cu nanoparticles reached 10%.

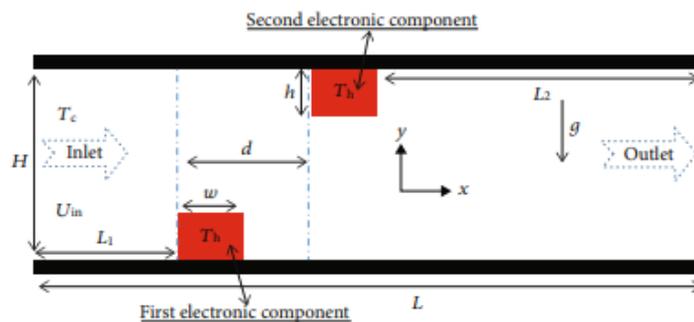


Figure I. 16 Schematic of the physical model study.

A. Hamouche, R. Bessaïh (2009) [13] performed a numerical investigation on laminar mixed-convection heat transfer to air from two identical protruding heat sources within a two-dimensional horizontal channel, simulating electronic components. The conservation equations of mass, momentum, and energy for mixed convection were solved using the finite volume method and the SIMPLER algorithm. The findings revealed a significant enhancement in heat transfer within a range of Reynolds numbers(Re) from 5 to 30 and a Prandtl number (Pr) of 0.71. Furthermore, increasing

the separation distance, height, and width of the components positively influenced heat transfer inside the channel.

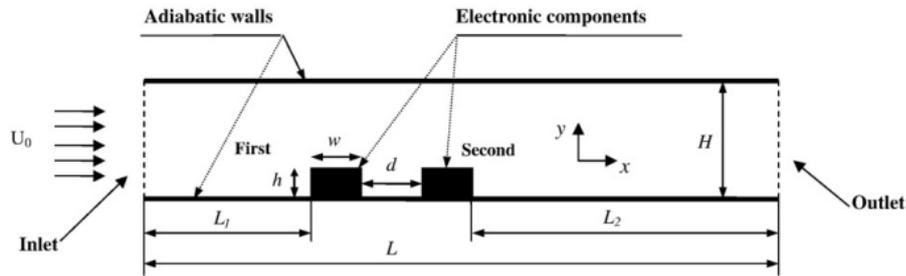


Figure I. 17 Geometry of the problem. The horizontal channel contains two protruding heat sources, which simulate electronic components.

I 8 2 Obstacles 3D

YJ. Kim et al. (2018) [14] investigated the cooling performance by analyzing the conjugate heat transfer and fluid flow of radiator used in power transformer. The flow and temperature distributions around the radiators were analyzed to inspect the fundamental mechanisms of radiator cooling in the hybrid cooling system. The oil flow rate in the radiators was varied in the range of 44.4 LPM ~ 309.6 LPM. Additionally, the position of the cooling fan was altered along the bottom and right surfaces of the radiators, and the impacts on cooling efficiency were assessed. When computational results using the common $k-\epsilon$ turbulence model were compared to measured data, it was found that there was good agreement with a difference of less than 5%. Due to the beneficial interaction between the vertical and horizontal air flows induced by cooling fans, the cooling performance of the cooling fans situated at the center of the bottom surface and the bottom of the right surface was the best regardless of the insulating oil flow rate, providing about 22% higher cooling performance than the worst cooling performance at all flow rates.

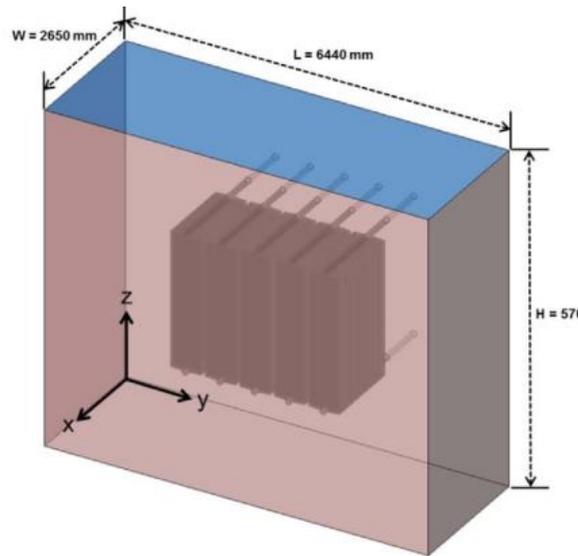


Figure I. 18 Full mode of the radiator cooling system used in a transformer.

G.Zhao et al. (2021) [15] Researched air-cooling battery thermal management systems (BTMS) for electric and hybrid electric vehicles. They identified that improving cooling channel design and incorporating advanced materials and technologies are popular methods for optimizing performance. They proposed design innovations in core structures and coupled cooling systems to overcome cooling limitations, and suggested novel inlet air pre-processing methods for cooling battery cells in hot weather conditions. They conducted that air-cooling BTMSs show promise in efficiently cooling high-energy-density battery systems in EVs and HEVs.

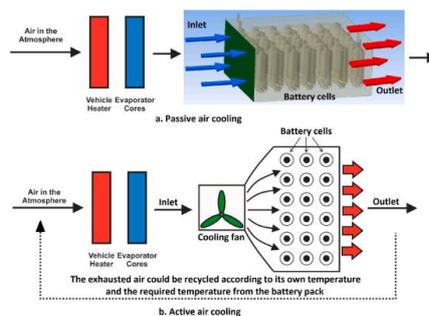


Figure I. 19 A schematic diagram of the air-cooling BTMS.

Abdelwafi Bouras et al.(2018) [16] Presented a study where they conducted a numerical simulation of forced convection in a cubic cavity with two cylindrical heat sources placed in the center. The cavity received an incoming air flow from the left side (center) and an outgoing flow from the right side, with both opening doors having dimensions of 0.1 H. the cavity walls were kept adiabatic. Using the FLUENT software, they solved the conservation equations that govern forced convection flow. They compared their numerical results with existing literature and found a satisfactory agreement. They also analyzed the impact of cavity size (Rayleigh number) and air

ventilation velocity (Reynolds number) on the flow. The results clearly demonstrated a significant correlation between the geometric conditions and the dynamic and thermal characteristics of the forced convection flow.

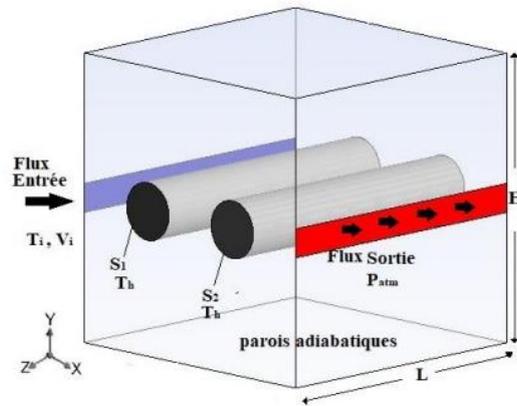


Figure I. 20 geometric configuration and boundary conditions of the problem.

I 9 Conclusion

this chapter provided a comprehensive introduction to the topic of cooling hot cylindrical blocks. It discussed the importance of heat transfer modes, particularly convective heat transfer, in the cooling process. Also it included a literature review that examined previous researches and studies related to our thesis.

CHAPTER II
MATHEMATICAL FORMULATION

II 1 Introduction

Fluid mechanics and heat transfer deal with the behavior and transfer of energy in fluids. They are important in engineering applications and involve complex partial differential equations that are challenging to solve analytically. Numerical methods are often used to obtain approximate solutions, which depend on the quality of the numerical methods used.

In the current chapter we are going to present the main conservation equations for the convective heat exchanges, for this will express the general conservation equations of continuity, momentum, and energy to understand the phenomena.

II 2 Free and Forced Convection Experiment(TD1005)

In the current study, we used the free and forced convection apparatus in order to understand the cooling process.

II 2 1 Description

The benchtop equipment includes a vertical duct that holds the chosen heat transfer surface and all instruments needed.

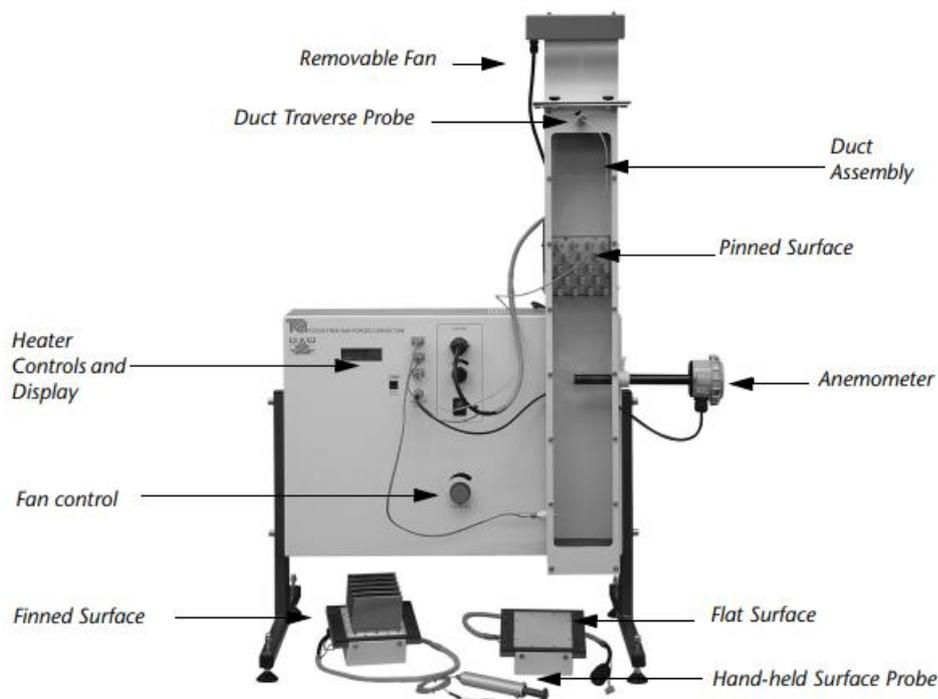


Figure II. 1 The Free and Forced Convection Apparatus (TD1005).

TecEquipment includes three different common heat transfer surfaces with the equipment:

- A flat plate .
- A pinned surface similar to a tubular heat exchanger
- A finned surface similar to the fins on air-cooled engines or electrical heat sinks

Each surface has its own built-in variable-power electric heater, in our study we use the pinned surface .

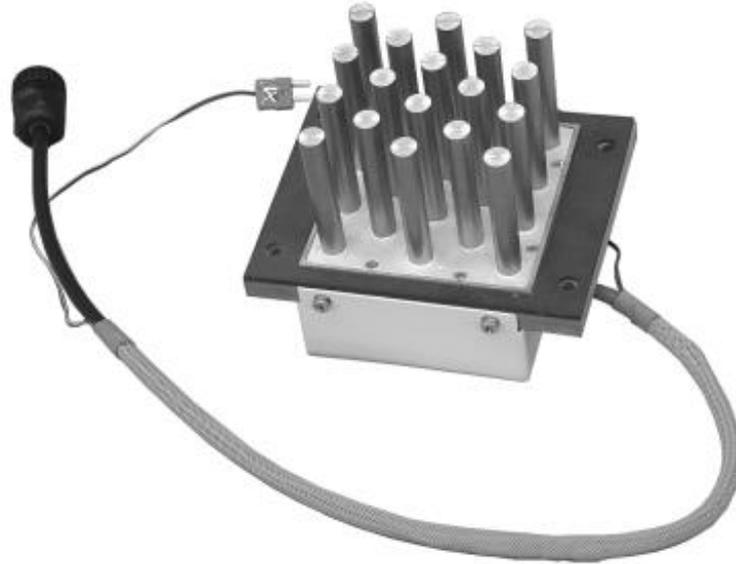


Figure II. 2 The Pinned Surface.

II 2 2 Objectives

- To find the surface temperature.
- To compare the surface temperature of the heat transfer surfaces in force and free convections for fixed input power[17]

II 3 Fluid kinematics

Fluid kinematics is a fundamental aspect of fluid mechanics that is concerned with the motion of fluids without considering the forces that cause the motion. It is a general concept that can be applied to all types of fluids, including gases and liquids, and is essential in understanding the behavior of fluids in various engineering applications.

The study of fluid kinematics involves the analysis of fluid motion in terms of its geometric and temporal characteristics, such as velocity, acceleration, and deformation. This analysis is typically done using mathematical equations, including the continuity equation and the Navier-Stokes

equations, as well as experimental techniques, such as flow visualization and particle image velocimetry.

Fluid kinematics is an essential component of fluid dynamics, which is the study of the forces that cause fluid motion. By understanding the kinematics of fluids, engineers can design and optimize fluid systems for various applications, including energy generation, chemical processing, and environment modeling. [18]

Overall, fluid kinematics is a general concept that is critical to understanding the behavior of fluids in many engineering applications. It is a foundational aspect of fluid mechanics that provides insight into fluid motion and can lead to the design and optimization of more efficient and effective fluid systems.[19]

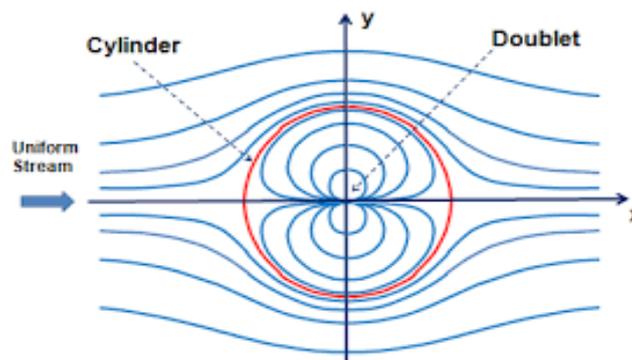


Figure II. 3 Potential flow around a cylinder.

II 4 Different flow regimes

In fluid dynamics, flow regimes refer to the patterns and behaviors of fluids as they move through different types of flow. The different flow regimes are characterized by different properties, such as flow velocity, viscosity, and Reynolds number. Some of the common flow regimes are:

II 4 1 laminar flow

Laminar flow is characterized by smooth, orderly movement of fluid particles in a parallel manner. The fluid particles move in layers or sheets, without mixing or crossing each other's paths. This type of flow is typically observed in low-speed or low Reynolds number flows, where the fluid viscosity dominates over its inertia.[7]

II 4 2 Turbulent flow

Turbulent flow is characterized by chaotic and random movement of fluid particles, with fluctuations and eddies occurring at different scales. The flow is highly irregular, with vortices and

turbulent structures causing mixing and diffusion of fluid particles. Turbulent flow typically occurs at high speeds or high Reynolds number flows, where the inertia of the fluid dominates over its viscosity.[20]

II 4 3 Transitional flow

Transitional flow is a mixture of laminar and turbulent flow, occurring in the range between the laminar and turbulent flow regimes. It is characterized by fluctuations and irregularities in the flow patterns, but with a general tendency towards laminar flow.

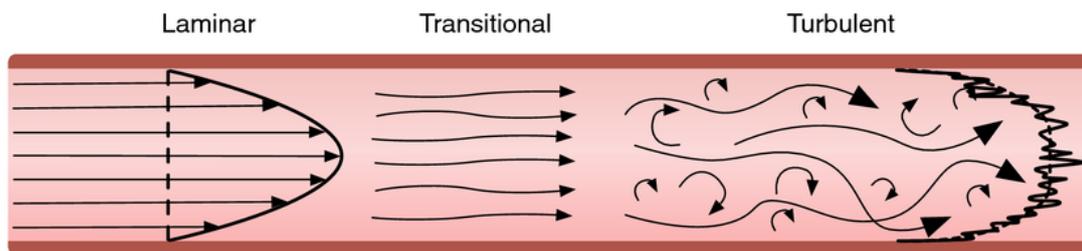


Figure II. 4 Laminar, turbulent and transitional flows.

In general, the type of flow that occurs depends on the fluid properties, the geometry of the flow, and the flow conditions such as velocity, pressure, and temperature. The type of flow can have a significant impact on the transport of heat, mass, and momentum in fluids, and is important in many engineering and natural phenomena.[2]

II 5 Turbulence

Turbulence is a state of fluid flow characterized by irregular and chaotic motion. It is a complex phenomenon that occurs when a fluid, such as air or water, flows in a non-uniform way, with the different parts of the fluid moving at different speeds and in different directions. Turbulence can be observed in a wide range of natural and human-made systems, including the atmosphere, oceans, rivers, pipes, and even in the wake of a moving vehicle.

Turbulence is often described in terms of its intensity or level of turbulence. This can be quantified using various measures, such as the Reynolds number, which is a dimensionless parameter that relates the velocity of the fluid to its viscosity and length scale. Turbulence can have both beneficial and harmful effects, depending on the context. For example, turbulence in a river can help to transport nutrients and oxygen to aquatic organisms, while turbulence in an aircraft can cause discomfort to passengers and increase fuel consumption.[21]

II 6 Turbulence models

Turbulence models are mathematical representations used to approximate the behavior of turbulent flows. They simplify the complexities of turbulence by making assumptions and solving equations for statistical quantities instead of resolving all turbulent structures.

Turbulence models are essential for simulating and predicting turbulent flows in various engineering applications. There are a lot of types of turbulent model, we will present some of them in the following:[22]

II 7 RANS (Reynolds-Averaged Navier-Stokes equations)

Also known as statistical methods, **RANS** models represent the most widespread approach for solving the Navier-Stokes equations. They directly involve averaging the Navier-Stokes equations by redefining variables as the sum of two values: a mean value and a fluctuating value. Thus, for any arbitrary variable (such as pressure , velocity , etc.), it can be written as [10]:

$$\phi_i(x, t) = \bar{\phi}_i(\bar{x}, t) + \phi_i'(\bar{x}, t) \quad \text{II. 1}$$

Where

$\bar{\phi}_i$ represent the mean values of pressure and velocity

ϕ_i' represent the fluctuations of these variables.

For closure of the problem, the calculation of Reynolds stresses can be approached in several ways. The oldest approach involves calculating the terms of Reynolds stresses by utilizing the concept of turbulent viscosity. This concept, represented by the Boussinesq hypothesis, allows expressing the Reynolds stresses in terms of gradients of the mean velocity of the flow.

Table II. 1 Ranking for closure relations.

closure relations	Characteristic
Algebraic Eddy viscosity or zero-equation model.	This model uses an algebraic relationship for the calculation of Reynolds stresses.

One-equation models Spalart-Allmaras	They use a partial differential equation for a scale of turbulent fluctuation velocity. Turbulent kinetic energy. Turbulent viscosity.
Two-equation models k- ϵ , k- ω , k-l, k-t, q-w	They use two partial differential equations: one for the turbulent length scale and the other for the scale of turbulent fluctuation velocity.
Reynolds stress models	They use multiple partial differential equations (typically seven) for all the components of the Reynolds stresses.

II 7 1 zero-equation model (Algebraic Eddy viscosity)

The zero equation model is a type of turbulence model used in CFD and fluid mechanics. Unlike more complex turbulence models that involve solving partial differential equations, it provides a simplified approach to estimate turbulent properties, specifically the eddy viscosity, directly from algebraic relationships without the need for additional transport equations. [5]

$$v_t = l_m^2 \left| \frac{\delta u}{\delta y} \right| \quad \text{II. 2}$$

where

l_m is the mixing length,

$\left| \frac{\delta u}{\delta y} \right|$ is the partial derivative of the velocity along the stream (x-direction).

The advantages of this model is that it is the computational efficiency of turbulence. This enables faster simulation.

II 7 2 One-equation models (Spalart-Allmaras)

This model has the advantage of being relatively simple and accounting for the history of turbulence. However, the choice of length scale is empirical, and extending it to three-dimensional cases is challenging. The main difference lies in the fact that the SST model uses the k-omega model in the near-wall region and the k-epsilon model in the far-field regions with high Reynolds numbers.

There is a modification in the formulation of the turbulent viscosity term to properly account for the transport effects of turbulent shear stress.[23]

In this model, the turbulent dynamic viscosity is calculated using the following relationship:

$$\mu_t = \rho \tilde{\nu} f_v \quad \text{II. 3}$$

f_v : is a damping function.

II 7 3 Two-equation models

A two-equation model refers to a type of turbulence model that utilizes two additional transport equations to capture the behavior of turbulence in a fluid flow. These equations are typically derived from the Reynolds-averaged Navier-Stokes (**RANS**) equations. The most commonly used two-equation models include:[24]

II 7 3 1 k-ε Model (Standard)

The standard k-ε turbulence model is a two equation model that aims to simulate turbulent flow more accurately than simpler models.in this model two partial differential equations are solved to calculate the evolution of turbulent kinetic energy and turbulent dissipation rate throughout a fluid domain. These equations account for the production, diffusion, and dissipation of turbulence. It is particularly effective for simulating a wide range of turbulent flows, from boundary layers to complex swirling flows in engineering application. We can observe this turbulence model in its entirety in the equations below: [14]

➤ Transport equations for standard k-epsilon model :

- For turbulent kinetic energy k :

$$\frac{\partial}{\partial t}(\rho k) + \frac{\partial}{\partial x_i}(\rho k u_i) = \frac{\partial}{\partial x_j} \left[\left(\mu + \frac{\mu t}{\rho k} \right) \frac{\partial k}{\partial x_j} \right] + P_K + P_b - \rho \varepsilon - Y_M + S_K \quad \text{II. 4}$$

- For dissipation ε :

$$\frac{\partial}{\partial t}(\rho \varepsilon) + \frac{\partial}{\partial x_i}(\rho \varepsilon u_i) = \frac{\partial}{\partial x_j} \left[\left(\mu + \frac{\mu t}{\rho \varepsilon} \right) \frac{\partial \varepsilon}{\partial x_j} \right] + C_{1\varepsilon} \frac{\varepsilon}{k} (P_K + C_{3\varepsilon} P_b) - C_{2\varepsilon} \rho \frac{\varepsilon^2}{k} + S_\varepsilon \quad \text{II. 5}$$

➤ turbulent viscosity in modelled as :

$$\mu_t = \rho C_\mu \frac{k^2}{\varepsilon} \quad \text{II. 6}$$

with C_μ is an empirical constant.

➤ **Model constants**

Table II. 2 Values of model constants $k - \varepsilon$.

C_μ	$C_{1\varepsilon}$	$C_{2\varepsilon}$	σ_k	σ_ε
0.09	1.44	1.92	1	1.3

The $k-\varepsilon$ turbulence model is easy to implement, shows good convergence due to stable calculations and fair predictions for a huge variety of flows. However, there are also flows with bad predictions where there are strong separations, axisymmetric jets or rotating flows. Furthermore, the model is only valid for fully turbulent flows, the ε -equation is considered as too simplistic.[24]

II 7 3 2 $k-\omega$ Model

Unlike the $k-\varepsilon$ (Standard) model, this model does not require the incorporation of non-linear functions for simulations at low Reynolds numbers. It is empirically similar to the $k-\varepsilon$ model with two transport equations: one for the modified turbulent kinetic energy (k) and one for the specific dissipation rate (ω), which is related to the ratio of ε to k . However, implementing this model requires a very fine near-wall mesh, which is not easily achievable in most cases. To address this issue, a wall proximity function is incorporated, ensuring a smooth transition from the low Reynolds number formulation to the wall law.

After several years of refinement, this model now offers an advantage in predicting free shear flows. It also considers the effects of low Reynolds numbers, compressibility, and jets of different configurations (planar, radial, etc.). For these reasons, it is particularly suitable for internal flows.[16]

The turbulent viscosity is calculated by combining k and ω as follows:

$$\mu_t = \alpha^* \frac{\rho k}{\omega} \quad \text{II. 7}$$

α^* is a coefficient that provides a correction to the turbulent viscosity at low Reynolds numbers.[5]

II 7 4 Reynolds stress models

The Reynolds stress model, also known as the second-moment closure model, calculates the turbulent stresses directly by solving a transport equation for each stress component, without relying on the concept of turbulent viscosity.[22]

II 8 Simplifying hypotheses

In order to make the computational model more detailed and accurate, some simplifying assumptions need to be introduced, which are distributed as follows:

- The fluid (air) is Newtonian and incompressible.
- The fluid flow and heat transfer are three-dimensional.
- The density of the fluid in the volume force term varies linearly with the temperature T according to the approximation of j. Boussinesq

II 9 Navier Stokes equations

The mathematical formula for convective phenomena depends on equations that link the various parameters, namely: velocity, pressure and temperature. These equations are obtained as special cases from the following general equations (continuity equation, momentum conservation equation and energy conservation equation).

II 9 1 Continuity equation

The continuity equation, also known as the conservation of mass equation, is a fundamental principle in physics that expresses the conservation of mass in a closed system. The equation states that the mass of a fluid is conserved, and therefore the mass flow rate through any given point in the fluid must be constant over time.[7]

The general form of the continuity equation is:

$$\frac{\partial \rho}{\partial t} + \rho \cdot \text{div} \vec{V} = 0 \quad \text{II. 8}$$

where:

ρ is the density of the fluid,

t is time,

\vec{V} is the velocity of the fluid,

The continuity equation can be used to derive many other equations and relationships that describe fluid behavior. It is applicable to both incompressible and compressible fluids, and can be extended to include other quantities such as energy or momentum.

II 9 2 Momentum equation

The principle of conservation of momentum allows to write the equation of motion in the following form:

$$\rho \frac{DV}{Dt} = -\nabla p + \mu \nabla^2 V + \rho g \quad \text{II. 9}$$

where:

V : fluid velocity vector (m/s)

g : gravity acceleration

μ : dynamical viscosity

p : pressure (pa)

II 9 3 Energy equation

The energy equation represents conservation of energy of a fluid element.

$$\rho C_p \left(\frac{\partial T}{\partial t} + (\vec{V} \cdot \vec{\nabla}) T \right) = \text{div}(\lambda \overrightarrow{\text{grad}} T) \quad \text{II. 10}$$

where:

λ : thermal conductivity of the fluid

T : fluid temperature

C_p : heat capacity of the fluid at constant pressure

II 10 The Boussinesq approximation

The Boussinesq equation is derived from the Navier-Stokes equations by applying the Boussinesq approximation. The Navier-Stokes equations describe the motion of fluid and are given by:

$$\frac{\partial u}{\partial t} + (u \cdot \nabla) u = -\nabla P + \mu \nabla^2 u + \rho g \quad \text{II. 11}$$

$$\nabla \cdot u = 0 \quad \text{II. 12}$$

In these equations:

u is the velocity vector of the fluid.

t is time.

∇ is the gradient operator.

P is the pressure.

μ is the dynamic viscosity.

ρ is the density.

g is the acceleration due to gravity.

The Boussinesq approximation assumes that the density variations in the fluid are small except for the buoyancy term. This approximation is valid for incompressible flows with small temperature-induced density changes. It allows us to treat the fluid as incompressible, with a constant density ρ_0 , except in the buoyancy term, where density variations are taken into account.[19]

By applying the Boussinesq approximation, the density term ρg in the Navier-Stokes equations is replaced with $\rho_0 g(T - T_0)$, where:

ρ_0 is the reference density.

T is the temperature.

T_0 is a reference temperature.

The resulting Boussinesq equation for incompressible flows is:

$$\frac{\partial u}{\partial t} + (u \cdot \nabla)u = -\nabla P + \mu \nabla^2 u + \rho_0 g(T - T_0) \quad \text{II.13}$$

$$\nabla \cdot u = 0$$

This equation retains the same structure as the Navier-Stokes equations but includes the temperature-induced buoyancy term, $\rho_0 g(T - T_0)$, which represents the buoyancy force due to temperature variations.

The Boussinesq equation is widely used in fluid dynamics and thermal sciences to study buoyancy-driven flows, natural convection, and heat transfer phenomena. It simplifies the analysis of incompressible flows with small density variations and allows for the investigation of important fluid flow behaviors induced by temperature gradients.

It is important to note that the Boussinesq equation is an approximation, and its validity depends on the magnitude of the density variations. For larger density variations or compressible flows, more accurate and comprehensive equations are required.[5]

II 11 Formulation of equations in Cartesian coordinates

The dimensional equations in vector form are expressed in Cartesian coordinates

with the consideration of simplifying assumptions.

II 11 1 Continuity equation

$$\frac{\rho u}{\partial x} + \frac{\partial v}{\partial y} + \frac{\partial w}{\partial z} = 0 \quad \text{II. 14}$$

Where \mathbf{u} , \mathbf{v} and \mathbf{w} are the velocity components in \mathbf{x} , \mathbf{y} and \mathbf{z} direction respectively

II 11 2 Equation of momentum

- According to the x-axis :

$$\rho \left(\frac{\partial u}{\partial t} + u \frac{\partial u}{\partial x} + v \frac{\partial u}{\partial y} + w \frac{\partial u}{\partial z} \right) = - \frac{\partial p}{\partial x} + \mu \left(\frac{\partial^2 u}{\partial x^2} + \frac{\partial^2 u}{\partial y^2} + \frac{\partial^2 u}{\partial z^2} \right) + \rho g_x \quad \text{II. 15}$$

- According to the y-axis :

$$\rho \left(\frac{\partial u}{\partial t} + u \frac{\partial u}{\partial x} + v \frac{\partial u}{\partial y} + w \frac{\partial u}{\partial z} \right) = - \frac{\partial p}{\partial y} + \mu \left(\frac{\partial^2 u}{\partial x^2} + \frac{\partial^2 u}{\partial y^2} + \frac{\partial^2 u}{\partial z^2} \right) + \rho g_y \quad \text{II. 16}$$

- According to the z-axis :

$$\rho \left(\frac{\partial u}{\partial t} + u \frac{\partial u}{\partial x} + v \frac{\partial u}{\partial y} + w \frac{\partial u}{\partial z} \right) = - \frac{\partial p}{\partial z} + \mu \left(\frac{\partial^2 u}{\partial x^2} + \frac{\partial^2 u}{\partial y^2} + \frac{\partial^2 u}{\partial z^2} \right) + \rho g_z \quad \text{II. 17}$$

II 11 3 Energy equation

$$U \frac{\partial T}{\partial x} + V \frac{\partial T}{\partial y} = \alpha \left(\frac{\partial^2 T}{\partial x^2} + \frac{\partial^2 T}{\partial y^2} \right) \quad \text{II. 18}$$

with

$\alpha = \frac{\lambda}{\rho c_p}$ is the thermal diffusivity.

II 12 Dimensional analysis

In many cases, it's advantageous to express the governing equations in dimensionless form to make the analysis of a physical problem more general. To do this, we need to identify characteristic quantities that represent the flow, such as a characteristic velocity, pressure... By using these characteristic quantities, we can derive different non dimensional parameters :[25]

$$x^* = \frac{x}{L} \quad , \quad y^* = \frac{y}{L} \quad , \quad z^* = \frac{z}{L} \quad , \quad u^* = \frac{u}{u_\infty} \quad , \quad v^* = \frac{v}{u_\infty} \quad , \quad w^* = \frac{w}{u_\infty}$$

$$t^* = \frac{t}{L/u_\infty} \quad , \quad P^* = \frac{P-P_\infty}{\rho u_\infty^2} \quad , \quad T^* = \frac{T-T_\infty}{\Delta T} \quad , \quad K = \frac{k}{k_S}$$

Where :

T^* is dimensionless temperature, K is thermal conductivity ratio.

By using these parameters we can obtain the following governing equations.

II 12 1 Continuity equation

$$\frac{\partial u^*}{\partial x^*} + \frac{\partial v^*}{\partial y^*} + \frac{\partial w^*}{\partial z^*} = 0 \quad \text{II. 19}$$

II 12 2 Momentum equation

- In x-direction:

$$\left(\frac{\partial u^*}{\partial t^*} + u^* \frac{\partial u^*}{\partial x^*} + v^* \frac{\partial u^*}{\partial y^*} + w^* \frac{\partial u^*}{\partial z^*} \right) = -\frac{\partial p^*}{\partial x^*} + \frac{1}{Re} \left(\frac{\partial^2 u^*}{\partial x^{*2}} + \frac{\partial^2 u^*}{\partial y^{*2}} + \frac{\partial^2 u^*}{\partial z^{*2}} \right) \quad \text{II. 20}$$

- In y-direction:

$$\left(\frac{\partial v^*}{\partial t^*} + u^* \frac{\partial v^*}{\partial x^*} + v^* \frac{\partial v^*}{\partial y^*} + w^* \frac{\partial v^*}{\partial z^*}\right) = -\frac{\partial p^*}{\partial y^*} + \frac{1}{Re} \left(\frac{\partial^2 u^*}{\partial x^{*2}} + \frac{\partial^2 u^*}{\partial y^{*2}} + \frac{\partial^2 u^*}{\partial z^{*2}}\right) + Ri.T^* \quad \text{II. 21}$$

• **In z-direction:**

$$\left(\frac{\partial u^*}{\partial t^*} + u^* \frac{\partial w^*}{\partial x^*} + v^* \frac{\partial w^*}{\partial y^*} + w^* \frac{\partial w^*}{\partial z^*}\right) = -\frac{\partial p^*}{\partial z^*} + \frac{1}{Re} \left(\frac{\partial^2 u^*}{\partial x^{*2}} + \frac{\partial^2 u^*}{\partial y^{*2}} + \frac{\partial^2 u^*}{\partial z^{*2}}\right) \quad \text{II. 22}$$

II 12 3 The energy equation

$$\frac{\partial T^*}{\partial t^*} + u^* \frac{\partial T^*}{\partial x^*} + v^* \frac{\partial T^*}{\partial y^*} + w^* \frac{\partial T^*}{\partial z^*} = \frac{1}{Re.Pr} \left(\frac{\partial^2 T^*}{\partial x^{*2}} + \frac{\partial^2 T^*}{\partial y^{*2}} + \frac{\partial^2 T^*}{\partial z^{*2}}\right) \quad \text{II. 23}$$

II 13 Dimensionless numbers

II 13 1 Grashof number

Grashof number **Gr** is a dimensionless parameters used in fluid mechanics and heat transfer to quantify the effect of buoyancy forces in relation to viscous forces within a fluid flow or heat transfer scenario. It is defined as the ratio of the buoyancy-induced forces to the viscous forces and plays a critical role in determining whether naturel convection dominates in a particular situation.[20]

$$Gr = \frac{g\beta.\Delta T.L^3}{\nu^2} \quad \text{II. 24}$$

II 13 2 Prandtl number

The Prandtl number is a dimensionless number used in fluid mechanics and heat transfer to characterize the relative importance of momentum diffusion to heat diffusion in a fluid. It is defined as the ratio of a fluid's kinematic viscosity to its thermal diffusivity. In simpler terms, its describes how heat is conducted through a fluid compared to how momentum is transported due to viscosity:[21]

$$Pr = \frac{\nu}{\alpha} = \frac{(\mu/\rho)}{(k/\rho Cp)} = \frac{\mu.Cp}{K} \quad \text{II. 25}$$

II 13 3 Reynolds number

The Reynolds number, denoted Re, is a dimensionless number used in fluid dynamics to determine whether a flow is laminar or turbulent. It's calculated by dividing the product of a fluid's velocity and characteristic length by its kinematic viscosity. This number helps identify the type of fluid flow : laminar at low values or turbulent at higher values: [26]

$$Re = \frac{\rho V_{max} \cdot D_h}{\mu} \quad \text{II. 26}$$

where :

ρ = density [kg/m^3] , V = velocity maximal [m/s] , D = hydraulic diameter [m] , μ = dynamic viscosity [$\text{kg}/\text{m}\cdot\text{s}$]

- the flow is laminar for $Re < 2300$
- the flow is turbulent for $Re > 2300$

II 13 4 Nusselt number

The Nusselt number, Nu, is a critical dimensionless parameter in fluid dynamics and heat transfer. It quantifies how efficiently heat is transferred through convection compared to conduction in a fluid boundary layer. It is used to optimize heat exchanges processes and design effective heat exchangers, ultimately enhancing various technological application.[23]

$$Nu = \frac{hL}{K} \quad \text{II. 27}$$

For our problem we use the following equation to calculate Nusselt number:

$$Nu = C \cdot Re^{1/2} \cdot Pr^{1/3} \quad \text{II. 28}$$

Where:

$$C = \frac{0.61 \cdot ST^{0.091} \cdot SL^{0.053}}{1 - e^{-1.09 \cdot SL}}$$

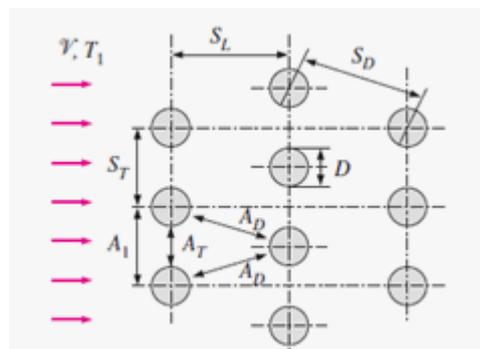


Figure II. 5 $ST=28\text{mm}$. $SL=21\text{mm}$.

II 13 5 Richardson number

Richardson number is a dimensionless number used in particular in thermodynamics which was developed by Lewis Fry Richardson, English physicist and mathematician.

This number represent a parameter used in fluid dynamics to quantify the relative importance of buoyancy forces to shear forces within a fluid flow. It is a valuable tool for assessing the stability of stratified fluids and helps classify flows as stable, unstable, or transitional, depending on its value

It can be calculated from the following equation.[1]

$$Ri = \frac{Gr}{Re^2} \quad \text{II. 29}$$

- forced convection $Ri < 0.1$
- Natural convection $Ri > 1.6$
- mixed convection $0.1 \leq Ri \leq 1.6$

II 14 Model Boundary conditions

Input speed : $0.5 \text{ m/s} < v < 3 \text{ m/s}$

Temperatures: $T_{left} = T_{right} = \text{adiabatic}$

At the inlet

$$u^* = 1, v^* = w^* = 0$$

At the outlet

$$\frac{\partial U}{\partial x} = 0, \frac{\partial U}{\partial y} = 0, \frac{\partial U}{\partial z} = 0,$$

II 15 Conclusion

In summary, this chapter serves as a comprehensive introduction to the key principles of fluid mechanics and heat transfer. These fields are vital in engineering and involve intricate equations that are often tackled through numerical methods. The chapter's focus on conservation equations, especially in mixed convection, lays the groundwork for understanding fluid behavior.

CHAPTER III
NUMERICAL METHODS

III 1 Introduction

To acquire an estimated numerical solution, it is imperative to convert the governing partial differential equations into a collection of algebraic equations that can be tackled through computational approaches. This simplification is typically performed on a localized portion of the domain where a numerical solution can be obtained. The process of discretization plays a crucial role in finding the solution and is equally important in the development of numerical programs.

III 2 Solution of differential equations

There are various sorts of problem-solving techniques, including the finite difference method(FDM), the finite element method(FEM), and the finite volume method(FVM), depending on how discretization is done.

To tackle a CFD problem, a variety of alternative approaches are available, such as BEM and SEM. In addition, there are a various software programs available today, including ANSYS which will be used in the current study, and it relies on the finite volume method.

In the following, we will provide a brief explanation of the aforementioned.

III 3 Finite volume methods

The finite volume method is a numerical technique used to solve partial differential equations (PDEs) on a discretized grid. It is a conservative method that discretizes the computational domain into a finite number of control volume or cells. The method then integrates the governing PDEs over each control by volume by considering the net flow of mass, momentum, and energy across the corresponding faces. This leads to a set of algebraic equations ,which can be solved numerically to obtain the solution of the PDE.[27]

In the FVM , the physical domain is divided into a collection of non-overlapping control volume. The value of the solution variables are defined at the centers of the control volumes, and the values on the faces are computed using suitable numerical approximations .[28]

The FVM is a versatile method that can handle a wide range of problems with complex geometries , non-uniform grids , and non-linear boundary conditions. It is commonly used in computational fluid dynamics (CFD), heat transfer, electromagnetics and many other physical and engineering phenomena .

The different steps of finite volume methods are:

- The discretization of the domain considered in control volume.

- Writing algebraic equations at the nodes of the mesh.
- Solving the algebraic system obtain.

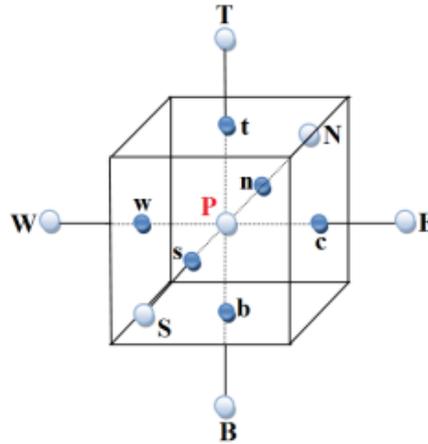


Figure III. 1 Control volume in three dimensions.

In the discretization scheme used, a control volume center is located at the center of each volume and is referred to as the principal node denoted by P . The neighboring volume nodes are labeled according to their positions as $NSWET$ and B , corresponding to the North, South, West, East, Top, and Bottom directions, respectively. [29]

III 4 Discretization of the governing equations

III 4 1 Discretization process

The discretization process is crucial in numerical methods as it allows the application of computational techniques to solve complex mathematical models or physical problems. It enables the transformation of continuous mathematical formulations into discrete representations that can be processed by computers, leading to approximate numerical solutions.

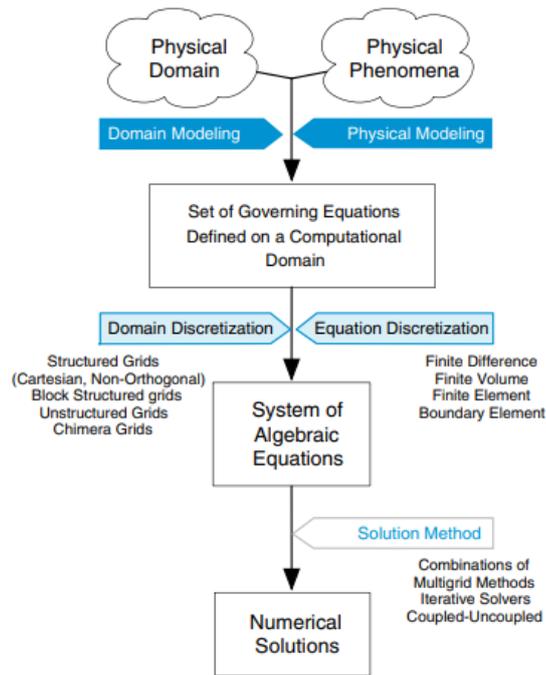


Figure III. 2 The discretization process.

III 4 2 Transport equation

The standard form of the transport equation for a scalar property ϕ :

$$\underbrace{\frac{\partial \rho \phi}{\partial t}}_{\text{temporal dervative}} + \underbrace{\nabla \cdot (\rho \mathbf{U} \phi)}_{\text{convection term}} = \underbrace{\nabla \cdot (\Gamma_\phi \nabla \phi)}_{\text{diffusion term}} + \underbrace{S_\phi(\phi)}_{\text{source term}} \tag{III. 1}$$

Where :

ϕ : transport quantity such as velocity, mass or temperature.

Γ_ϕ : transport quantity’s diffusion coefficient.

The table Bellow represent a different parameters for the governing equation mentioned in chapter two.[30]

Table III. 1 Cases for transport equation for fluid domain.

Quantity	ϕ	Γ_ϕ	S_ϕ
Continuity equation	1	0	0
Momentum equation in x direction	u^*	$\frac{1}{Re}$	$-\frac{\partial P^*}{\partial x^*}$
Momentum equation in y direction	v^*	$\frac{1}{Re}$	$-\frac{\partial P^*}{\partial y^*} + Ri.T^*$
Momentum equation in z direction	w^*	$\frac{1}{Re}$	$-\frac{\partial P^*}{\partial z^*}$
Energy equation	0	$\frac{1}{Re.pr}$	0

III 4 2 1 Discretization of transport equation

The integration of transport equation over a three-dimensional control volume (cv):

$$\int_{cv} \frac{\partial(\rho\phi)}{\partial t} dV + \int_{cv} \nabla(\rho\phi u) dV = \int_{cv} \nabla(\Gamma\nabla\phi) dV + \int_{cv} S_\phi dV \quad \text{III. 2}$$

The convective term and the diffusive term are rewritten by Gauss's divergence theorem as integral over the entire bounding surface of the control volume, for a vector \mathbf{a} :

$$\int_{cv} \nabla(\mathbf{a}) dV = \int_A \mathbf{n} \cdot \mathbf{a} dS \quad \text{III. 3}$$

The physical interpretation of $\mathbf{n} \cdot \mathbf{a}$ is that it represents the projection of vector ' \mathbf{a} ' onto the direction of vector ' \mathbf{n} ', which is perpendicular to the surface element dS . Consequently, the integral of the divergence of vector ' \mathbf{a} ' over a volume is equal to the summation(or integration) of the component of ' \mathbf{a} ' in the direction perpendicular to the surface that encloses the volume, considering the entire bounding surface 'S'.

Applying Gauss's divergence theorem equation **III.2** can be written as :

$$\frac{\partial}{\partial t} \left(\int_{CV} \rho \phi dV \right) + \int_S \mathbf{n} \cdot (\rho \phi \mathbf{u}) dS = \int_S \mathbf{n} \cdot (\Gamma \nabla \phi) dS + \int_{CV} S_\phi dV \quad \text{III. 4}$$

This equation expresses the principle of conservation, indicating that the alteration of ϕ within the specified area is equivalent to the combined effects of convective and diffusive fluxes across its boundaries, alongside the rate at which the quantity is generated within the said area.[31]

III 4 2 2 Approximation of surface and volume integral

The values of ϕ are determined at the midpoint of the control volume, to assess the surface integral in the equation III. 3. we need to make a presumption that ϕ changes proportionally along all faces f of control volume. So we can use the mean value of ϕ at the center applying the mind-point rule, by approximating the surface integral as the product of the transported quantities at the face centroid f and the area of the face. This approximation assist the calculating of the surface integral, by using an available data at the face centers of the control volume.

The fluxes in equation III. 3, using those assumptions and approximations can be written :

$$\oint_S (\rho u \Phi) \mathbf{n} \cdot dS = \sum_f \int_S (\rho u \Phi \cdot \vec{n})_f dS \approx \sum_f S_f \cdot (\overline{\rho u \Phi})_f = \sum_f S_f \cdot (\rho u \Phi)_f \quad \text{III. 5}$$

$$\oint_S (\Gamma_\Phi \nabla \Phi) \mathbf{n} \cdot dS = \sum_f \int_S (\Gamma_\Phi \nabla \Phi \cdot \vec{n})_f dS \approx \sum_f S_f \cdot (\overline{\Gamma_\Phi \nabla \Phi})_f = \sum_f S_f \cdot (\Gamma_\Phi \nabla \Phi)_f \quad \text{III. 6}$$

In equation III. 3, when approximating volume integral, we adopt a comparable assumption, which is that Φ changes linearly across the control volume where we perform the integration, allowing us to write:

$$\begin{aligned} \int_S \Phi(\mathbf{x}) dV &= \int_V [\Phi_p + (\mathbf{x} - \mathbf{x}_p) \cdot (\nabla \Phi)_p] dV \\ &= \Phi_p \int_V dV + \left[\int_V (\mathbf{x} - \mathbf{x}_p) \cdot (\nabla \Phi)_p dV \right] \cdot (\nabla \Phi)_p \\ &= \Phi_p V \end{aligned} \quad \text{III. 7}$$

This approximation is exact when Φ varies linearly or constant, and it considered as a second order approximation. When we introduce The equation III.4 into equation III.3 :

$$\frac{\partial}{\partial t} \rho \Phi V + \sum_f S_f \cdot (\rho u \Phi)_f = \sum_f S_f \cdot (\Gamma_\Phi \nabla \Phi)_f + S_\Phi V_p \quad \text{III. 8}$$

After all variables are calculated and retained at the centroid of the control volume , we need to define the convective flux and the diffusive flux in or out faces in equation III.7, using different form of interpolation from the centroid and the neighboring control volume.[32]

III 4 2 3 Convection term spatial discretization

From equation III.7, we can write :

$$\int_V \nabla \cdot (\rho U \Phi) dV = \sum_f S_f (\rho U \Phi)_f = \sum_f F_f \Phi_f \quad \text{III. 9}$$

When F is the mass flux through the face

$$F = S_f (\rho U)_f \quad \text{III. 10}$$

The flux is calculated from the interpolation values of ρ and U which calculated similarly to Φ_f .

With the consideration that the velocity field must satisfy the continuity equation from which the fluxes are derived.[31]

Here we present two different schemes which we can use to discretize the convection term:

➤ Centrale differencing schemes

The central difference scheme is a commonly used FVM scheme for solving partial differential equations . it is a second-order accurate scheme that approximates the fluxes across each face of a control volume using a central difference approximation .

For a uniform grid, cell face values are:

$$\Phi_f = \frac{\Phi_P + \Phi_N}{2} \quad \text{III. 11}$$

We can calculate the face values according to the following equation, assuming the straight-line correlation of Φ between P and N:

$$\Phi_f = f_x \Phi_P + (1 - f_x) \Phi_N \quad \text{III. 12}$$

f_x denotes the quotient of the distance fN and PN that :

$$f_x = \frac{\overline{fN}}{\overline{PN}} = \frac{|x_f - x_N|}{|d|}$$

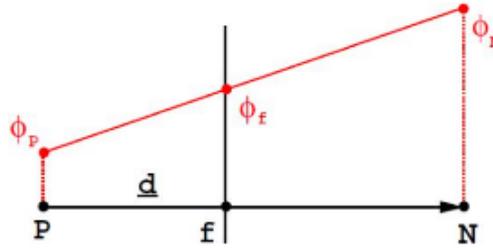


Figure III. 3 Face interpolation.

➤ **Upwind differencing scheme (UD)**

The upwind scheme is a discretization method that ensures bounded solutions, it determines the face value of a quantity based on the direction of the flow as :

$$\Phi_f = \begin{cases} \Phi_f = \Phi_P & \text{For } F \geq 0 \\ \Phi_f = \Phi_N & \text{For } F < 0 \end{cases} \quad \text{III. 13}$$

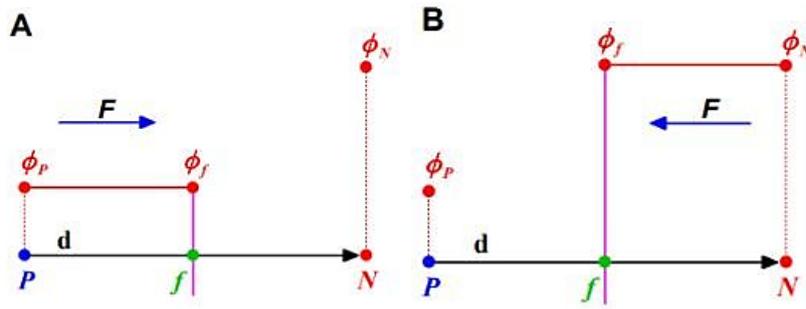


Figure III. 4 Face interpolation UD scheme, (A) $F \geq 0$, (B) $F < 0$.

The solution’s boundedness is ensured through the sufficient boundedness criterion for systems of algebraic equation. However, the introduction of a numerical diffusion term in the UD method compromises accuracy and leads to considerable distortions in the solution due to the violation of the discretization’s order of accuracy.

In the present study we are going to use the second order upwind scheme, also the first order of it for the momentum and energy equations.[30]

III 4 2 4 Diffusion term spatial discretization

The diffusion term will be discretized in a comparable manner using the following interpolation:

$$\int_V \nabla(\rho \Gamma_\Phi \nabla \Phi) dV = \sum_f S_f (\rho \Gamma_\Phi \nabla \Phi)_f = \sum_f (\rho \Gamma_\Phi)_f S_f (\nabla \Phi)_f \quad \text{III. 14}$$

Γ_Φ represent the diffusion coefficient, which when it is uniform its values is the same for all the control volumes. Then when Γ_Φ is non-uniform we have to calculate it using another linear interpolation between the control volume V_P and V_N .

The interpolation used in the calculation of Γ_Φ can be explained as :

$$(\Gamma_\Phi)_f = f_x(\Gamma_\Phi)_P + (1 - f_x)(\Gamma_\Phi)_N \quad \text{III. 15}$$

In the case where we have a uniform control volume where f is between V_P and V_N , f_x equal to 0.5 and Γ_Φ equal to the arithmetic mean. When $(\Gamma_\Phi)_N$ is zero this mean that there is no diffusion from face f .

For an improved estimation of the fluctuation, and as a resolution to this problem we employ the harmonic average that :[31]

$$(\Gamma_\Phi)_f = \frac{(\Gamma_\Phi)_N(\Gamma_\Phi)_P}{f_x(\Gamma_\Phi)_P + (1 - f_x)(\Gamma_\Phi)_N} \quad \text{with} \quad f_x = \frac{\overline{fN}}{\overline{PN}} = \frac{|x_f - x_N|}{|d|} \quad \text{III. 16}$$

III 4 2 5 Source term spatial discretization

We can say that all the terms in the transport equation are considered as sources, where the source term $S_\Phi(\Phi)$ represent a general function of Φ . [33]

When we select the type of discretization for the source term, it is essential to investigate how it interacts with other terms in the equation and its impact on boundedness and precision.

It's necessary to linearize the source term :

$$S_\Phi(\Phi) = S_c + S_p \Phi \quad \text{III. 17}$$

Where S_c represent the constant part of the source term, when S_p depends to Φ .

As integral of the source term we can write:

$$\int_V S_\Phi(\Phi) dV = S_c V + S_p V \Phi_p \quad \text{III. 18}$$

III 4 2 6 Temporel Discretization

The integration of transport equation should be performed in time as an expression called “ semi-discretized” form of transport equation, where :

$$\int_t^{t+\Delta t} \left[\frac{\partial}{\partial t} \int_V \rho \Phi dV + \int_V \nabla(\rho u \Phi) dV - \int_V \nabla \cdot (\rho \Gamma_\Phi \nabla \Phi) dV \right] dt = \int_t^{t+\Delta t} (\int_V S_\Phi(\Phi) dV) dt \quad \text{III. 19}$$

By using the connection between equations, III.8, and III.18, and without changes in the control volume time, we find:

$$\int_t^{t+\Delta t} \left[\left(\frac{\partial \rho \Phi}{\partial t} \right)_P V + \sum_f F \Phi_f - \sum_f (\rho \Gamma_\Phi)_f S. (\nabla \Phi)_f \right] dt = \int_t^{t+\Delta t} (S_c V + S_p V \Phi_p) dt \quad \text{III. 20}$$

With taking into consideration the presumed change of the function in time, we can compute the temporal integral and the time derivative, as:

$$\left(\frac{\partial \rho \Phi}{\partial t} \right)_P = \frac{\rho_P^n \Phi_P^n - \rho_P^0 \Phi_P^0}{\Delta t} \quad \text{III. 21}$$

$$\int_t^{t+\Delta t} \Phi dt = \frac{1}{2} (\Phi^0 + \Phi^n) \Delta t \quad \text{III. 22}$$

That:

$$\Phi^n = \Phi t + \Delta t$$

$$\Phi^0 = \Phi t)$$

All of equations, III.20, III.21, III.22, presuming that density and diffusivity remain constant over time give:

$$\begin{aligned} \frac{\rho_P^n \Phi_P^n - \rho_P^0 \Phi_P^0}{\Delta t} V + \frac{1}{2} \sum_f F \Phi_f^n - \frac{1}{2} \sum_f (\rho \Gamma_\Phi)_f S. (\nabla \Phi)_f^n + \frac{1}{2} \sum_f F \Phi_f^0 \\ - \frac{1}{2} \sum_f (\rho \Gamma_\Phi)_f S. (\nabla \Phi)_f^0 = S_u V + \frac{1}{2} S_p V \Phi_f^n + \frac{1}{2} S_p V \Phi_f^0 \end{aligned} \quad \text{III. 23}$$

This equation represent the crack-Nicholson method specified to second order.

Now to create our linear algebraic system, which we will solve it with ANSYS Fluent ,and an appropriate algorithm, we can use the differencing scheme for diffusion and convection term, and we write:

$$a_P \Phi_P^n + \sum_N a_N \Phi_N^n = R \quad \text{III. 24}$$

For every control volume, an equation of this structure is formulated. When the value of the variable is determined in the neighboring cells, by the data with creating an algebraic equations system:

$$[A][\Phi] = [R]$$

Where:

A : is a square matrix.

a_p : on the diagonal / a_N : off the diagonal

Φ : the transported quantity vector for all control volumes and R is the source term vector.

After obtaining our system of linear equation, the next step is to solve it, many algorithms to solve the Navier-Stokes equations numerically exist such as SIMPLEC (Semi Implicit Method For Pressure Linked Equations Consistent) which we going to use it in the present study and it was developed by Van Doormal and Raithby in 1984.[31]

III 4 3 SIMPLEC Algorithm

The SIMPLEC Algorithm (Semi Implicit Method For Pressure Linked Equations Consistent) is frequently employed in the realm of CFD for the purpose of solving the Navier-Stokes equations, it parallels the process of the SIMPLE algorithm. Notably, it adjusts the momentum equations to refine the velocity correction equations in SIMPLEC. This adjustment is aimed at excluding terms of lesser significance than those featured in the original SIMPLE approach.[30]

The steps of SIMPLEC algorithm which are same as SIMPLE, and represent in the following figure are:

- Specify the boundary conditions and guess the initial values.
- Determine the velocity and pressure gradients.
- Calculate the pseudo velocities.

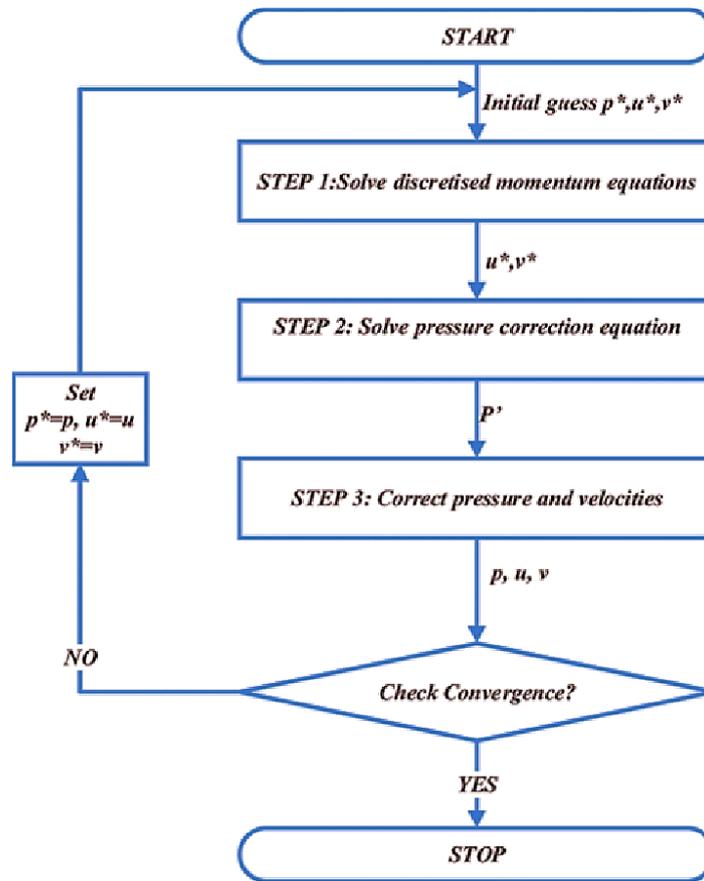


Figure III. 5 SIMPLEC Algorithm.

III 5 The computational fluid dynamics (CFD) :

CFD stands for computational fluid dynamics ,which is a branch of fluid mechanics that uses numerical methods and algorithms to analyze and solve problems related to fluid flow .

In other word ,CFD is a technique that uses computer simulation to analyze the behavior of fluids (such as liquids and gases) as they move through or interact with object in a given environment .it is widely used in variety of fields ,including aerospace ,automotive ,to optimize designs , improve performance , and reduce costs associated with testing and prototyping physical model.[30]

III 6 ANSYS Fluent :

ANSYS Fluent is a commercial CFD software developed by ANSYS Inc .It is one of the most widely used CFD software package in the world and is used in a wide range of industries , including aerospace, automotive ,chemical engineering ,and more .

ANSYS Fluent employs the finite volume method to solve equations governing fluid behavior and heat exchanges. This approach involves subdividing the domain into small interconnected cells, within which variable value are calculated at the centroid.

Through an iterative process, ANSYS Fluent achieves a convergent solution, enabling accurate modeling of fluid flow and thermal transfers.[34]

➤ **ANSYS Fluent interface**

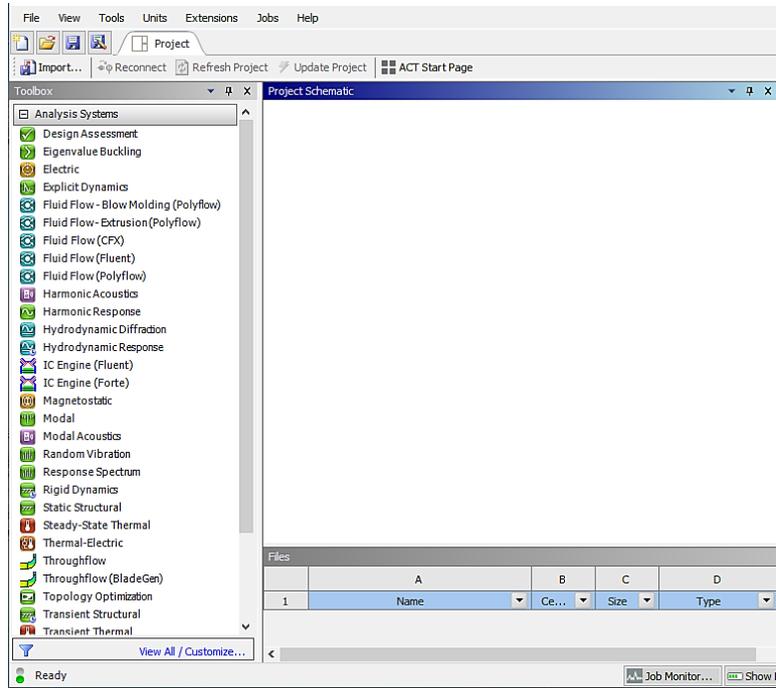


Figure III. 6 ANSYS Fluent interface.

To conduct the current study, we employed Fluent for fluid flow analysis.

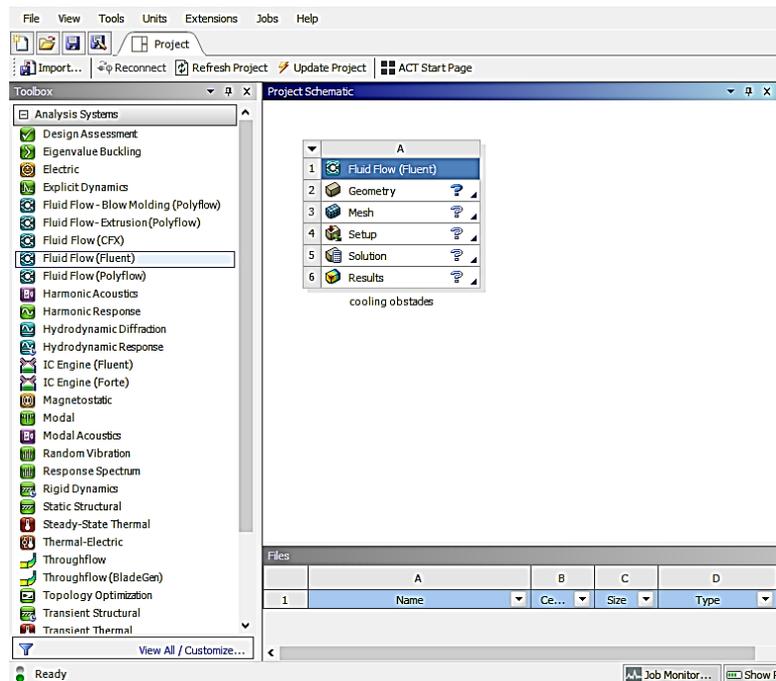


Figure III. 7 Fluid flow (fluent).

ANSYS fluent offers a comprehensive set of features for preprocessing ,solving ,and post-processing CFD simulations some of its key features include:

III 6 1 Pre-processing

it is used to define the geometry , boundary conditions ,and other input parameters required for the simulation. It include tools for meshing , importing CAD models , and setting up simulation parameters.

➤ Geometry model

When we have all the necessary informations. In the coming step we will elaborate on the geometric model. And for this we use ANSYS Design Modeler to built our geometry.

Which is function as a geometry editor for computer-aided design models.

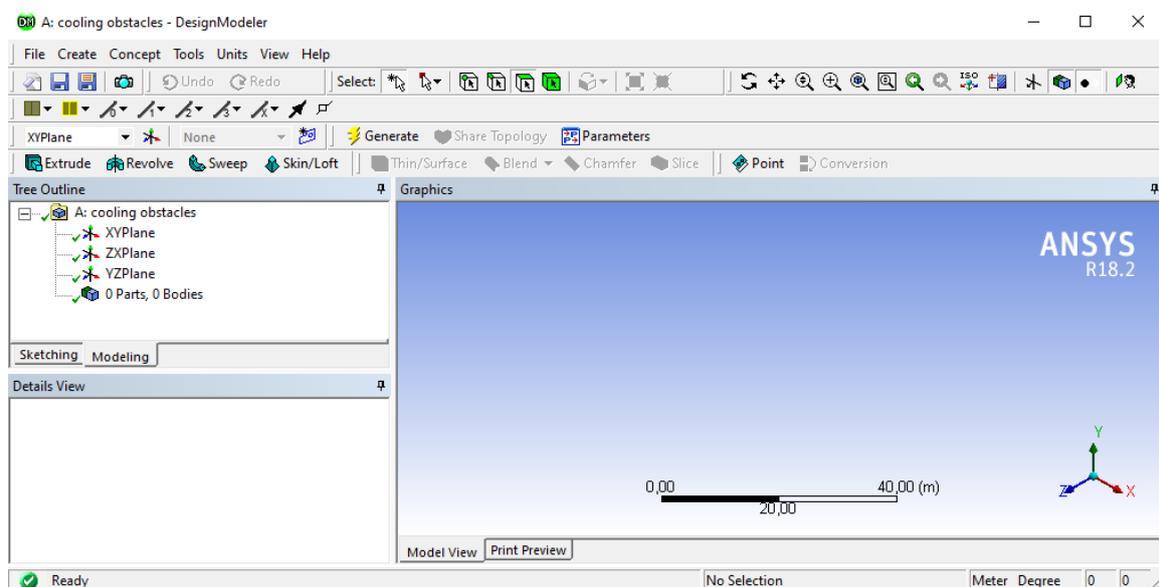


Figure III. 8 Design Modeler interface.

The geometry model for present study consist a part of the free and forced apparatus TD1005:



Figure III. 9 Geometry part of TD1005.

, which represent a box with 0.291 m length in y direction, 0.078 m thickness in z direction, and 0.128 m width in x direction, and contain a pinned surface with a plate surface $0.106 \times 0.106 \times 0.003$ m contains 18 pins with 0.012×0.073 m. the distance between the top wall and the plate surface is 0.03 m, and between the side walls and the plate is 0.011 m, both of pins and the plates are considered as one parts using Boolean, units and named Pin Fin and considered as solid when the surrounding box was considered as fluid domain, which contain inlet bottom wall, outlet top wall, and three adiabatic walls surrounding the pinned surface, when the pinned surface considered as a source term. The final results present in the following figure:

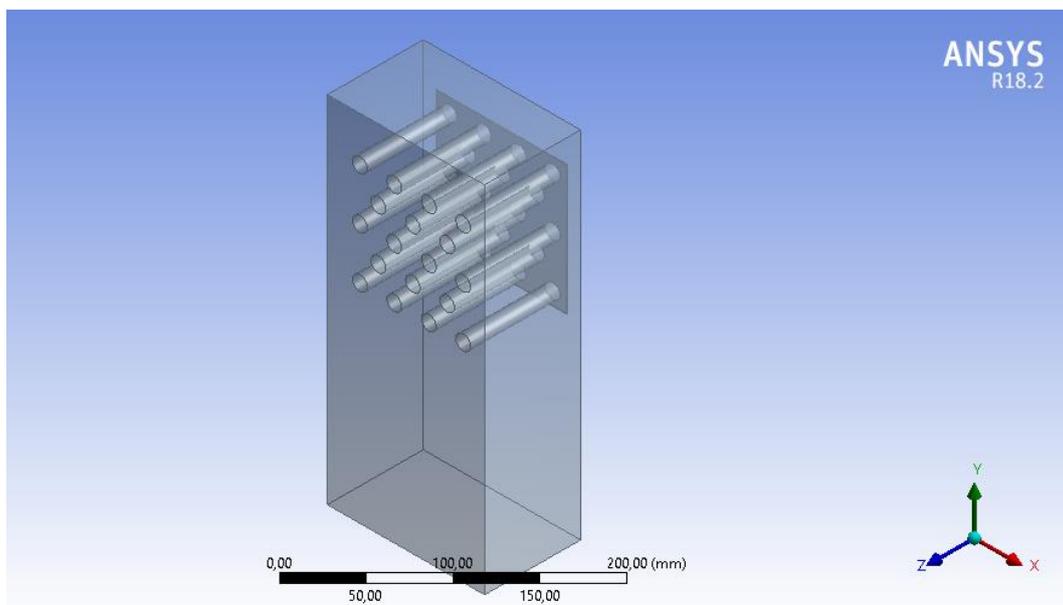


Figure III. 10 The computational model geometry.

➤ Meshing

Meshing in ANSYS Fluent is a fundamental step in the CFD simulation process. It involves dividing the geometric domain into a grid or mesh of interconnected cells to discretize the computational domain. ANSYS Fluent offers a range of meshing options including structured unstructured, and hybrid meshes. It also includes tools for mesh quality control and refinement.

In the present study we have determined a small mesh with about two a million elements which was used to precise the solution, this mesh has bodies sizing of 0.002m, in order to enhance precision further, an inflation at the pins boundary of 18 cylinders was added to achieve a more comprehensive grasp of the phenomena.

For the heat transfer between the solid and the fluid, a contact region was settled to ensure the interaction solid-fluid it was selected as a coupled wall.

The following figures observed the details of the mesh and the process of meshing, including the features and the different geometrical faces and volume entities assigned to them.

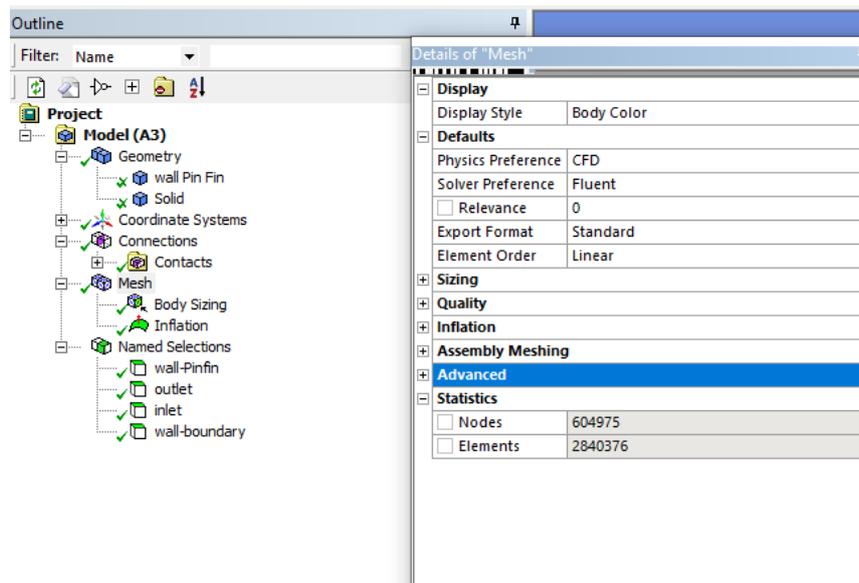


Figure III. 11 Different geometrical faces and volume entities, and mesh specifics.

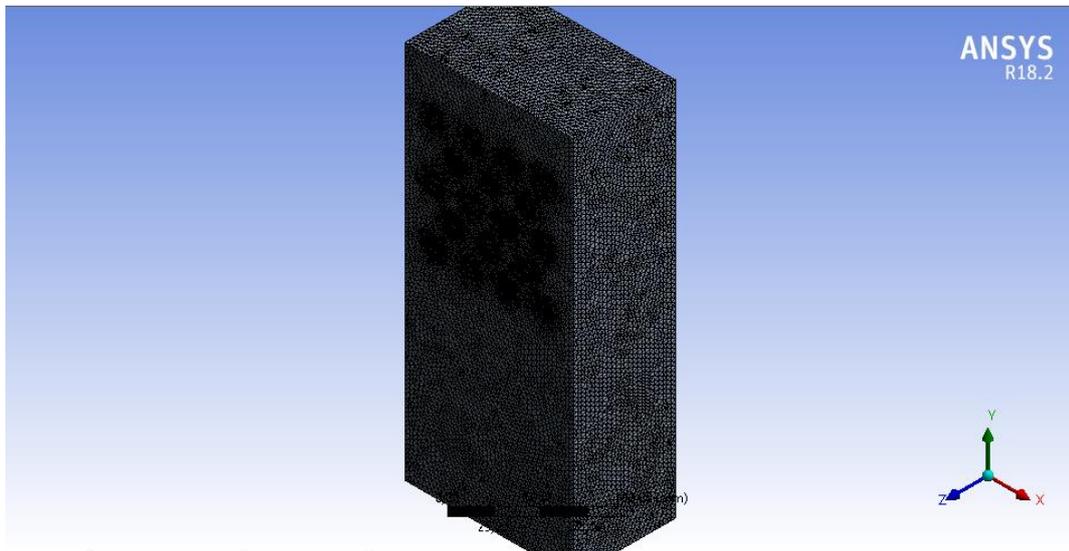


Figure III. 12 The discretized domain.

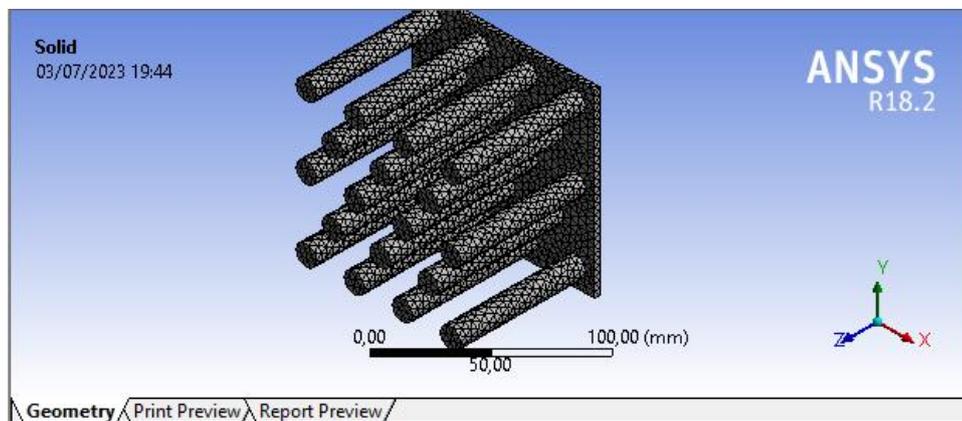


Figure III. 13 Meshing of Pinned surface.

III 6 2 Processing

➤ Solver type

In the current study we use the pressure-based solver which is a computational method used to solve fluid flow and heat transfer problems. It's particularly suited for steady-state simulations, where fluid flow and temperature distributions do not change with time. It employs a segregated approach to iteratively solve the governing equations for fluid dynamics and pressure-velocity coupling. In our study we use the segregated Pressure-Based algorithm which works as following:[34]

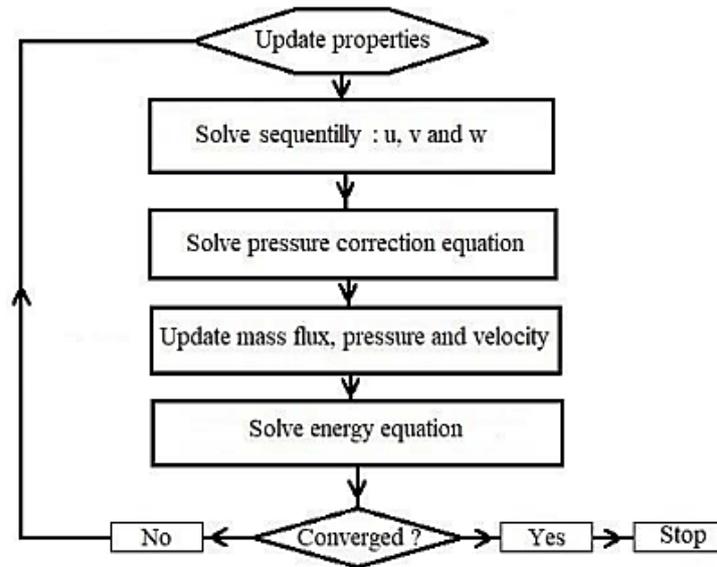


Figure III. 14 The segregated Pressure-Based Algorithm.[34]

After selecting the solver, we enter the value of gravity with negative sign in the y acceleration, as it is opposite to the direction of velocity. By clicking in the general task.

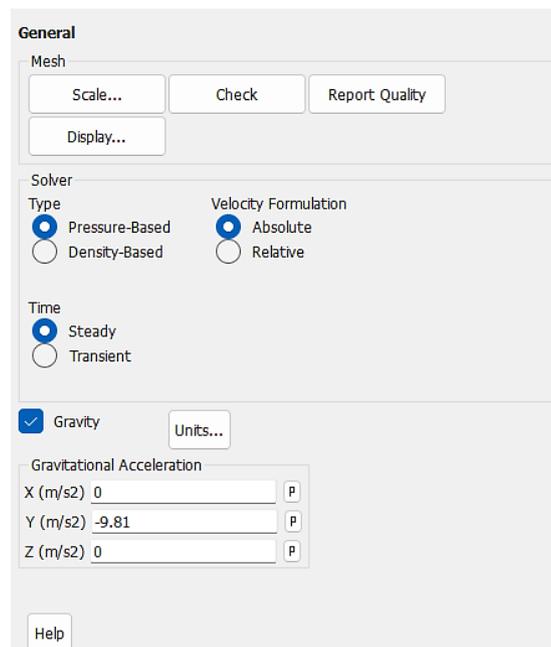


Figure III. 15 Setting up physics.

➤ Physical model

The next step is to use Models task for enabling :

- The heat transfer by activating the energy equation
- The k- ϵ turbulence model

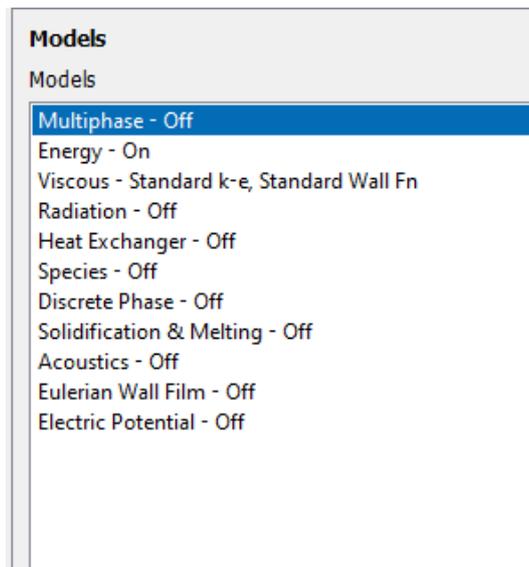


Figure III. 16 Models selecting.

➤ Materials properties

The next step is to modify the air properties by accessing the Materials box, that in the current study we used the Boussinesq approximation for buoyancy flow. The air flow properties was taken under 20° of temperature as follow:

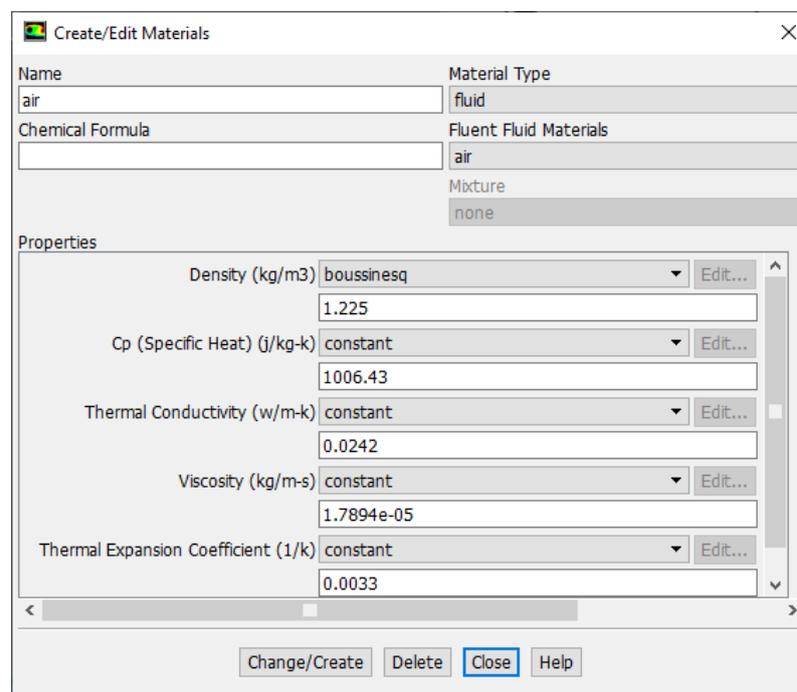


Figure III. 17 Air properties.

➤ **Boundary conditions**

boundary condition is a specification applied to the edges of the computational domain. It defines how the system interacts with its surrounding and provides information such as temperature, velocity, or other relevant parameters at the domain’s boundaries. Our computational domain has three principal boundaries which are:

Velocity inlet: in the current study we set the temperature of the inlet air at 294 k, while the velocity is vary from 0.5m/s to 3 m/s :

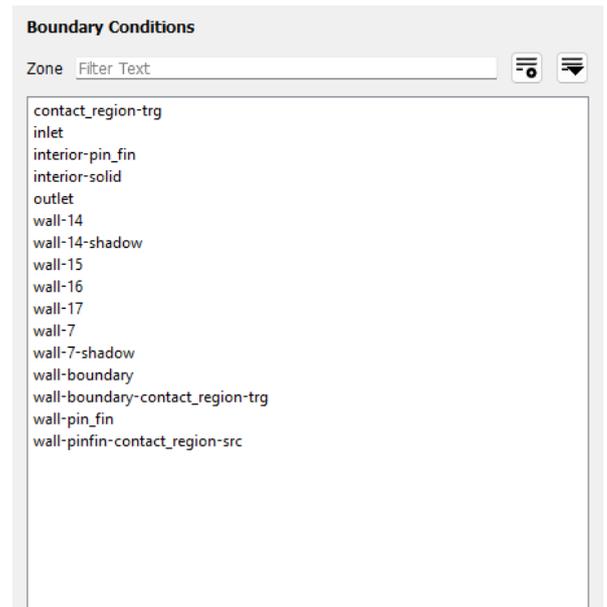


Figure III. 18 Boundary conditions.

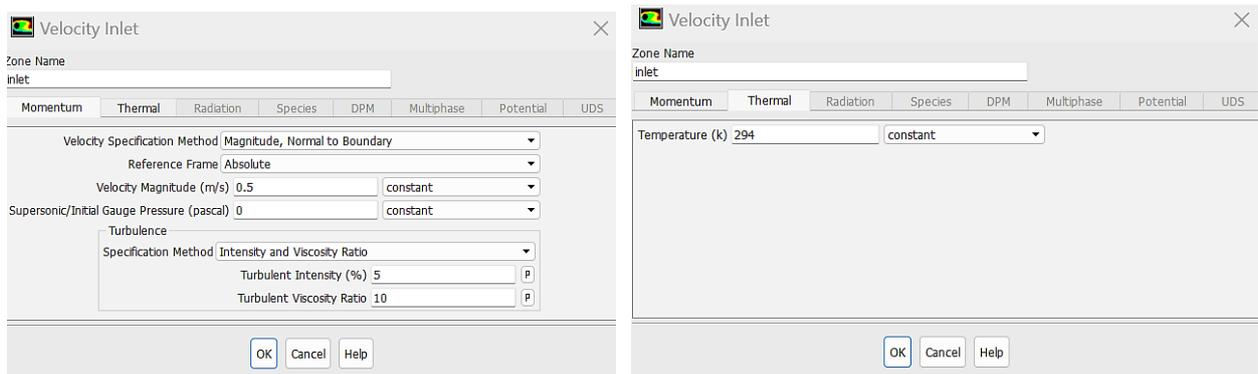


Figure III. 19 Velocity inlet parameters.

Outlet: which considered as outflow.

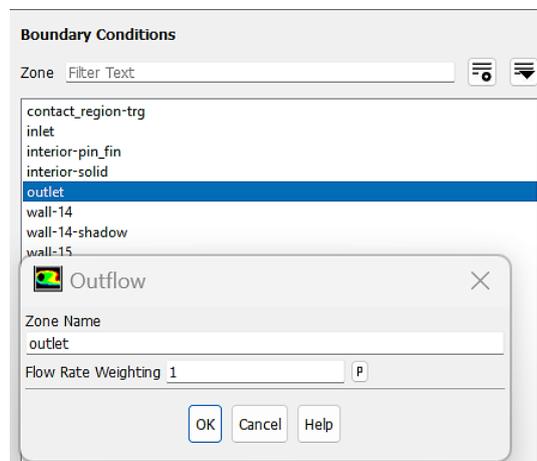


Figure III. 20 Outlet.

Wall Pin Fin: it considered as a hot wall where we entered a value of thermal flux, which we calculated it by dividing the power on watt by the area of Pin Fin subtracting on it the area of 18 pins. That because in the study we use different values of power 70W and 50W. so we calculated the thermal flux as follow :

$$q = \frac{P}{A}$$

such as q is the thermal flux in W/m^2 , P is the power in W, and A is the area in m^2 .

The first value of thermal flux we entered is $7609 W/m^2$.

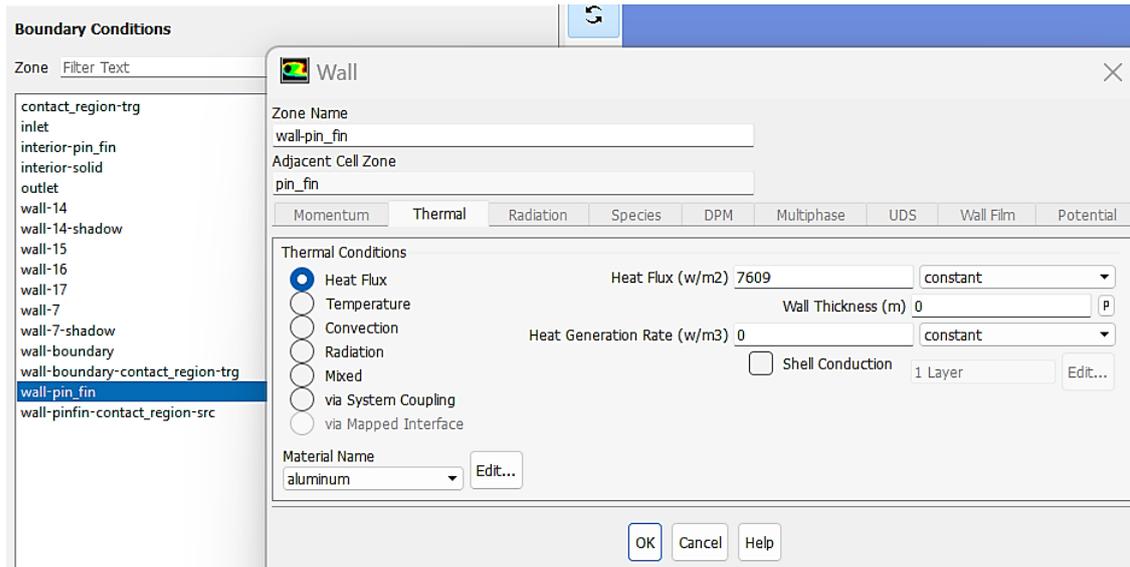


Figure III. 21 Wall Pin Fin properties.

➤ The solution Methods

To solve a CFD problem we have first to choose the scheme for the solving algorithms by setting up the solution methods. In the present study we use the SIMPLEC Algorithm to solve the problem. Least squares cell based for gradient term, second order upwind scheme for momentum and energy equations, as presented in the following figure:

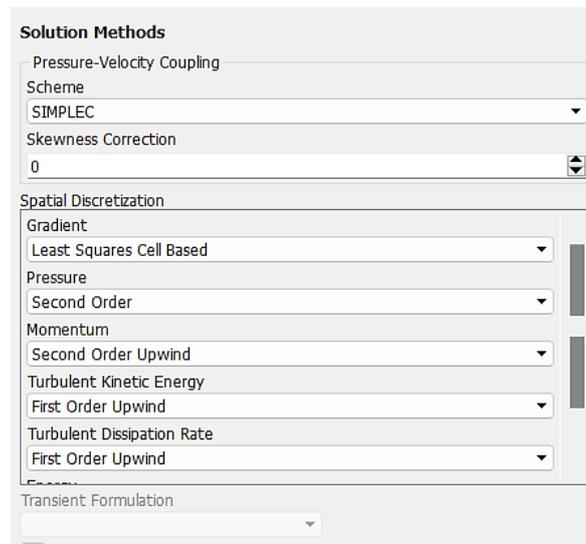


Figure III. 22 Solution Methods.

➤ Solution Monitoring

In the solution monitoring which is an important part for determining the accuracy of meshing, physical model and problem setup. In the current work we set the residual at 10^{-06} for the energy equation, and at 10^{-03} for all of continuity, velocity, and k-epsilon equations this gives :

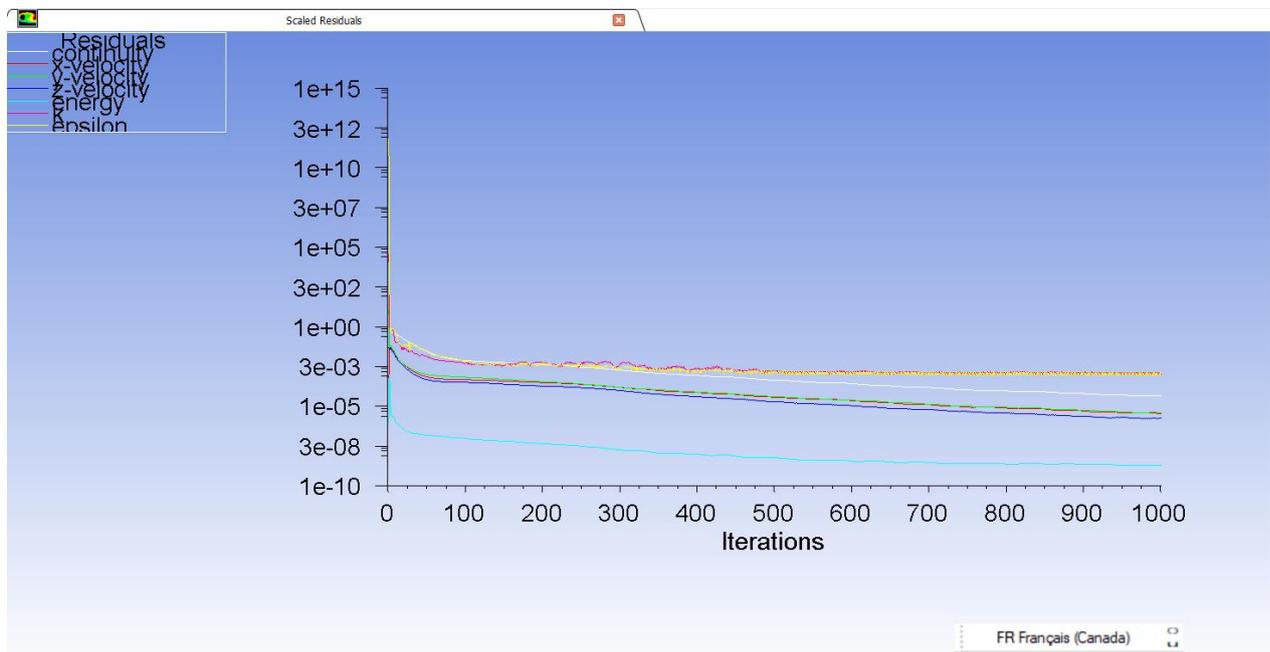


Figure III. 23 Scaled Residuals.

III 7 Conclusion

In this chapter we discussed discretization techniques, including volume methods and CFD . we explored the application of ANSYS Fluent for simulations and emphasized our work's post-

processing Using ANSYS to Analyze the results. It serves as a comprehensive overview of our approach and findings in the field of numerical analysis and simulations.

In the next chapter we will delve into the presentation of the results derived from the numerical methods and simulation discussed. This will provide a clear and detailed understanding of the outcomes of our work and the insights gained from the application of these techniques.

CHAPTER IV
RESULTS AND DISCUSSION

IV 1 Introduction

In this last chapter we will present our results of the Numerical study obtained by the calculation code used. Which was titled Numerical study of the influence of air velocity on the cooling of hot cylindrical blocks. We have used ANSYS Fluent 18.2, which we have discussed in the previous chapter, to solve our problem.

In the current study we investigated the impact of air velocity on cooling. We conducted experiments of forced convection with two different power value, 50 watts, and 70 watts, for number of Prandtl of air $Pr=0.7$, that we varied the air velocity from 0.5m/s to 3m/s for each power value, and this is what we will discuss in this chapter.

IV 2 Mesh choice

Mesh		Noeuds	Elements
A	2	605062	2841007
B	2.5	328324	1473696
C	3	204233	880257

Table IV. 1 Noeuds and elements for different meshes.

The table above represent different meshes which we defined for the choice of our study .we did it for , then we got the following results:

For the temperature exchanges we got for the three different mesh as follow:

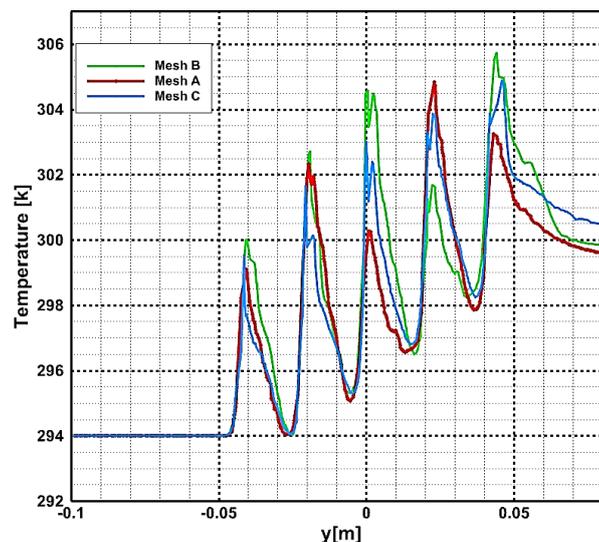


Figure IV. 1 Temperature profile for different Mesh in y direction.

And for the velocity profile for these different meshes we got the following profile:

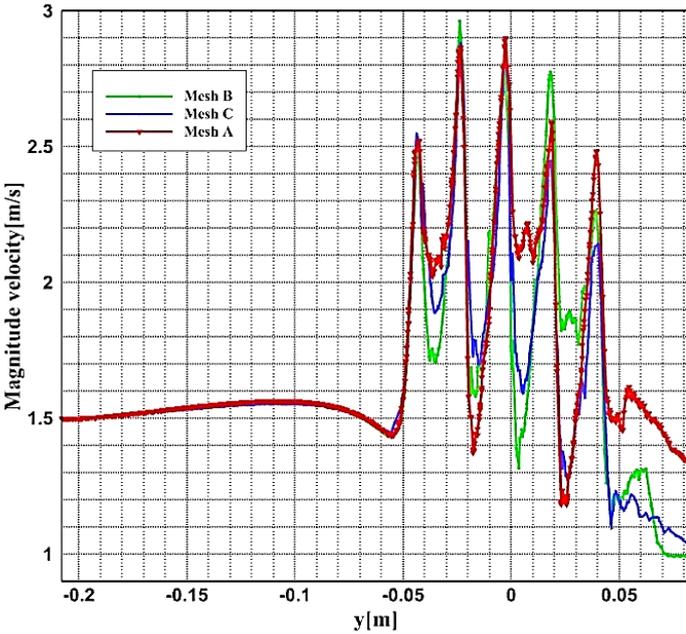


Figure IV. 2 Velocity profiles for different meshes in y direction.

In the current study we use Mesh A which has the biggest number of nodes and elements, this allow for a high level of accuracy and precision in our calculation. Knowing that our model is complex and has a lot off detailed, this why a finer mesh can provide more intricate details and more reliable results.

The following results was done in different planes , horizontal plane with $z = 5\text{ mm}$ for temperature contours, vertical plane with $x = 0\text{ mm}$ for temperature exchanges through pins, when the profiles was in a middle line in y direction.

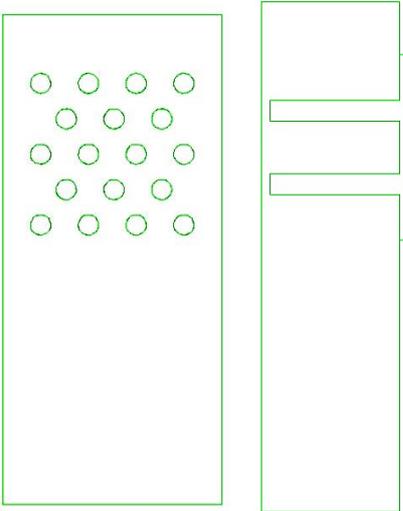


Figure IV. 3 xy plane and yz plane.

IV 3 Volume rendering

The volume rendering is a tool for visualizing and understanding the behavior of airflow in the complex 3D model, in our domain its show us the behavior of the fluid over the pins fin surfaces as its presented in the following figures:

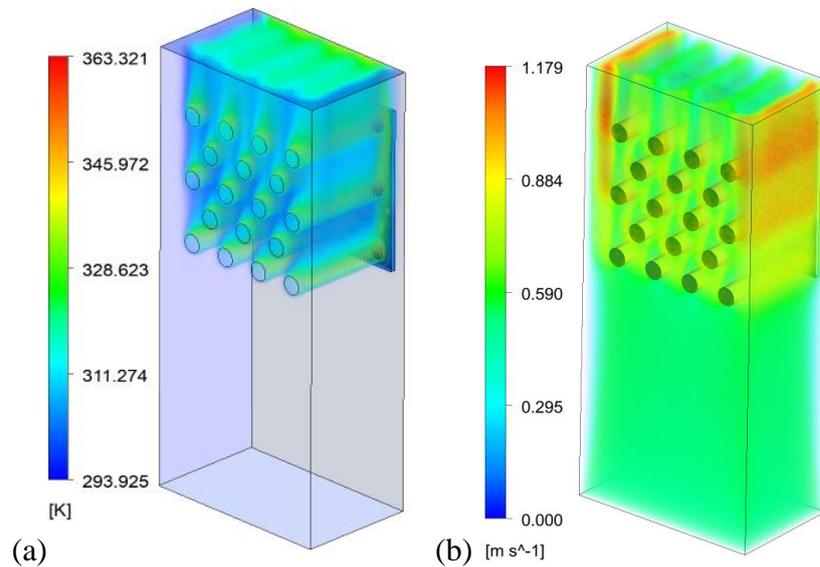


Figure IV. 4 (a) Temperature volume rendering, (b) velocity volume rendering, $V=0.5$ m/s, $P= 70$ watts.

IV 4 Velocity influence

IV 4 1 For $P= 50$ watts

IV 4 1 1 Contours and streamlines

We have an air flow around a row of hot tubes, there is a forced convection between the tubes surfaces and the incoming air , causing the increase of air temperature due to the heat transfer process involved, when air is forced to circulate around the hot tubes its absorb the heat from them, thereby increasing its temperature. This is what causes the pipes to lose their heat as result of the cooling process.

When the air velocity is low compared to the temperature of the pins , the effect on tubes temperature is minimal. However, as we increase the air velocity, we observe a noticeable improvement in the air's ability to cool. This acceleration of air results in enhanced cooling efficiency, meaning that the higher the air velocity, the more effective and rapid cooling becomes.

About the velocity exchanges we find that it increase around the tubes.

In this case we present the result of different air velocity $V= 0.5, 1, 1.5, 2, 2.5, 3$ m/s on the cooling of the tubes the grashof number is varied as $Gr = 4 \times 10^6, Gr = 3 \times 10^6$,

$Gr = 2.9 \times 10^6$, $Gr = 2.7 \times 10^6$, $Gr = 2.5 \times 10^6$, $Gr = 4 \times 10^6$. The results are explained in the following figures

➤ **Velocity = 0.5m/s, $Gr = 4 \times 10^6$**

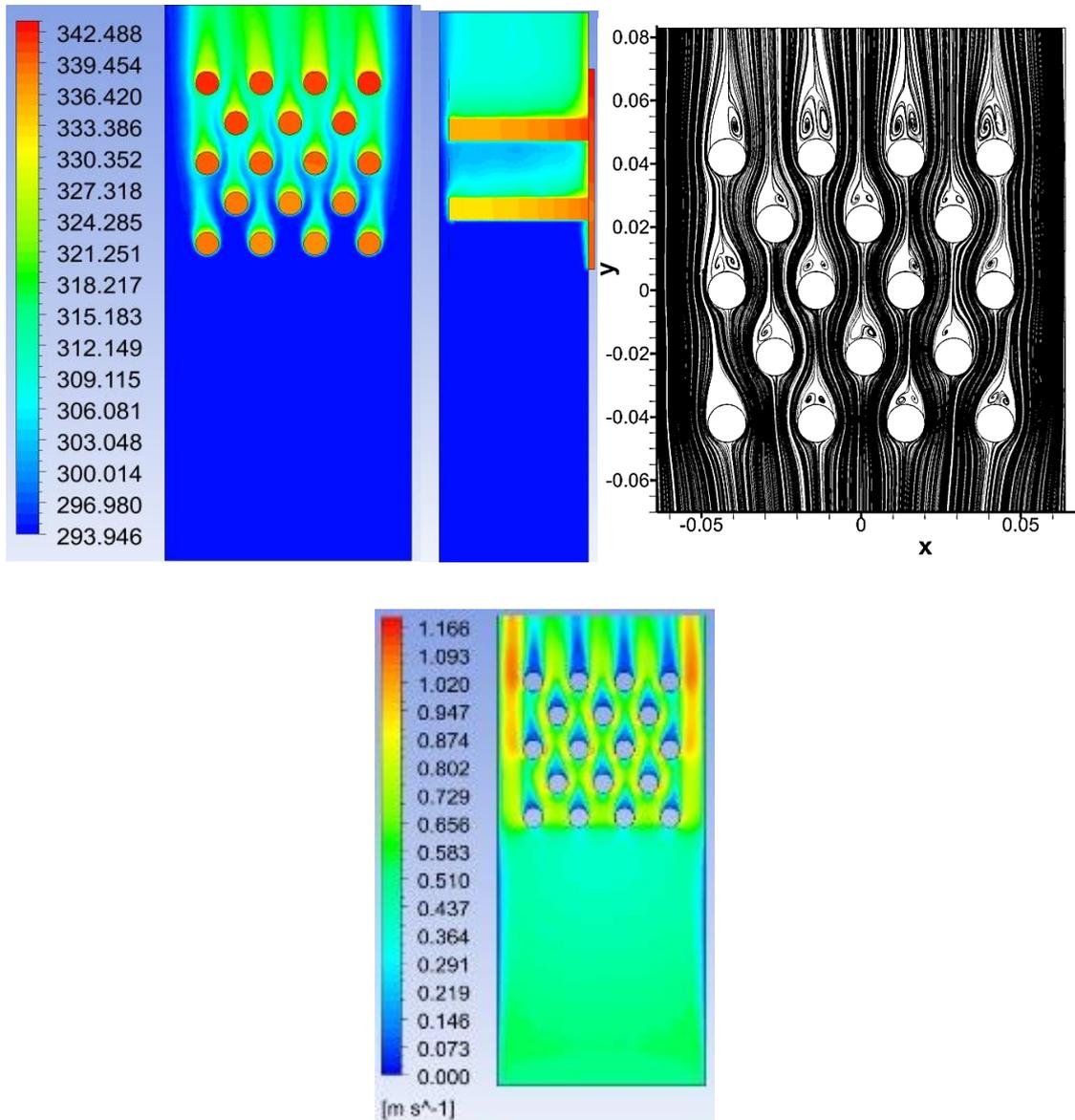


Figure IV. 5 Temperature, velocity contours and streamlines $v=0.5\text{m/s}$.

➤ Velocity = 1m/s, $Gr = 3 \times 10^6$

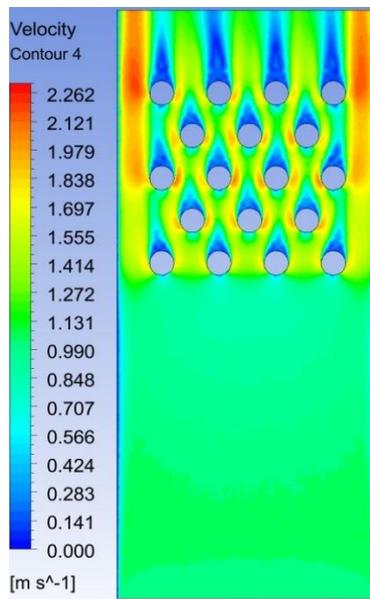
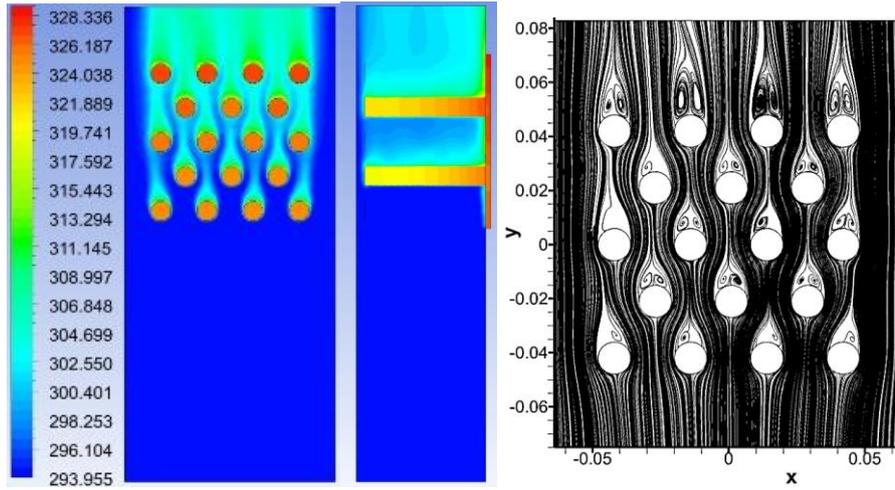
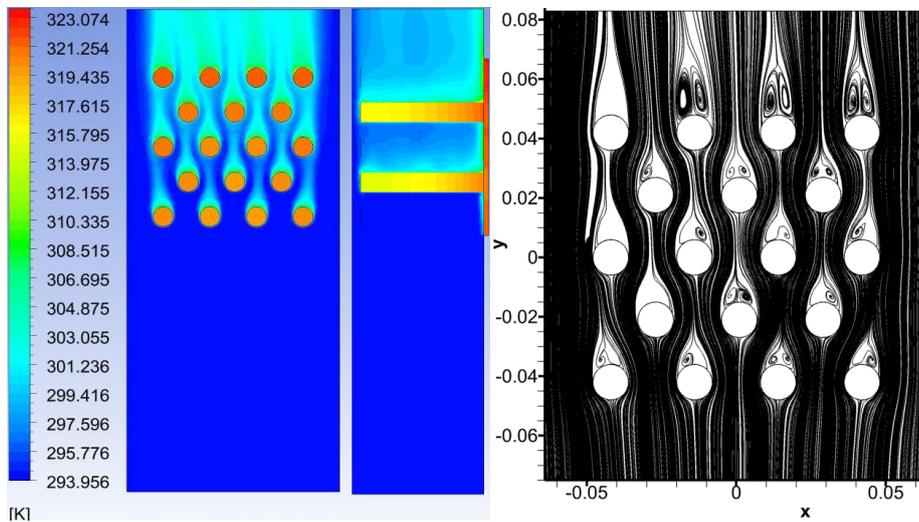


Figure IV. 6 Temperature, velocity contours and streamlines $v=1$ m/s.

➤ Velocity = 1.5m/s , $Gr = 2.9 \times 10^6$



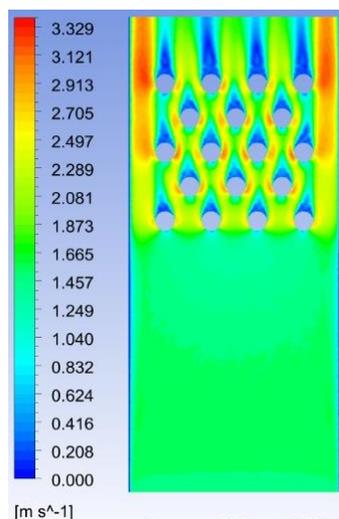


Figure IV. 7 Temperature, velocity contours and streamlines $v = 1.5$ m/s.

➤ Velocity = 2m/s , $Gr = 2.7 \times 10^6$

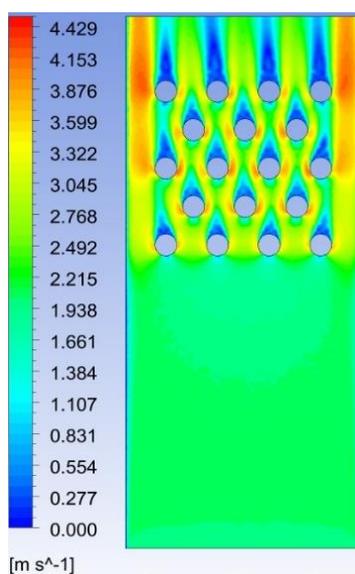
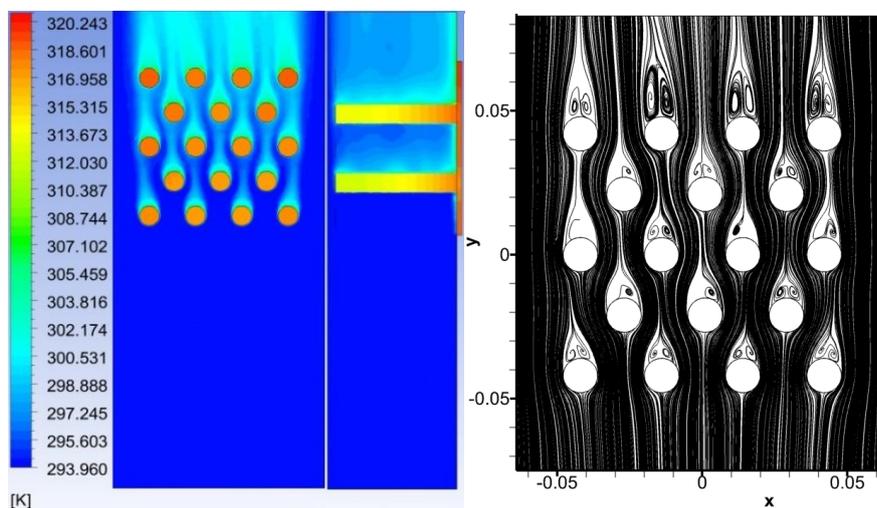


Figure IV. 8 Temperature, velocity contours and streamlines $v = 2$ m/s.

➤ Velocity = 2.5 m/s, $Gr = 2.5 \times 10^6$

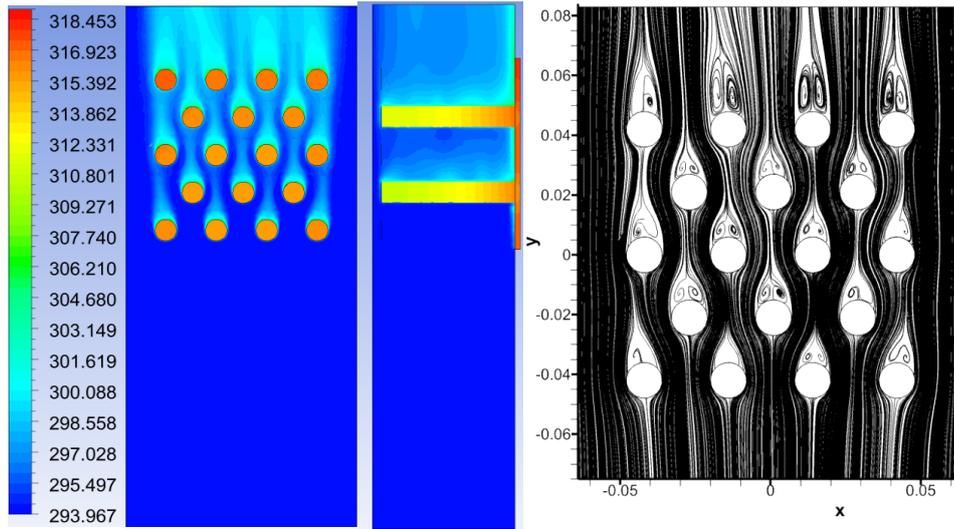
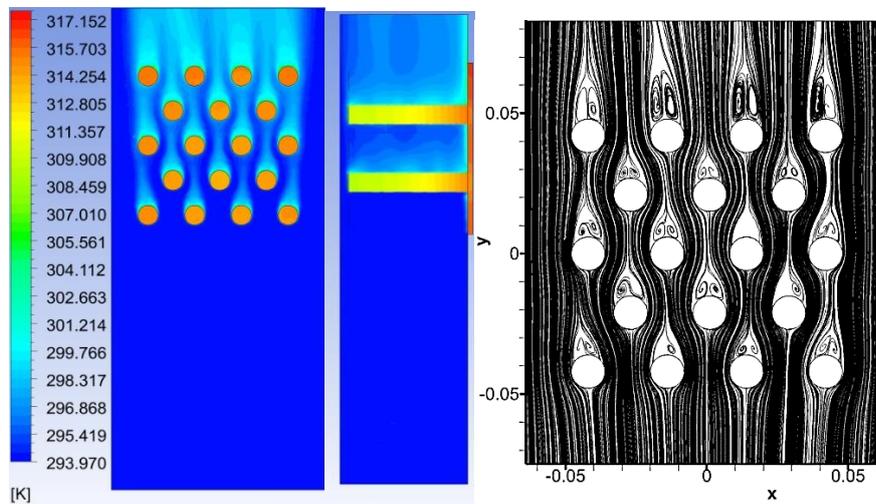


Figure IV. 9 Temperature, velocity contours and streamlines $v=2.5\text{m/s}$.

➤ Velocity = 3 m/s, $Gr = 2.4 \times 10^6$



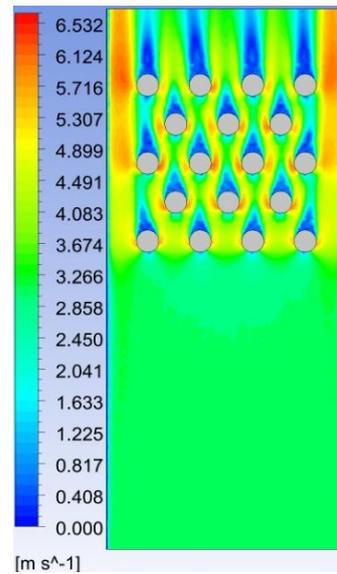


Figure IV. 10 Temperature, velocity contours and streamlines $v=3$ m/s.

IV 4 1 2 Profiles

– Temperature profile in y direction

As its shown in the following profile the temperature in y direction which we did it in a middle line, show the influence of air velocity on the cooling of hot pins.

When the air velocity is low , the air absorbs more temperature then in the higher velocity. This why the air temperature when $V=0.5$ m/s is the highest temperature compared to the other velocities.

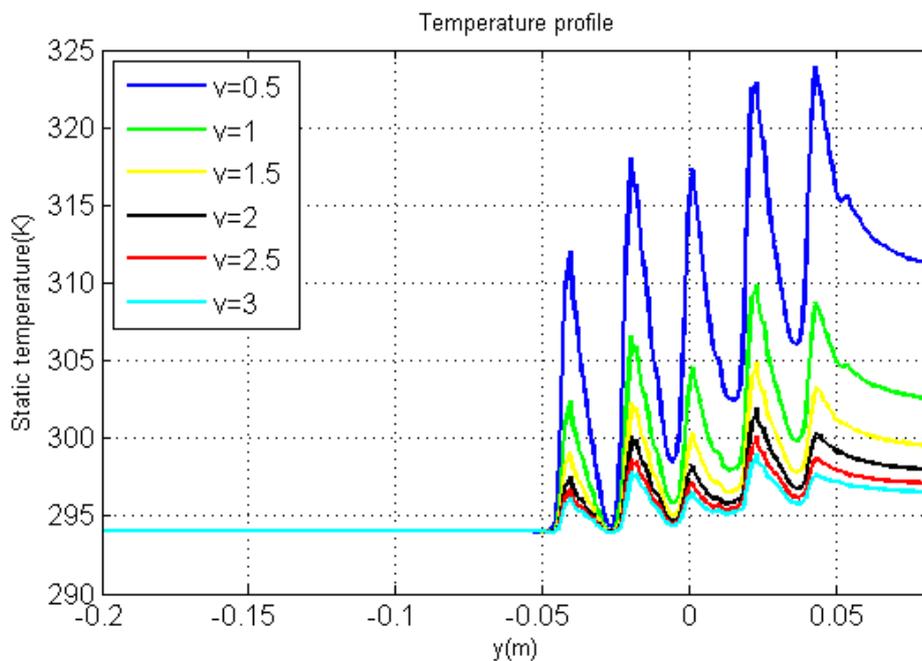


Figure IV. 11 Temperature profiles for $P=50$ Watts.

– **Pins temperature profile**

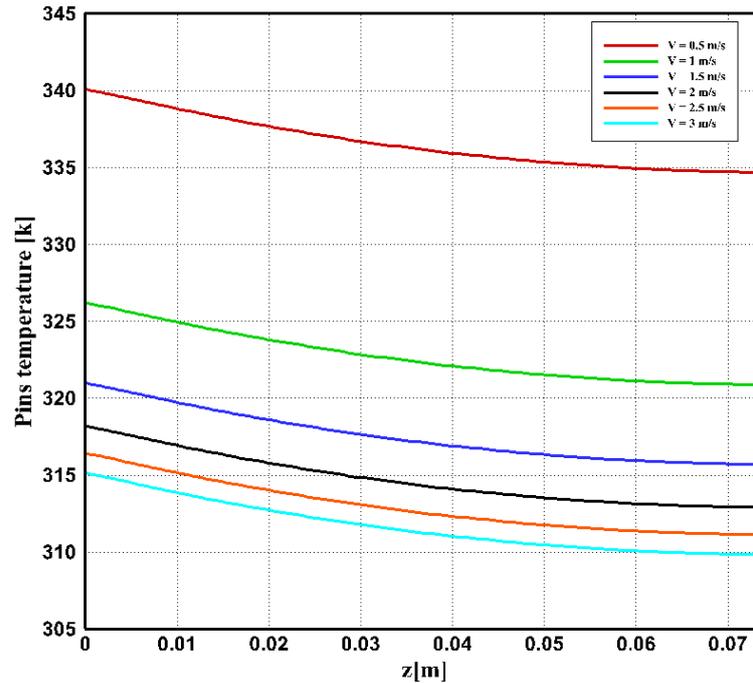


Figure IV. 12 Temperature profile in pins for $P=50$ watts.

In the pins, the temperature decrease by the increase of air velocity. And the temperature changes of the pins compared to the changes in air temperature are inversely related, as when the pins temperature decreases, the air temperature increases, along with its speed.

– **Velocity profile**

The different air velocity changes over the position of air, as its shown in the following figure the air velocity increase when the air surrounding the pins, this due to the increase of its temperature in the contact with the pins surfaces.

Increasing the airflow speed around the cylinders contributes to their cooling process. When the air moves at a higher speed around the cylinders, heat transfer from these cylinders to the air is enhanced. And this helps effectively reduce the temperature of the cylinders and maintains their good performance.

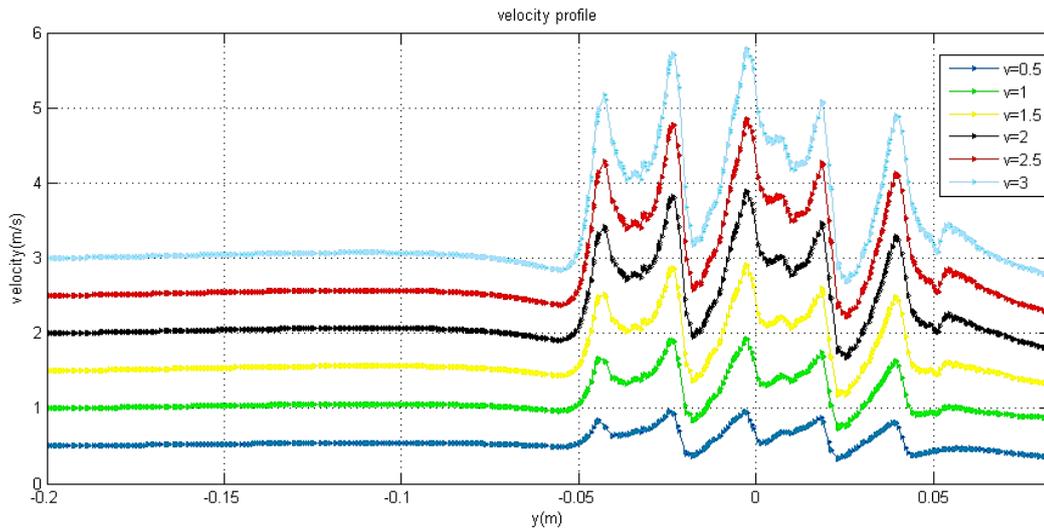


Figure IV. 13 Velocity profiles for $P=50\text{Watts}$.

IV 4 1 3 Average Nusselt number and Reynolds number

For the variation of the velocity from 0.5 to 3 m/s we calculated the Average Nusselt number and Reynolds number, presented in the table below.

Based on these results we find that there is a proportional relationship between Reynolds number and Nusselt number, where this last increases with the increase in Reynolds number and air velocity.

Table IV. 2 Average Nusselt number, and Reynolds number values for V from 0.5 to 3 m/s.

Velocity magnitude m/s	Reynolds number	Average Nusselt number
0.5	950.45	26.74
1	1844.08	37.25
1.5	2770.09	45.65
2	3711.92	52.85
2.5	4693.33	59.42
3	5548.095	64.60

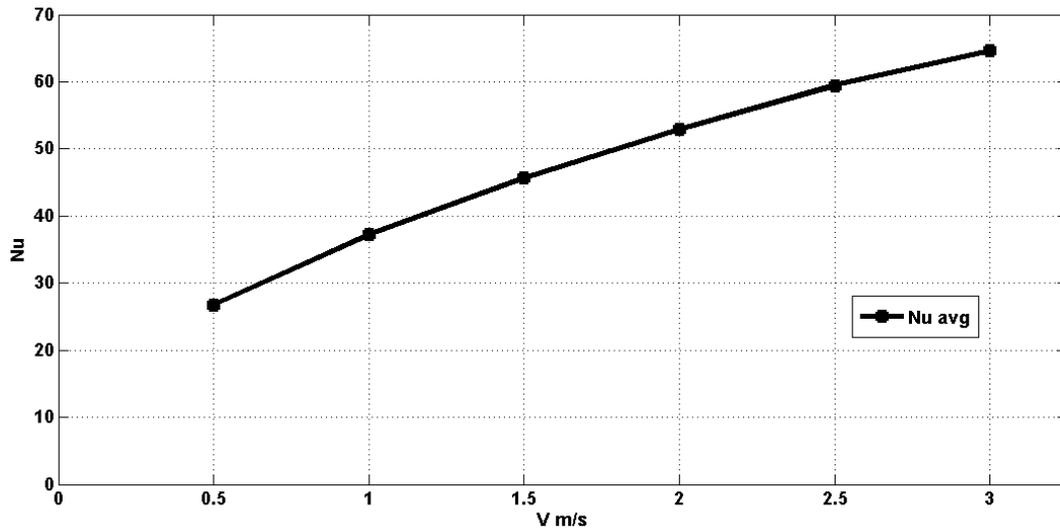


Figure IV. 14 Average Nusselt number VS velocity from 0.5 to 3m/s.

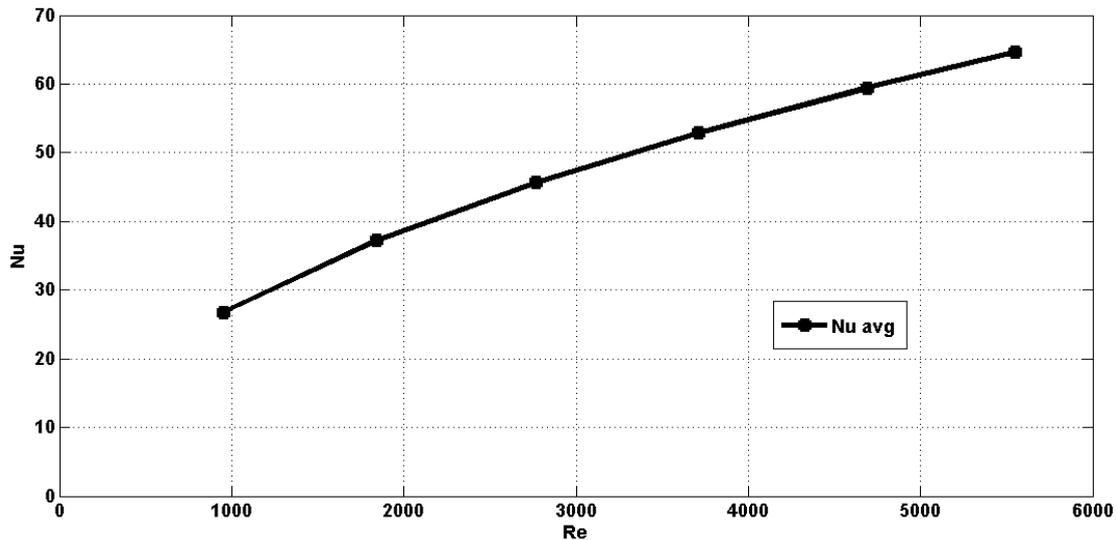


Figure IV. 15 Average Nusselt number VS Reynolds number.

As the Reynolds number increase within the turbulent flow regime, the Nusselt number typically also increase. This indicates that as the flow becomes more turbulent, heat transfer generally becomes more efficient due to increased convective heat transfer.

IV 4 2 For P =70 watts

IV 4 2 1 Contours and streamlines

➤ **Velocity =0.5m/s , $Gr = 5 \times 10^6$**

In the second case we changed the power, by kipping the same mesh and same other conditions and change the velocity from 0.5 to 3m/s this presented in following result :

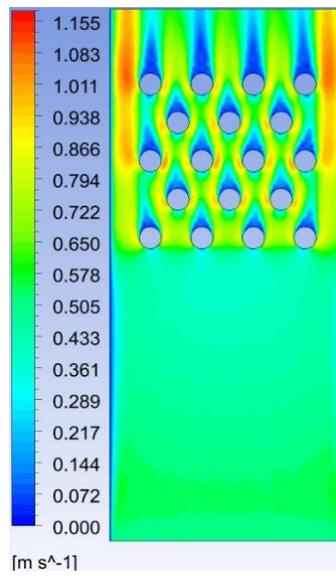
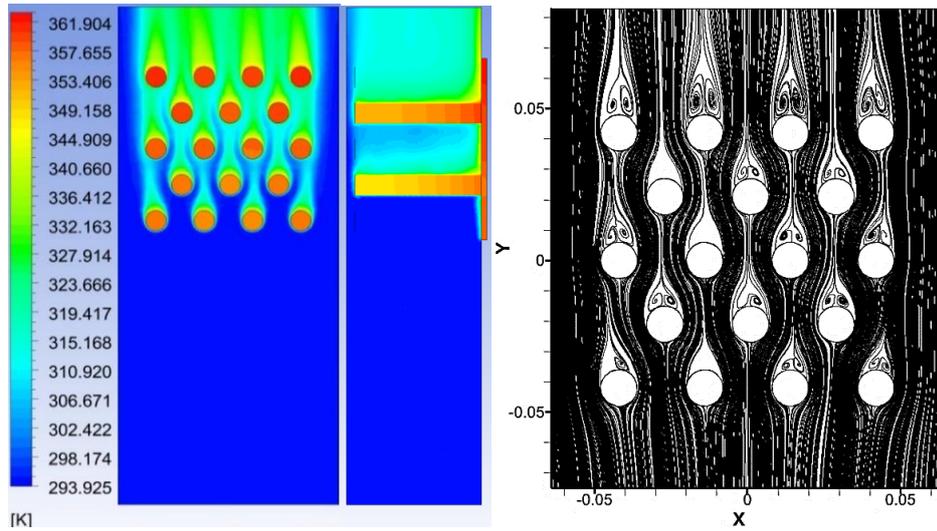
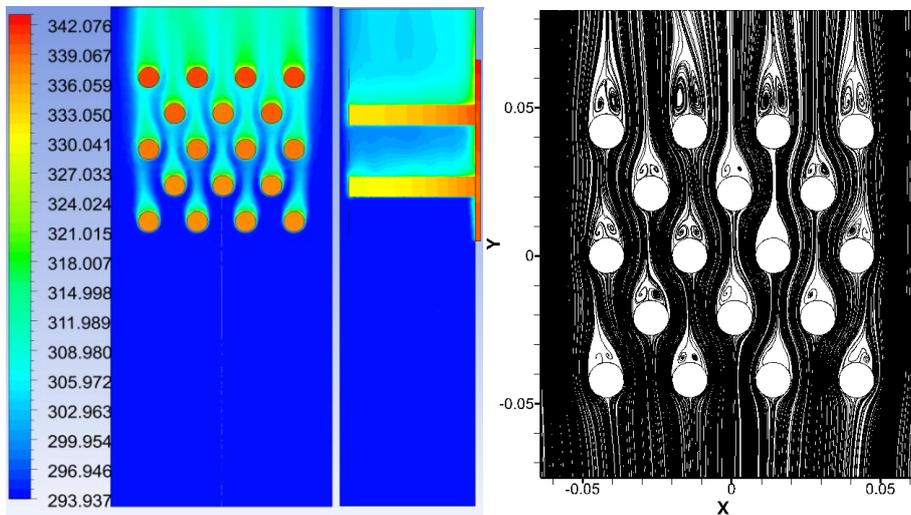


Figure IV. 16 Temperature, velocity contours and streamlines $v=0.5\text{m/s}$.

➤ Velocity =1 m/s , $Gr = 4 \times 10^6$



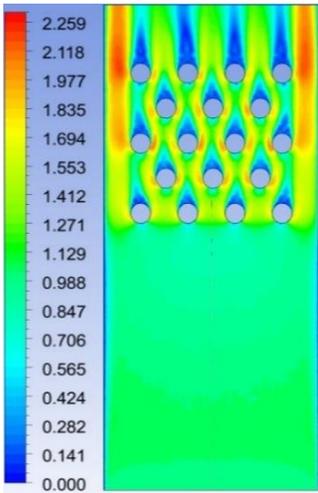


Figure IV. 17 Temperature, velocity contours and streamlines $v=1m/s$.

➤ Velocity =1.5 m/s , $Gr = 3 \times 10^6$

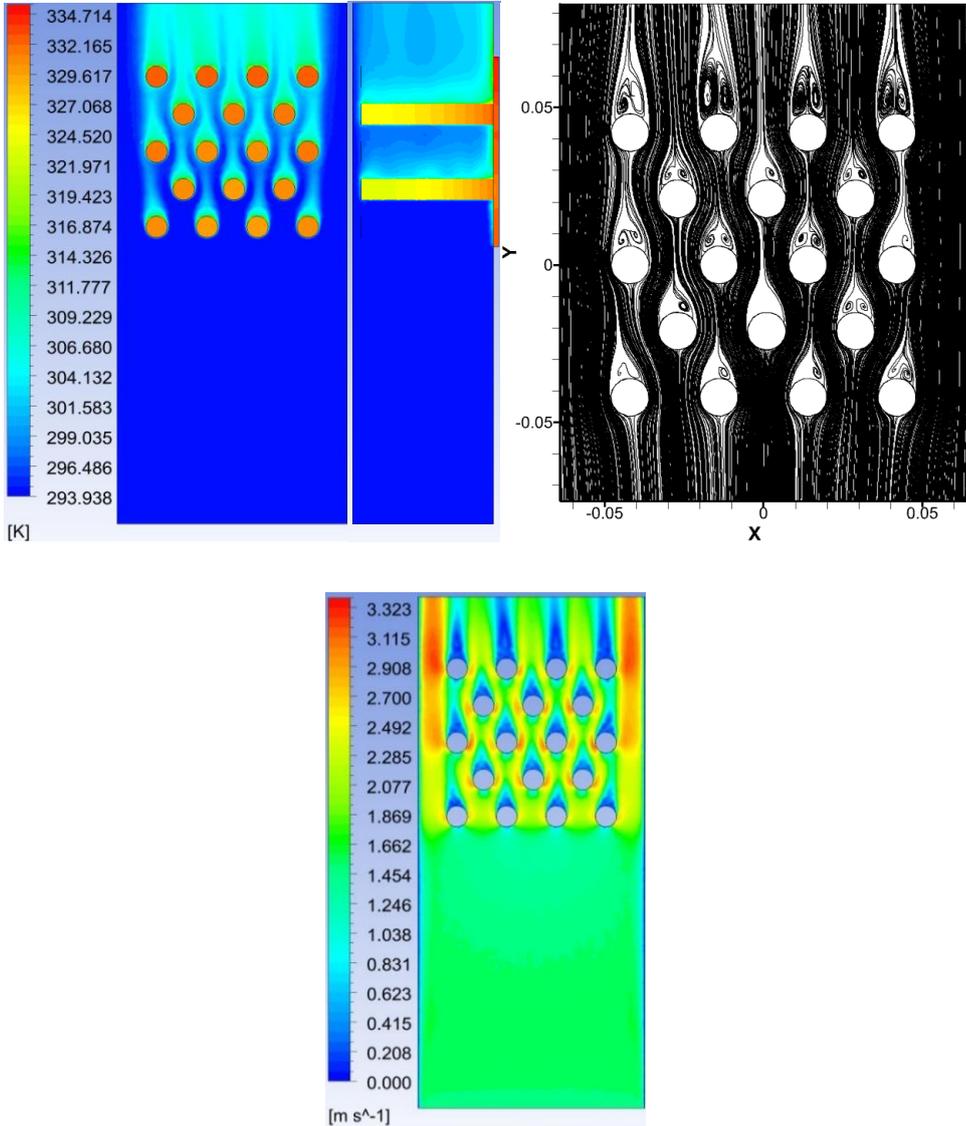


Figure IV. 18 Temperature , velocity contours and streamlines $v=1.5m/s$.

➤ Velocity = 2 m/s, $Gr = 3 \times 10^6$

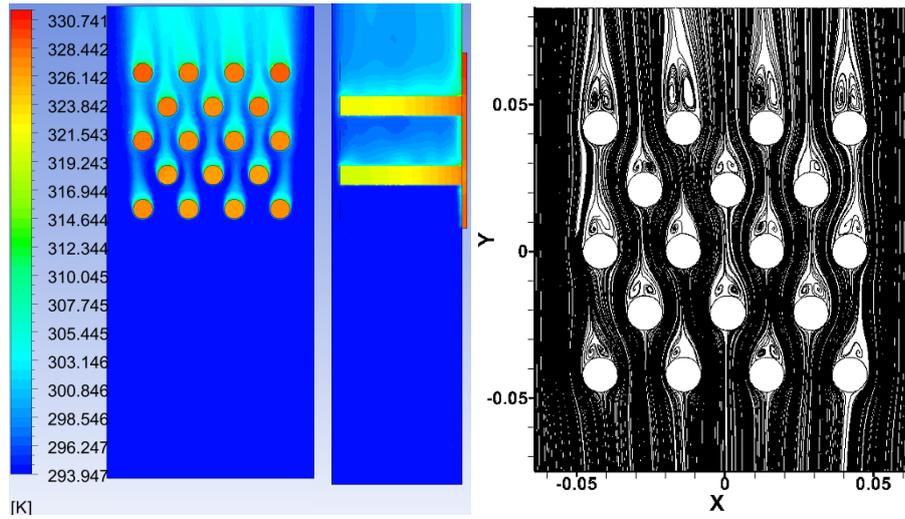
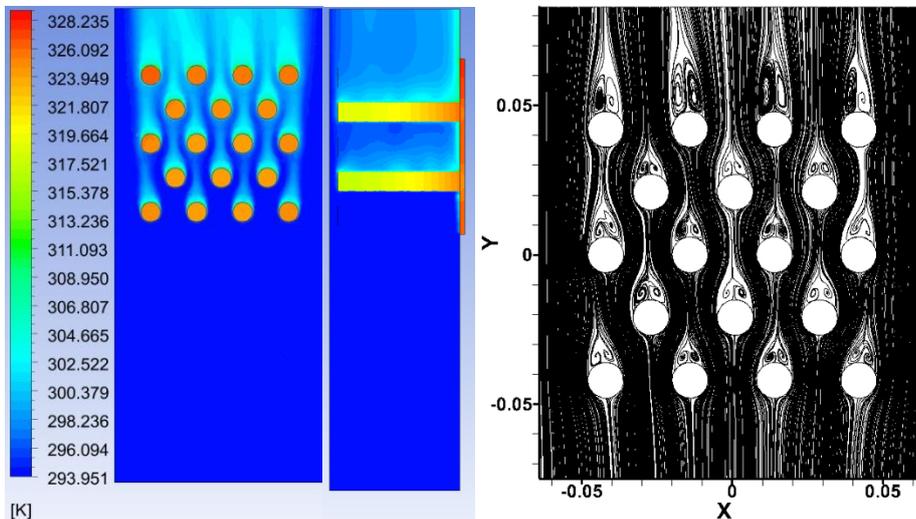


Figure IV. 19 Temperature, velocity contours, and streamlines $v = 2\text{m/s}$.

➤ Velocity = 2.5 m/s, $Gr = 2 \times 10^6$



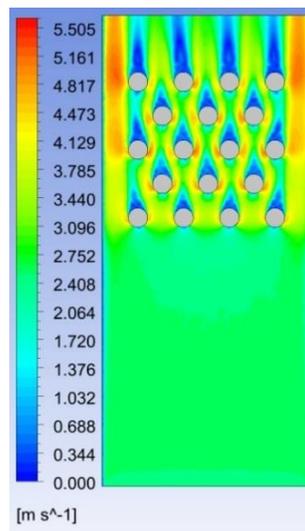


Figure IV. 20 Temperature, velocity contours, and streamlines.

➤ Velocity = 3 m/s, $Gr = 2 \times 10^6$

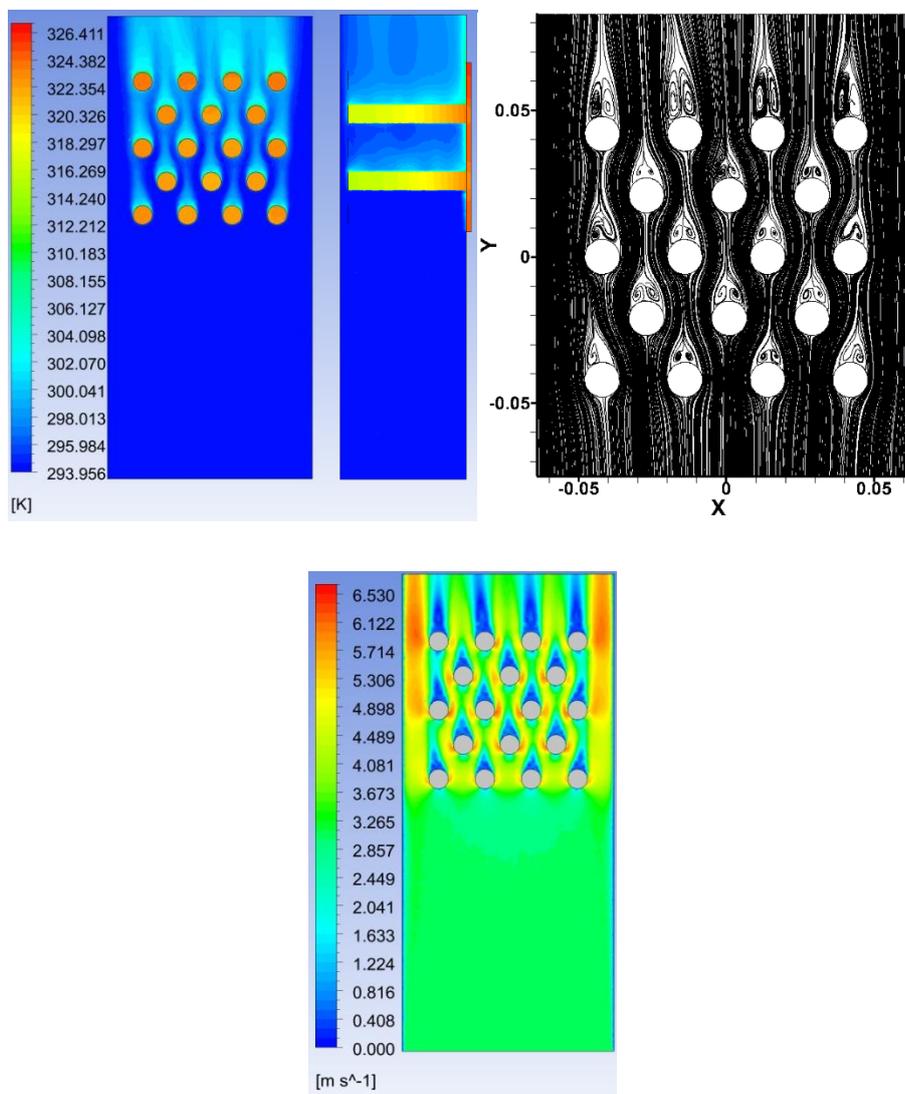


Figure IV. 21 Temperature, velocity contours, and streamlines $v=3\text{m/s}$.

IV 4 2 2 Profiles

➤ Temperature profile

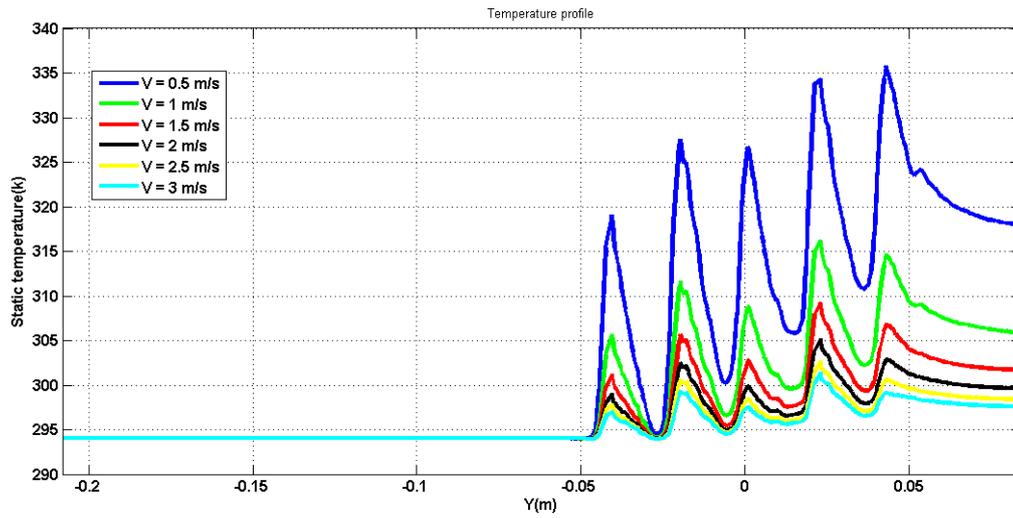


Figure IV. 22 Temperature profile for $P=70$ watts, Velocity from 0.5 to 3m/s.

➤ Pins temperature profile

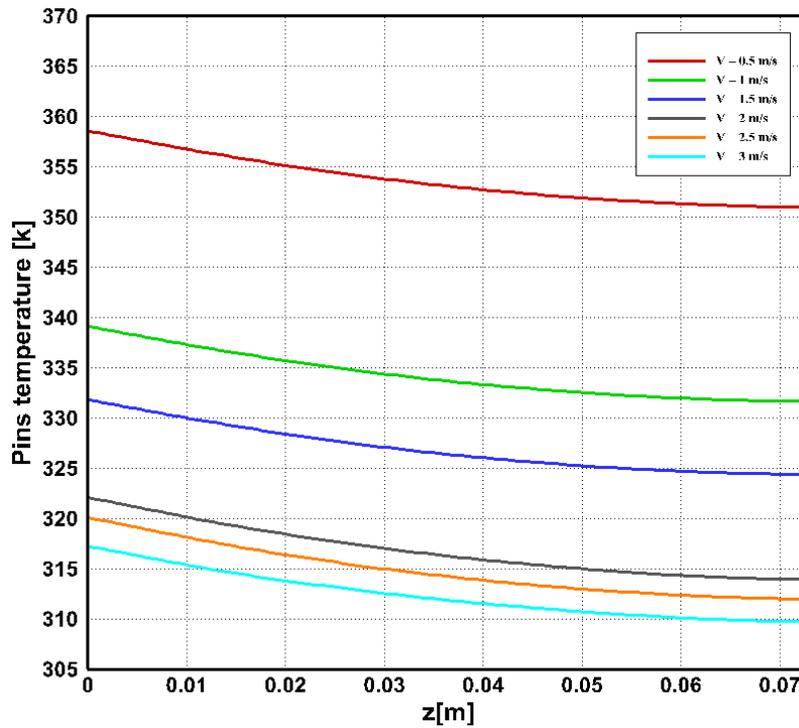


Figure IV. 23 Temperature profile through Pins.

➤ **Velocity profile**

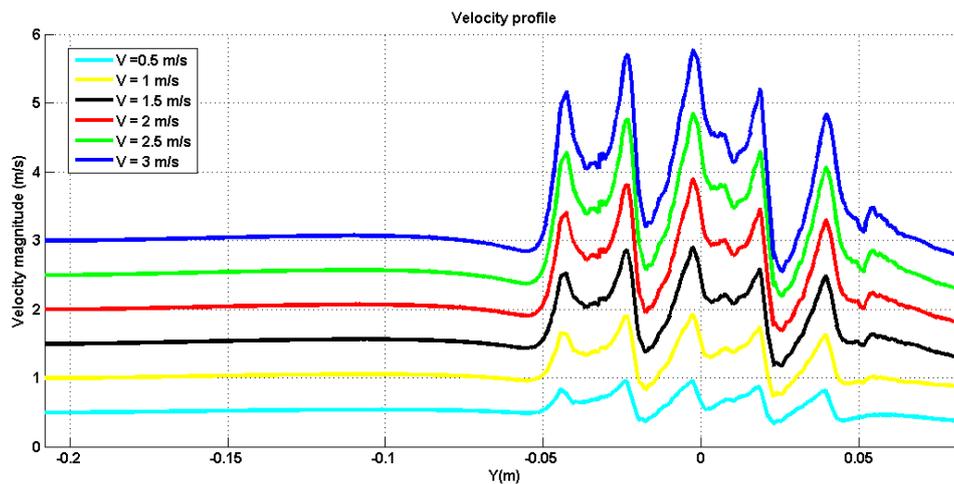


Figure IV. 24 Velocity profile for $P=70$ watts, velocity from 0.5 to 3m/s.

IV 4 2 3 Average Nusselt number and Reynolds number for $P=70$ watts

For power $P = 70$ watts, the average number and Reynolds number changed as the same manner as in $P=50$ watts, and we remark a little different between them due to the heat increase in the pins fin surfaces.

Table IV. 3 Average Nusselt number and Reynolds number for V from 0.5 to 3 m/s.

Velocity magnitude m/s	Reynolds number	Average Nusselt number
0.5	933.92	26.51
1	1852	37.33
1.5	2809.66	45.98
2	3719.84	52.9
2.5	4701.24	59.47
3	5546.52	64.59

The following figures represent the graphics of the table values :

The following curves represent the changes of Nusselt number as function of velocity and Reynolds number.

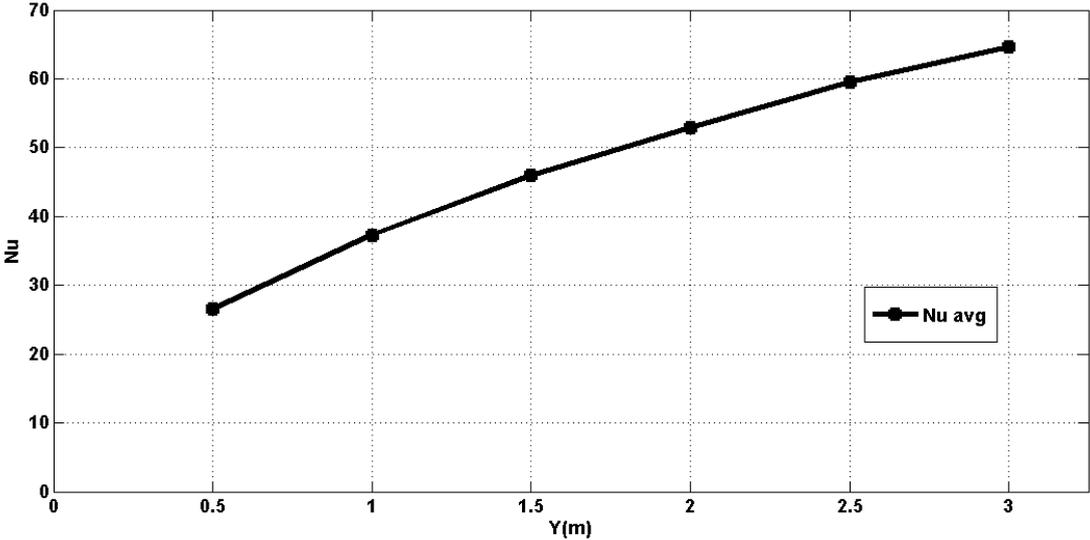


Figure IV. 25 Average Nusselt number Vs velocity magnitude.

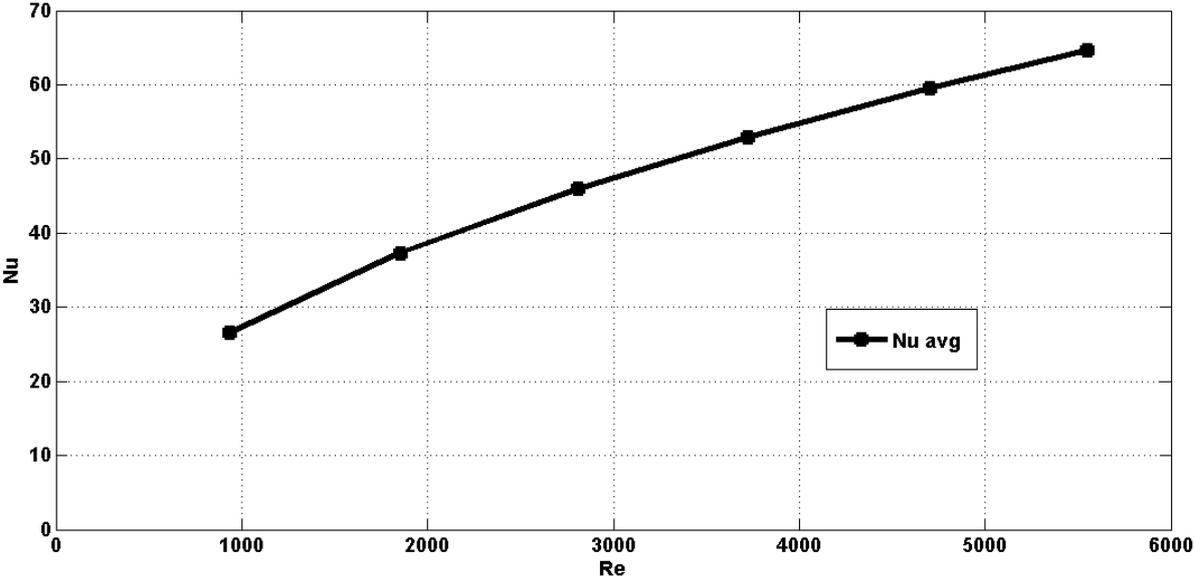


Figure IV. 26 Average Nusselt number Vs Reynolds number.

IV 5 Power influence

In the first section we were presented the influence of air velocity on the result, in this section we are going to talk about the influence of power on the results. To do this, we adjusted the velocity to a value of 1.5 m/s and changed the power, this what we clarify in the following pictures:

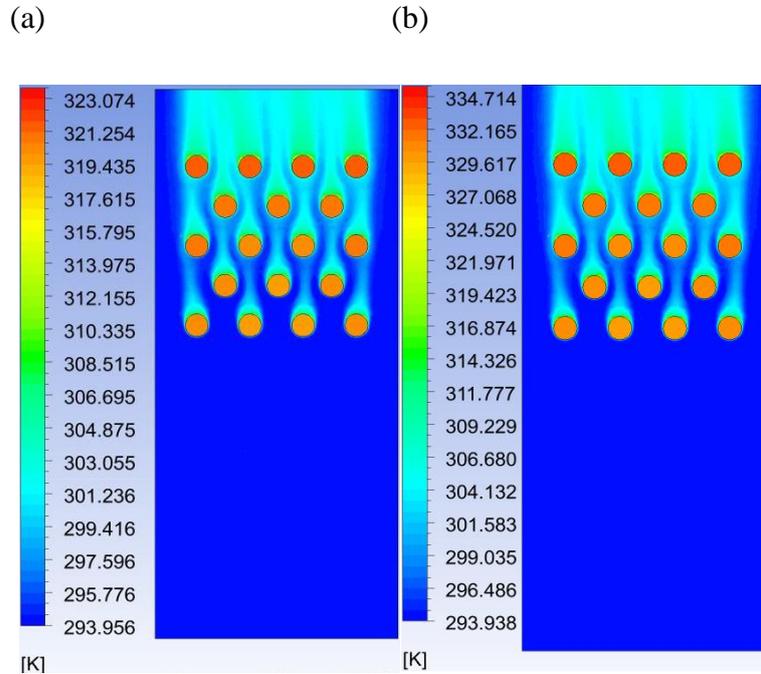


Figure IV. 27 Temperature contours for $v=1.5\text{m/s}$. (a) $P=50\text{ W}$. (b) $P=70\text{ W}$.

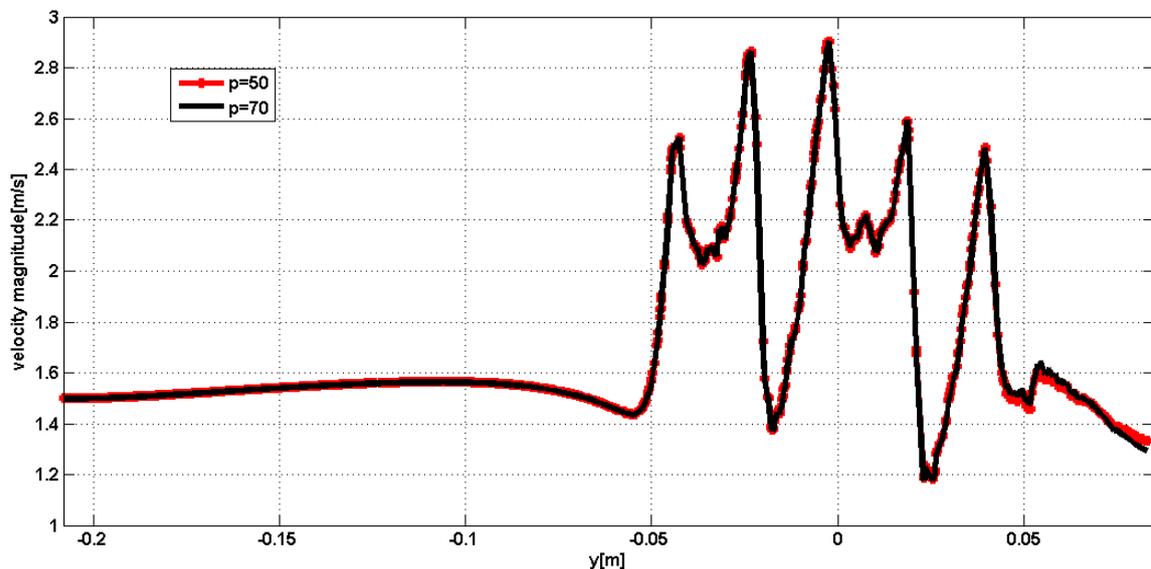


Figure IV. 28 Influence of power on air velocity.

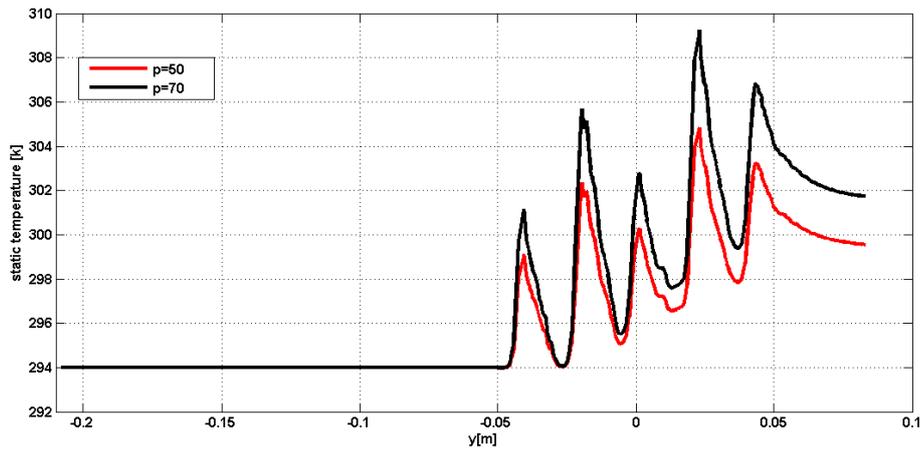


Figure IV. 29 Influence of power on temperature.

The results indicate that the change of power which involved change of the heat flux through the pin fin. When we increase the power value from 50 watt to 70 watt, the heat flux over the pin fin typically increase this what makes the temperature of pins fin higher than the temperature for 50 watt. For that it need more high air velocity and time for the cooling.

Also the air when the power is $P=70$ watts, gains more heat than when it's 50 watts.

IV 6 Turbulence

IV 6 1 Turbulent kinetic energy contours and profiles

We did the study for three different velocity 1m/s, 2 m/s, 3 m/s respectively and we obtained the following results:

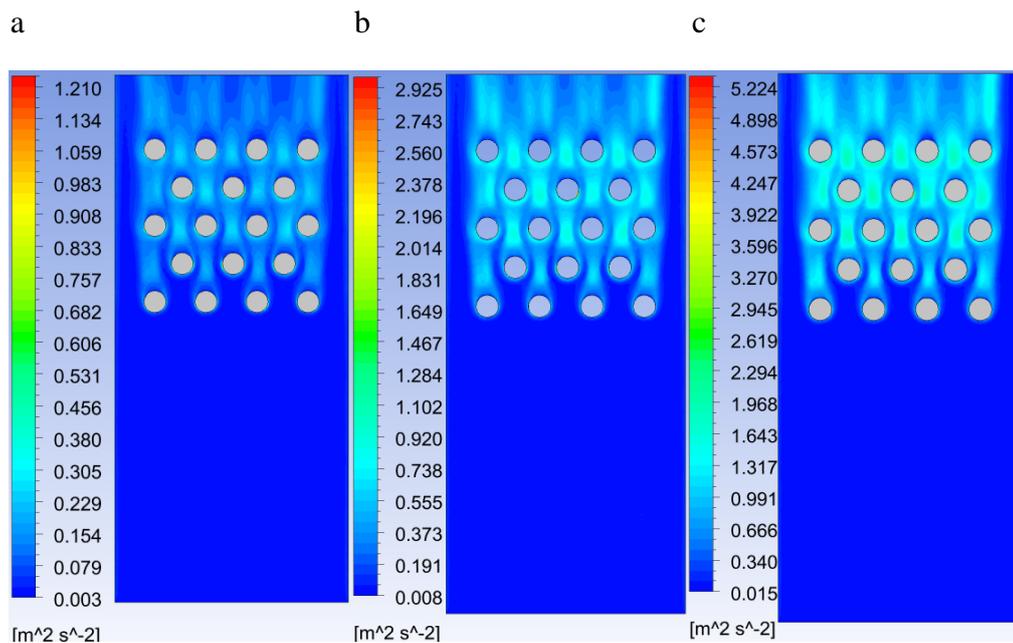


Figure IV. 30 Turbulent kinetic energy contours, a) 1m/s, b)2m/s, c) 3 m/s.

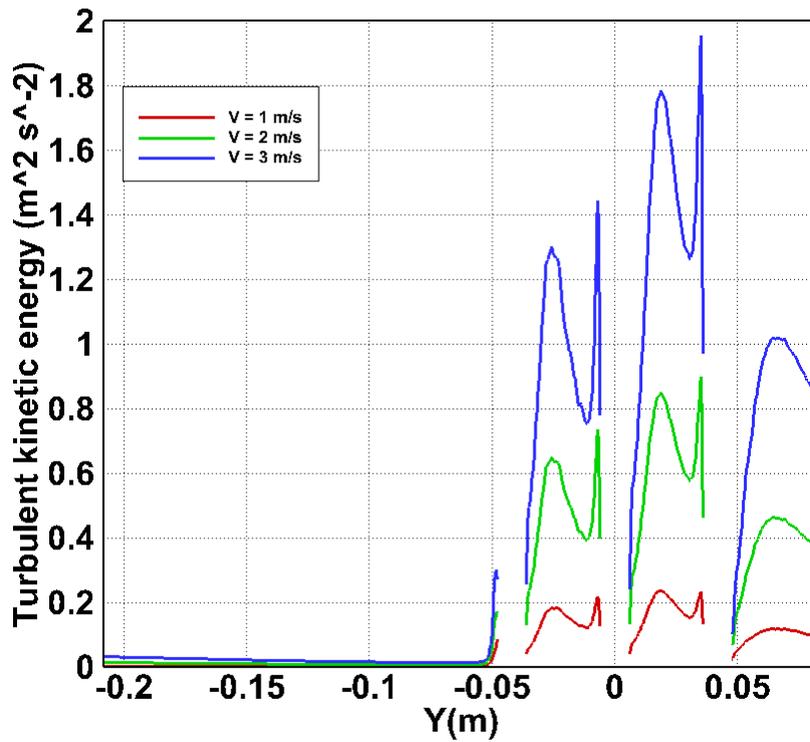


Figure IV. 31 Turbulent kinetic energy profiles.

IV 6 2 Eddy viscosity contours and profiles

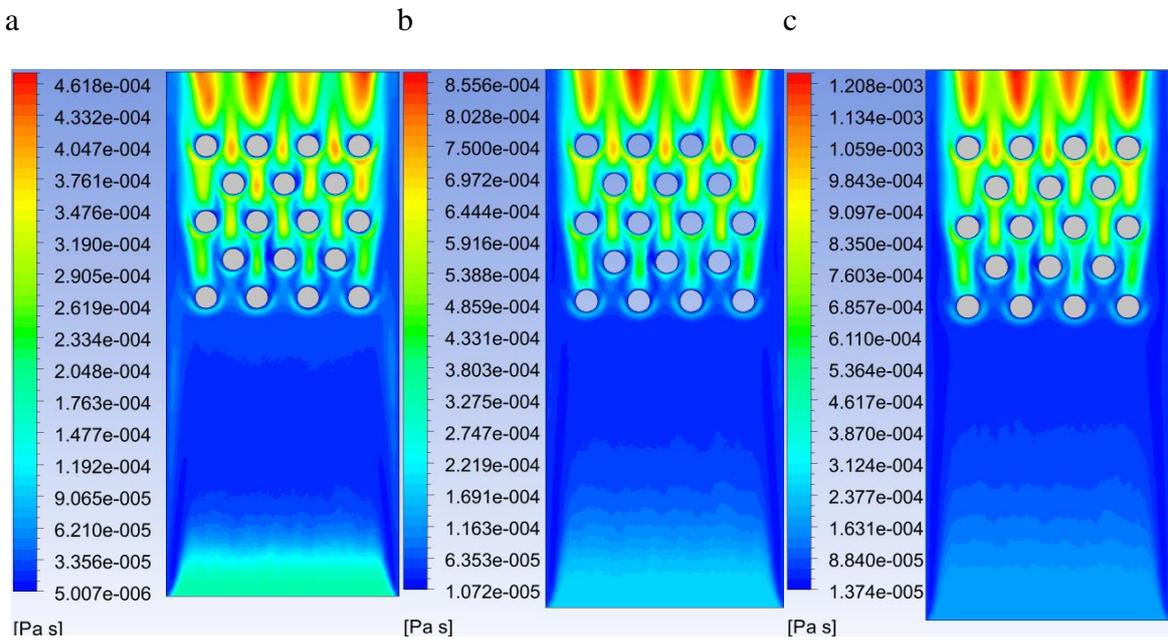


Figure IV. 32 Eddy viscosity, a) 1 m/s, b) 2 m/s, c) 3 m/s.

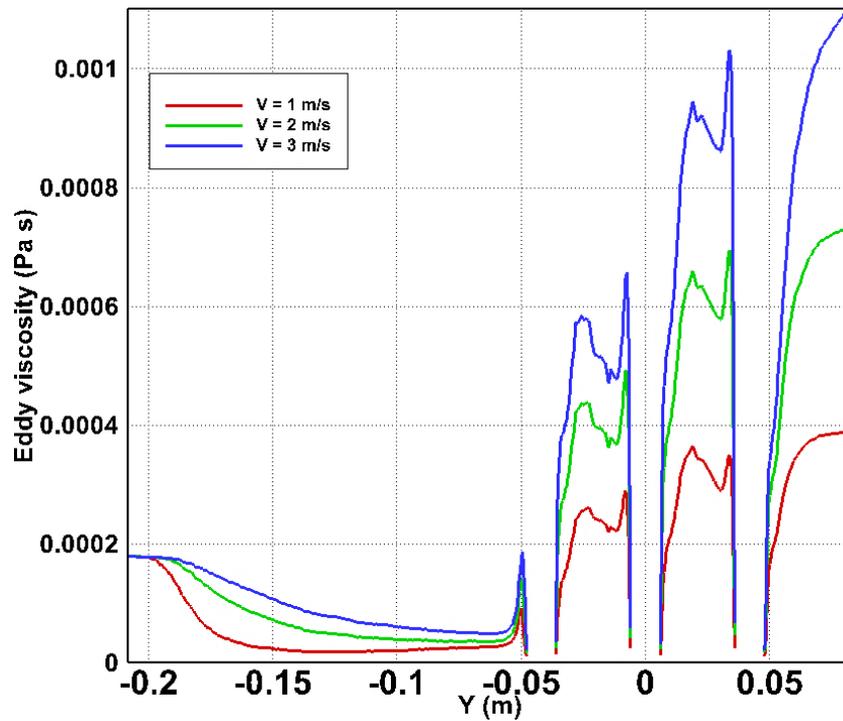


Figure IV. 33 Eddy viscosity profiles.

The increase in turbulent kinetic energy and viscosity in the areas between the hot cylinders can be explained as follow:

As air passes between these hot cylinders, it repeatedly changes direction and speed to flow around the obstacles, this continuous change in direction and speed leads to the formation of many vortices and turbulent disturbances in these areas. These vortices represent an additional source of kinetic energy in these regions, increasing the kinetic energy of the air.

Due to the increase in interference and disturbances in these areas, the level of air viscosity also increases. Eddy viscosity which represents the internal resistance to turbulent flows, increases in parallel with the increase in turbulent kinetic energy, as there are more vortices, making the air more resistant to flow.

IV 7 Conclusion

In light of the findings derived from our study on the influence of air velocity on the cooling of heated cylinders, it has been determined that diverse methodologies can be employed to enhance the efficiency and expeditiousness of the cooling process.

Elevating the airspeed induces augmented airflow velocity surrounding the cylinders, consequently amplifying their cooling capacity and swiftness. Furthermore, the implementation of intelligent control systems for the modulation of cooling velocity in accordance with operational

conditions has proven to be advantageous. Moreover, the utilization of advanced cooling techniques, such as rapid cooling, offers promise in further optimizing cooling processes.

GENERAL CONCLUSION

GENERAL CONCLUSION

This study examined the influence of air velocity on the cooling of hot cylindrical blocks using a three-dimensional numerical simulation. The findings indicated that the air velocity has a relevant impact on the cooling process, with increasing air velocity provoking a higher heat transfer rate. The optimum air velocity for cooling the cylindrical block based on the dimensions and configurations of the block, as well as the properties of the fluids involved.

The study was conducted using ANSYS Fluent, a commercial computational fluid dynamics (CFD) software package. The geometry of the cylindrical block was created in CAD software and imported into Fluent. The boundary conditions were set to represent the actual conditions of the cooling process. The air velocity was varied from 0.5 to 3 m/s, and the heat transfer rate was calculated at each velocity.

We also found that the air velocity has a considerable impact on the flow field around the cylindrical block. With increasing air velocity, the flow becomes more turbulent. Turbulence is a chaotic motion of the fluid, and it enhances the mixing of the warm and chilly fluids. This mixing increases the temperature gradient.

The optimum air velocity for cooling the cylindrical block also depends on the properties of the fluids involved. For example, the heat transfer rate is higher for fluids with a higher thermal conductivity.

The results of this study can be utilized to improve the the engineering of air-cooled heat exchangers and related equipment. It also provides insights into the complex interplay between air velocity and convective heat transfer.

In summary, the following are the key findings of the study:

- The air velocity profoundly influences the cooling of hot cylindrical blocks
- Increasing the air velocity causes an elevated thermal transfer rate.
- The optimum air velocity for cooling the cylindrical block based on the dimensions and configurations of the block, as well as the properties of the fluids involved.
- The air velocity has profoundly affects the flow characteristic surrounding the cylindrical blocks.
- Turbulence enhances the heat transfer rate.
- The results of current work can be made use of to develop the design of heat transfer devices and other devices that use air cooling.

REFERENCES

- [1] L. Area, V. Velocity, D. Force, M. Pressure, and D. V. Kinematic, “heat transfer tenth edition,” *Princ. Met. Manuf. Process.*, pp. 310–311, 1999, doi: 10.1016/b978-034073162-8/50017-5.
- [2] M. Moshinsky, *heat and mass transfer fundamentals & Applications*, vol. 13, no. 1. 1959.
- [3] M. Moshinsky, *introduction to heat transfer*, vol. 13, no. 1. 1959.
- [4] Imane, “Mechanisms of heat transfer Lecture 4,” *heat mass Transf. V5.p55*.
- [5] S. Mostafa Ghiaasiaan, *Convective Heat and Mass Transfer*.
- [6] H. Duz, “Numerical Investigation of the Transition Length at the Entrance Region of Pipe Flows,” vol. 2, no. 2009, pp. 101–110, 2018.
- [7] Y. A. Cengel and J. M. Cimbala, *Fluid Mechanics: Fundamentals and Principles*. 2010.
- [8] K. Thulukkanam, *Heat Exchanger Design Handbook, SECOND EDITION*. 2013. doi: 10.1201/b14877.
- [9] S. Steel and C. Plastics, “Types of Heat Exchangers and Their Selection (PDF) Classification of Heat Exchangers,” pp. 1–6, 2022.
- [10] T. J. Young and K. Vafai, “Convective cooling of a heated obstacle in a channel,” *Int. J. Heat Mass Transf.*, vol. 41, no. 20, pp. 3131–3148, 1998, doi: 10.1016/S0017-9310(97)00323-2.
- [11] S. O. O. Al-Omar and O. M. Ali, “Mixed convection from two horizontally aligned hot and cold circular cylinders in a vented square enclosure,” *Ain Shams Eng. J.*, no. November, p. 102048, 2022, doi: 10.1016/j.asej.2022.102048.

- [12] M. A. Hssain, R. Mir, and Y. El Hammami, “Numerical Simulation of the Cooling of Heated Electronic Blocks in Horizontal Channel by Mixed Convection of Nanofluids,” *J. Nanomater.*, vol. 2020, 2020, doi: 10.1155/2020/4187074.
- [13] A. Hamouche and R. Bessaïh, “Mixed convection air cooling of protruding heat sources mounted in a horizontal channel,” *Int. Commun. Heat Mass Transf.*, vol. 36, no. 8, pp. 841–849, 2009, doi: 10.1016/j.icheatmasstransfer.2009.04.009.
- [14] Y. J. Kim, M. Jeong, Y. G. Park, and M. Y. Ha, “A numerical study of the effect of a hybrid cooling system on the cooling performance of a large power transformer,” *Appl. Therm. Eng.*, vol. 136, no. March 2017, pp. 275–286, 2018, doi: 10.1016/j.applthermaleng.2018.03.019.
- [15] G. Zhao, X. Wang, M. Negnevitsky, and H. Zhang, “A review of air-cooling battery thermal management systems for electric and hybrid electric vehicles,” *J. Power Sources*, vol. 501, no. January, p. 230001, 2021, doi: 10.1016/j.jpowsour.2021.230001.
- [16] A. Bouras, S. Bouabdallah, B. Ghernaout, and A. Ghazel, “Convection forcée 3D dans un box contenant deux sources de chaleurs cylindriques,” 2018.
- [17] S. Ben L. and A. M., “Free and Forced Convection Effects,” *J. Hydraul. Eng.*, vol. 109, no. Paper No. 18234, pp. 1216–1229, 1983.
- [18] Pijush K. Kundu, I. M. Cohen, and David R Dowling, *Fluid Mechanics (6th edition)*. 2016.
- [19] Y. Cengel, M. Boles, and M. Kanoglu, *Thermodynamics_An Approach_Yunus Cengel*. 2019.
- [20] D. G. Hurst, “Engineering Heat Transfer,” *Nucl. Sci. Eng.*, vol. 18, no. 4, pp. 539–540, 1964, doi: 10.13182/nse64-a18784.

- [21] S. S. Mukrimaa *et al.*, *TURBULENCE*, vol. 6, no. August. 2016.
- [22] H. Rubin and J. Atkinson, “Introduction To Turbulence,” *Environ. Fluid Mech.*, 2001, doi: 10.1201/9780203908495.ch5.
- [23] P. R. & A. S. . (La R. A. Spalart, “RechAerosp_1994_SpalartAllmaras.pdf.” pp. 5–21, 1994. [Online]. Available: https://turbmodels.larc.nasa.gov/Papers/RechAerosp_1994_SpalartAllmaras.pdf
- [24] F. R. Menter, “Two-equation eddy-viscosity turbulence models for engineering applications,” *AIAA J.*, vol. 32, no. 8, pp. 1598–1605, 1994, doi: 10.2514/3.12149.
- [25] S. V. Patankar, “Numerical_Heat_Transfer_and_Fluid_Flow_Patankar.pdf.”
- [26] C. H. Forsberg, “Front Matter,” in *Heat Transfer Principles and Applications*, 2021, p. iii. doi: 10.1016/b978-0-12-802296-2.01001-5.
- [27] F. Moukalled, L. Mangani, and M. Darwish, *The finite volume method in computational fluid dynamics [Fluid Mechanics and Its Applications]*, vol. 113. 2016. doi: 10.1007/978-3-319-16874-6_21.
- [28] T. Barth, R. Herbin, and M. Ohlberger, “Finite Volume Methods: Foundation and Analysis,” *Encycl. Comput. Mech. Second Ed.*, vol. m, pp. 1–60, 2017, doi: 10.1002/9781119176817.ecm2010.
- [29] R. Eymard, T. Gallouët, and R. Ele Herbin, “Finite Volume Methods,” vol. 6632, no. October, pp. 713–1020, 2006.
- [30] C. F. Dynamics *et al.*, *11.1 an Introduction To Computational Fluid Dynamics*, vol. 113, no. 2. 1951. doi: 10.1007/978-3-319-16874-6_21.
- [31] Hrvoje Jasak, “Error Analysis and Estimation for the Finite Volume Method with Applications to Fluid Flows,” vol. M, no. septembre, p. 200, 1992, [Online].

Available: https://books.google.com.co/books?id=_ghlHAAACAAJ

- [32] C. R. Maliska, “The Finite Volume Method,” *Fluid Mech. its Appl.*, vol. 135, pp. 41–83, 2023, doi: 10.1007/978-3-031-18235-8_3.
- [33] J. Boudet, “Finite volume methods,” *Comput. Fluid Dyn.*, vol. M, no. 6, pp. 1–24, 2011, doi: 10.1007/978-3-319-99693-6_4.
- [34] ANSYS Inc., “ANSYS Fluent 18 - Tutorial.” 2018.

